Exploring the Mechanistic Role of Oncostatin M in *Dnmt3a*-Mutant Clonal Hematopoiesis

A thesis submitted by

Logan Sari Schwartz

In partial fulfillment of the requirements for the degree of

PhD

in

Genetics

Tufts University

Graduate School of Biomedical Sciences

October 2023

Advisor: Jennifer Trowbridge, PhD

Abstract

Hematopoietic stem cells (HSCs) are essential for the process of or the lifelong production of all blood lineages; therefore, their specification and maintenance are tightly regulated. With aging this process becomes dysregulated due to the deteriorating support of the hematopoietic niche and chronic inflammation. Mutations in the stem cell pool increase in frequency with age and while some have no effect, others can confer a competitive advantage causing a clonal HSC expansion. This clonal expansion is known as clonal hematopoiesis (CH) and is present in 10-15% of individuals aged 70 years or older. Individuals with CH have a 10- to 15-fold increased risk of progression to hematologic malignancy compared to age-matched controls, as well as 2-fold higher risk of coronary heart disease and 2.6-fold higher risk of ischemic stroke. While CH can be detected using next-generation sequencing, this information is not sufficient to predict which individuals with CH will develop hematologic malignancy, coronary heart disease, ischemic stroke, or other complications. This prediction is currently not possible due to a lack of understanding of the mechanisms by which clonal HSC expansion and disease development occurs. The inflammatory environment plays a role in driving the selective advantage of mutant cells CH and we do not yet understand how this is initiated or how to intervene. To address this, we explored the previously identified target gene, Oncostatin M (OSM), as a candidate contributor to age-related *Dnmt3a*-mutant CH (Chapter 2). Our studies revealed a negative feedback mechanism whereby OSM signaling led to increased transcription and stability of anti-inflammatory genes to provide a selective advantage to young *Dnmt3a*-mutant HSCs within the context of CH. We also explored the effect of chronic inflammation how this might disrupt the

regulatory mechanisms that normally resolve inflammatory states in young *Dnmt3a*-mutant HSCs. In Chapter 3 we test the utility of a conditional *Osmr*$^{fl/fl}$ mouse model to study the role of OSM in CH. While validating this model we found that loss of *Osmr* exon 2 variably impacts mRNA and protein expression. Overall, this work has contributed to the field of CH by identifying OSM as a novel master regulator of an inflammatory cytokine network active in *Dnmt3a*-mutant CH.

Dedication

To my parents, Lori and Michael Schwartz and sister Morgan Schwartz for their unconditional love and support.

Acknowledgments

This endeavor would not be possible without the support and patience of my PI, Dr. Jennifer Trowbridge. It is difficult to put into words how grateful I am for having you as my mentor over these years to guide me through the many ups and downs. You have been a fundamental role model in my personal and professional life. I am truly honored to be a graduate student in your laboratory, and the opportunity to work under your supervision has made me a better scientist and taught me lessons I will never forget.

I also express deep gratitude to my committee members, Dr. Carol Bult, Dr. Ryan Tewhey, Dr. Phil Hinds, and Dr. Clifford Rosen, who generously provided me with knowledge and expertise towards completing my thesis. Dr. Carol Bult provided critical feedback and was an incredibly supportive committee chair throughout the process; thank you for always being my biggest supporter. I also want to thank my unofficial mentors, and there are many, especially Dr. Greg Cox, for providing much-needed advice, car support, and an outside perspective. Lastly, this endeavor would not have been possible without the generous support from the National Institute of Health NIDDK F31, the Burroughs Wellcome Endowed Fellowship through The Jackson Laboratory, and the Scheer-Tomasso Endowment award through Tufts University.

I would like to thank all the scientific and writing staff at The Jackson Laboratory who made this work possible. A special thank you to Stephen Sampson for his extremely thoughtful and insightful feedback on my fellowship writing. A huge thank you and deep gratitude to everyone in the Flow Cytometry Core: Will Schott, Danielle Littlefield, Krystal-Leigh Brown, and all past members who have helped to support me. I truly could

not have done this without all your expertise, advice, and friendship over the years. Additional thanks to everyone in Computational Infrastructure, the Research Administrative Assistants, Genome Technologies, the Center for Biometric Analysis, the Histology Services, the Research Necropsy Services Group, the Scientific Instrument Services, the Rosen Laboratory, and the Monoclonal Antibody and Protein Production Service for teaching me and helping me complete any experiment I wished to achieve during my time in graduate school.

I would like to thank the directors of Pre- and Postdoctoral education at The Jackson Laboratory, Dr. Carrie Cowan (former) and Dr. Meredith Theeman (current), and the Genetics Program coordinators at Tufts University Graduate School of Biomedical Sciences, Diana Pierce (former) and Hannah Hanemann (current), for their support in facilitating the graduate program.

A huge thank you to past and current members of the Trowbridge lab, who have made being part of the lab feel like a team and a family. I specifically would like to thank the incredible mentors I have had throughout the years, including Dr. Jennifer SanMiguel, Dr. Jayna Mistry, Elizabeth Eudy, Dr. Maria Telpoukhovskaia, and Dr. Kira Young. Kira, I am incredibly fortunate to have had such a fun, brilliant, supportive, and dedicated role model to learn from over these years. Your mentorship has been instrumental in this process, and I could not have done it without you.

I am also grateful to my fellow graduate students, past and present. Thank you for being incredible colleagues and friends. I have learned so much from you over the years, and you have made this experience memorable. You have made Bar Harbor feel like home and made even the worst days feel tolerable. I am grateful for all the brainstorming sessions, feedback, fun in classes, and moral support.

This community has provided me with lifelong friends who mean the world to me. I would like to thank all my friends, especially Dr. Sarah Vogel, Katharine Hickey, Ezra Hallett, and Elli Hartig, for sticking with me through this process. Thank you for the long phone calls, delivered meals, and travels out here to visit, even though Bar Harbor can be difficult to travel to. Specifically, I would like to thank Elli Hartig for being my buddy, rock, and shoulder to cry on at any time. Thanks for talking sense into me when I needed it the most, telling me I could carry on when I felt most hopeless, and for the care and love you have given me over the years. I am so grateful to every one of you, and I could not have done this without you cheering me on every step of the way.

I would also like to thank Lucy Benjamin and Clifton Page for taking me in as your daughter and providing me with a home away from home. Thank you for the farmers market fun, dinner parties, food, and friendship. I am so lucky to have a second family like you!

Lastly, I would not be here if not for the support of my immediate and extended family, especially my parents, who have worked hard their entire lives and have served as an

incredible example for me. My mother, Lori, for fostering my interest in science as a precocious sixth grader, and my father, Michael, for his unwavering support. I want to thank my sister Morgan for being the kind of sister people wish for; I don’t know what I would do without your love and support. Thank you for always being motivational, understanding, and supportive, no matter what. All I have been able to accomplish is thanks to you.

Table of Contents

List of Tables

List of Figures

List of Abbreviations

AML – Acute myeloid leukemia
ARCH – Age related clonal hematopoiesis
ASXL1 – Additional sex combs-like transcriptional regulator 1
BM – Bone marrow
Bp – Base pair
CFU – Colony-forming unit
CH – Clonal hematopoiesis
CHIP – Clonal hematopoiesis of indeterminate potential
CMPs – Common myeloid progenitors
CLOUD-HSPCs – a Continuum of LOw primed UnDifferentiated hematopoietic stem- and progenitor cells
CLPs – Common lymphoid progenitors
CNTF – Ciliary neurotrophic factor
CT-1 – cardiotrophin 1
CLCF1 – cardiotrophin-like cytokine factor 1
DNA – Deoxyribonucleic acid
DNMT3A – DNA methyltransferase 3 alpha
FACS – Fluorescence-activated cell sorting
GMP – Granulocyte-macrophage progenitors
gp130 – Glycoprotein 130 or IL6ST
hOSM – Human OSM
hlOSM – Human-like OSM
HSCs – Hematopoietic stem cells
HSCT – Hematopoietic stem cell transplant
HSPCs – Hematopoietic stem and progenitor cells
IFNg – Interferon gamma
IL-6 – Interleukin 6
JAK/STAT3 – Janus-activated kinase/signaling transducer and activator of transcription 3
JNK – c-Jun N-terminal Kinase
Kb – Kilobase
LIF – Leukemia inhibitory factor
LIFR – Leukemia inhibitory factor receptor alpha
LPS – Lipopolysaccharides
LT-HSCs – Long-term hematopoietic stem cells
mAbs – Monoclonal antibodies
MAPK/ERK – Mitogen-activated protein kinase/extracellular regulator kinase
MEPs – Megakaryocyte-erythrocyte progenitors
MMRRC – Mutant Mouse Resource and Research Centers
MPPs – Multipotent progenitor populations
mOSM – Mouse Oncostatin m
NMR – Nuclear magnetic resonance
OSM – Oncostatin m
OSMRβ – Oncostatin m specific receptor subunit beta

OSMi – OSM inhibitor
PB – Peripheral blood
PI3K/AKT – Phosphotydylinositol-3-kinase protein kinase B
PolyI:C – Polyinosinic-polycytidylic acid
PVA – Polyvinyl alcohol
RNA – Ribonucleic acid
scRNA-seq – Single cell RNA seq
ST-HSCs – Short-term hematopoietic stem cells
TET2 – ten-eleven translocation 2
TNFα – Tumor necrosis factor alpha
XCI – X chromosome inactivation

Chapter 1: Introduction

1.1 Overview: Hematopoietic Stem Cells, Hierarchy, Function

Throughout an individual's lifetime, the cellular components of blood are constantly replenished through a process known as hematopoiesis. This process has been studied for centuries from the ancient Egyptians who believed that blood was the source of life to 17th century researcher, William Harvey who uncovered that blood circulates throughout the body and the bone marrow (BM) is responsible for producing blood cells[1-3]. This intricate delicate system is composed of a variety of specialized cells, each with their own distinct roles, including oxygen transportation and immune protection[4]. The blood and BM composition are both regenerative and plastic as millions of "old" blood cells are replenished and turned over with new ones every second[5]. Organizing the hematopoietic cells by most multipotent to least, we get a resulting hematopoietic hierarchy with self-renewing HSCs and multipotent progenitor (MPP) cells sitting at the very top.

1.1.1 Defining the Classic Hematopoietic Hierarchy

How do we know what types of cells HSCs can produce? In 1961 Till and McCulloch performed and published a series of experiments that showed that hematopoiesis could be quantified, hematopoietic cells in the marrow had multi-lineage potential as well as self-renewal properties and lastly murine spleens contained cells that were capable of producing lymphocytes[6]. By performing colony forming unit assays (CFUs) the authors proposed that the cells capable of self-renewal and producing all blood cell types must be HSCs. The process of differentiation is tightly regulated to ensure that an adequate supply of each blood cell type is produced. Differentiation occurs due to the activation of

specific genes and the suppression of others either transcriptionally or epigenetically, leading to changes in cellular morphology, function, and gene expression[7,8].

To define the different mature lineage populations, monoclonal antibodies (mAbs) are used to distinguish between lineage subsets. With the onset of fluorescence-activated cell sorting (FACS) capabilities combined with *in vitro* CFU or *in vivo* transplantation assays researchers were able to parse apart the first hematopoietic hierarchy (Figure 1.1A)[6,9,10]. There are two populations of HSCs, the first is a long-term HSC (LT-HSCs) comprised mostly of quiescent cells with a self-renewal capacity that can be retained for greater than 6 months[11]. The other population of HSCs are short-term HSCs (ST-HSCs), which are lineage-committed depending on intrinsic and extrinsic signals and cannot sustain their self-renewal properties for more than a month[12]. ST-HSCs can differentiate into MPPs and these cells further segregate into pre-GM/pre-Mk/E (formerly known as CMPs) and common lymphoid progenitors (CLPs). The pre-GM/pre-Mk/E cells give rise to granulocyte-macrophage progenitors (GMPs) and megakaryocyte-erythrocyte progenitors (MEPs). The GMPs can make granulocytes, monocytes, and dendritic cells, while MEPs transform into erythrocytes and megakaryocytes. The CLPs, on the other hand, can give rise to T, B, NK, and dendritic cells[13-15]. The culmination of these findings resulted in a traditional hierarchical tree diagram generally accepted by which HSCs differentiate to lineage-committed precursor cells in a stepwise manner through multipotent, oligopotent

and bipotent stages.

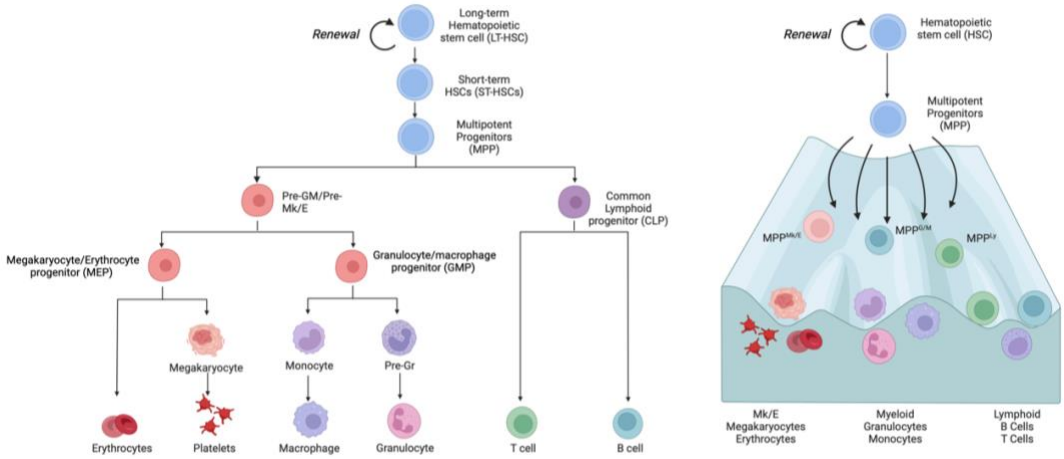

Figure 1.1: Classic and revised models of hematopoiesis
Hematopoiesis conceptualized as a hierarchical process in which hematopoietic stem cells (HSCs) differentiate into increasingly lineage-restricted, non-self-renewing hematopoietic progenitors. (B) Re-envisioned hematopoietic differentiation trajectory. With the advent of more sophisticated methods of fate tracking and molecular analysis in HSC and progenitor cells**,** it has become evident that individual HSCs can exhibit molecular features consistent with lineage priming. Created with BioRender.com licensed by The Jackson Laboratory.

1.1.2 Deviations from the Classical Hematopoietic Hierarchy

Our current understanding of HSC differentiation is limited as in reality it is context dependent, a continuum and plastic[16]. Recent studies using single cell RNA seq (scRNA-seq) in combination with unbiased clustering methods have revealed that there is an immense amount of heterogeneity within these previously defined populations[17-22]. The production of particular cell types is context dependent and changes with the demand of the individual: for example, fetal hematopoiesis[22], aged hematopoiesis[18] or emergency hematopoiesis in response to a stimulus such as chronic infection with Mycobacterium avium[23]. Up until recently our knowledge of the hematopoietic hierarchy relied heavily on flow cytometry markers used to isolate discrete steps in the differentiation of HSCs

but these methods only capture a discrete population/timepoint. The HSC fate and lineage priming decisions occur due to specific epigenetic and transcriptional circuits that can be altered on both the DNA and chromatin level resulting in different types and proportions of differentiated cells. These distinct gene expression modules work together to regulate HSC stemness, early lineage priming, and the progression into all major branches of hematopoiesis. For example, the transcription factor PU.1 has been identified as a myeloid "master regulator" that is expressed robustly in HSCs and can limit their proliferative activity in times of inflammatory stress[24-26]. In another example deletion of cohesin complex member STAG2 resulted in decreased chromatin accessibility and transcription of lineage-specification genes leading to increased self-renewal and reduced B cell lineage commitment[27]. A more accurate model of hematopoiesis may be the one detailed by Velten et al. which proposed the existence of a Continuum of LOw primed UnDifferentiated hematopoietic stem- and progenitor cells" (CLOUD-HSPCs)(Figure 1.1B)[28]. The ongoing studies of hematopoiesis at the single cell resolution reveal a continuous landscape downstream of HSCs in which unipotent progenitors may emerge directly from multipotent HSCs. These findings provide a basis for greater understanding of hematopoietic malignancies.

1.2 Hematopoietic Stem Cell Self-Renewal

The first idea of a stem cell that can give rise to the blood lineages was described in the 1950's by a British biologist Dr. Peter Medawar[29]. He contributed greatly to the uncovering of the HSC by understanding the immunological aspects of transplantation

and rejection of foreign grafts[30]. His work not only led to the development of immunosuppressive drugs that are still used today but in 1958, Medawar and his colleagues successfully transplanted BM between genetically distinct mice[31]. Medawar's contributions to the field of transplantation earned him the Nobel Prize in Physiology or Medicine in 1960[30,32]. This breakthrough paved the way for human BM transplantation and has since saved countless lives.

While HSCs are essential to maintaining hematopoietic homeostasis, this rare population of cells also has the capability to self-renew. This property is unique to HSCs in the hematopoietic hierarchy and therefore they are positioned at the top of the classical lineage model. The balance between differentiation and self-renewal is tightly regulated as excessive differentiation would deplete the HSC pool and uncontrolled self-renewal is associated with myeloproliferative disease, leukemia, and BM failure[5,33,34]. Each HSC can undergo a self-renewal, symmetric differentiation, or asymmetric division. Self-renewal division results in the production of two HSCs or while symmetric differentiation division results in two early hematopoietic progenitor cells. HSCs that undergo asymmetric division generate one progenitor cell and one HSC per division[35-40]. HSCs are controlled by the complex interplay of factors that are cell-intrinsic such as transcriptional regulators, epigenetic regulators, and metabolic pathways or cell-extrinsic, including long-range humoral and neural signals or local cues from the BM microenvironment, which is commonly known as the “stem cell niche”[41]. Studying self-renewal remains unclear and difficult to track directly in real-time. Currently, to study the

self-renewal properties of HSCs scientists must utilize a series of functional assays to retrospectively or indirectly study HSC self-renewal.

1.2.1 Assays to Study HSC Self-Renewal:

1.2.1.1 *In vitro* Colony Forming Unit Assays

Utilizing mouse models and advanced flow cytometry tools scientists have made great efforts at the ability to study self-renewal in murine HSCs. *In vitro* CFU assays have been utilized to study isolated HSCs and their ability to proliferate to form colonies and/or differentiate into mature cell types[42]. Studying the ability to generate mature cell types, such as myeloid cells, requires the use of cell-type specific media that will bias the HSC's ability to make that particular cell type. In the case of myeloid cell potential cells are cultured in Methocult 3434 (Stem Cell Technologies), a semi-solid media containing pro-myeloid cytokines and growth factors. These assays take about 7-12 days and can be serially re-plated to assess self-renewing cells by their ability to form colonies on the new plates. Unfortunately, due to the use of cell-type specific medias these assays are limited and require the use of in vivo transplant studies to understand the full self-renewal and differentiation capacity of HSCs.

1.2.1.2 Transplantation Studies

The current standard for mouse transplantation assays involves ablation of the recipient marrow with irradiation or chemical agents followed by transplant of new donor marrow containing HSCs into the recipient mice[43]. Only multipotent HSCs from the donor

marrow have the capacity for stable engraftment and multilineage blood reconstitution following transplantation into conditioned recipients. Many times, competitor or support BM may be transplanted alongside the donor cells to help with survival or study competition dynamics[44]. Studying the donor contributions or chimerism is possible by unique cell surface markers such as *Ptprc*, encoding the pan-leukocyte surface marker CD45. Different mouse strains contain different alleles of *Ptprc*, known as CD45.1 and CD45.2 (the marker used in strains that are C57BL/6 in background)[45-49]. Monoclonal antibodies for CD45.1 and CD45.2 can be used to track donor cells within the recipient mice in combination with other antibodies to quantify the mature hematopoietic cell types in the peripheral blood (pb) following transplant. The transplanted recipients are typically monitored once a month for a determined period and the BM chimerism is studied at the termination of the experiment. The harvested BM can be re-transplanted into new conditioned recipients to measure self-renewal potential. Only through HSC self-renewal can the primary recipient BM reconstitute the secondary recipient[50]. The best assay to assess the self-renewal capacity of individual HSCs is a daughter cell transplantation assay[51,52]. In this experiment a single HSC is sorted and allowed to divide exactly once *ex vivo*. Following division each individual daughter cell is transplanted into a conditioned recipient mouse and the reconstitution capability is measured for each of the daughter cells. Transplantation can also be paired with retroviral or lentiviral barcoding as well as fluorescent markers (rainbow or confetti) to trace individual HSC clones following transplantation[43].

1.2.1.3 Ex-vivo HSC Culture Systems

Given the importance of HSC transplants in human medicine, many groups have attempted to culture human HSCs *ex-vivo*. Studies using mouse HSCs and human HSCs have attempted to create favorable culture conditions for *in vitro* HSC expansion for use in transplantation. As of now hematopoietic stem cell transplant (HSCT) is still the only curative option for hematologic malignancies and other non-malignant blood disorders. Commonly in *ex vivo* cultures, HSCs are cultured in liquid growth media containing cytokines and fetal bovine serum, but HSCs general do not expand well in these cultures and survive for only approximate one week[43]. Alternatively recent studies have utilized a synthetic polymer: polyvinyl alcohol (PVA) in HSC ex-vivo liquid cultures[53]. In combination with cytokines and growth factors the use of PVA allows for a long-term and large-scale expansion of mouse HSCs ex-vivo[54]. PVA cultures are a novel way to culture HSCs ex-vivo, but many more studies are required to optimize conditions to support true HSC expansion for future use in human medicine.

1.3 Decline in Hematopoietic Function with Age

With age, changes to BM hematopoiesis have downstream impacts on health and longevity. Overall, human HSCs become less quiescent and as a result they have an increase in both their cell number and cell dividing capacity[55]. This is supported by studies that have demonstrated that allogenic BM transplantation with HSCs from aged donors have diminished engraftment potential and reduced self-renewal capacity compared to HSC from younger donors[56]. Skewing toward an increase in the myeloid lineage becomes prominent with age as well as increase in incidence of myeloid

malignancy[57]. This increase in myeloid cells comes at the expense of reduced T-cell production, resulting in a decrease in lymphocytes, which may contribute to a decrease in immunity seen in the elderly[58]. The observed increased number of HSCs is hypothesized to be a compensatory mechanism to maintain blood production and indicates that aged HSCs have a diminished functional capacity[59]. These features, in turn, drive an increased risk of autoimmunity and hematological malignancies[60].

1.3.1 Aged HSC Studies in Mice

Many of our insights into aged HSCs have come from extensive studies carried out on C57BL/6J mice. The average lifespan of a laboratory mouse is about two years while the average human lives to about 80 years old (Figure 1.2)[61]. Mice are characterized as young mature adults from three months old until about six months old and middle age after 10 months old until about 14-15 months. Finally, mice are considered aged if they are at least 18 months old[62]. These age groups are determined by the onset of a well characterized group of biomarkers of general aging[63,64]. The uncovered hallmarks of hematopoietic stem cell aging include age-dependent expansion of the HSC pool, with decreased homing capacity and reduced ability to repopulate transplanted recipients[60,65]. Additionally, the HSC pool differentiation potential is skewed toward production of myeloid at the expensive of lymphoid cell production[57]. Lastly the old HSCs have an increased and more sensitive stress-response therefore less of the aged HSCs are in a state of quiescence[66]. Unfortunately, the molecular mechanisms controlling these age-related changes are still under investigation. Both cell-intrinsic and cell-extrinsic influences play a role in the functional decline of HSCs. One key factor in cell-intrinsic dysfunction of

aged HSCs is the accumulation of Deoxyribonucleic acid (DNA) damage, which can lead to genomic instability[67]. Additionally, there is evidence of a deficiency in DNA repair mechanisms with simultaneous age-related replication stress[68]. On the other hand, cell-extrinsic factors such as the development of a proinflammatory environment and decreased HSC-support from the aging BM niche can also contribute to HSC functional decline[65,69,70]. Changes in the bone and vasculature are present in both old mice and elderly humans including pronounce thinning, defects in the regeneration potential of the niche and reduced hormone production which can begin to occur around middle age[60,71]. The remodeling of the BM niche and the presence of pro-inflammatory cytokines co-occur and make a less favorable environment for HSCs leading to age-associated dysfunction[72].

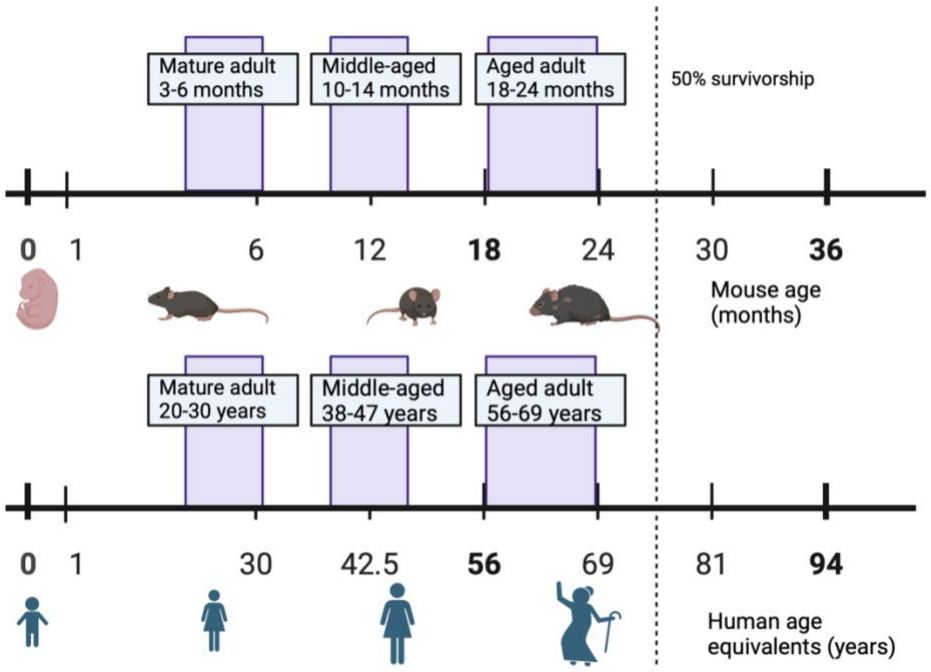

Figure 1.2: Aging with grace
Age ranges for mature life history stages in C57BL/6J mice (young adult: 3–6 months, middle-aged: 10–14 months, old: 18–24 months) and relative human age equivalents. Adapted from Flurkey et al[73]. Created with BioRender.com licensed by The Jackson Laboratory.

1.4 Global Increase in Aged Populations

In many developed nations, the average life expectancy has doubled, due to various factors such as enhanced food quality, better hygienic practices, safer housing conditions, healthier lifestyles, and advancements in medical care. The discovery of antibiotics and vaccines to combat infectious diseases has also played a significant role in prolonging life expectancy[74-76]. Population studies show that, around the year 2000, there were more people over 60 years old than under 15 years old in Europe[77]. This increase in aged individuals is attributed to the falling mortality rates in infants or young individuals and increasing longevity. However, the growth of the population over 80 years old represents a concurrent increase in the number of individuals that are susceptible to age-related malignancies, chronic illnesses, and disability. This "epidemic of frailty"[78] will exert pressure on the available health care resources and result in an increase in the number of individuals requiring consistent medical care[77,79,80]. Almost half of the cancers diagnosed in the early 2000's developed in people aged 65 or older and this number only continues to rise[81]. Recent studies have found that hematologic malignancies contribute significantly to the overall global tumor burden with various leukemias having the highest burden[82]. Since 1990, hematologic malignancies have been increasing in incidence globally, with a total of 1343.85 thousand cases in 2019[82,83]. There is an urgent need to understand the mechanisms governing homeostatic hematopoiesis as well as the onset and prevention of these malignant or mutated hematopoietic cell types. With this knowledge, we can continue to improve the health span of aged individuals, and contribute to the development of effective prevention, early detection, and management strategies for hematologic malignancies.

1.5 Clonal Hematopoiesis:

Advances in sequencing technology and the curation of large datasets have made studying human hematopoiesis possible on a large scale. A population-wide study comparing individuals with overt clinical phenotypes to "normal" aged individuals, revealed a surprising finding. Genetic alterations that were previously associated with patients diagnosed with hematologic malignancies were found to be widely present among "normal" aged individuals with no evidence of cancer[84-86]. The accumulation of somatic mutations and subsequent expansion of the hematopoietic stem and progenitor (HSPCs) cells containing this mutation is characterized as a non-malignant condition known as clonal hematopoiesis (Figure 1.3)[87]. The first observations of a skewed clonal hematopoietic output were first described in the 1960's studying the patterns of X-chromosome inactivation (XCI) in the blood cells of healthy females[88]. In these studies, it was noted that older females were more likely to exhibit skewing of their inactive X-chromosome. These women with skewed XCI also harbored a mutation in blood cancer driver gene, ten-eleven translocation 2 (*TET2*). These studies suggest that this pre-leukemic mutation was responsible for promoting the XCI skewing observed in these individuals[89]. Interestingly more than 90% of age-related CH mutations (ARCH) identified so far occur in TET2 and other genes encoding epigenetic modification enzymes, including DNA methyltransferase 3 alpha (DNMT3A), and additional sex combs-like transcriptional regulator 1 (ASXL1)[89-91]. CH of indeterminate potential (CHIP) constitutes a subset of CH, defined specifically by the presence of somatic mutations in individual hematological malignancy-associated genes at an allele frequency greater than 2%[92].

Clonal growths have been identified in individuals of all ages, but the prevalence depends on the assays being used and the sequencing depth. High-throughput sequencing coupled with error-correction strategies employ panels of targeted leukemia associated genes and can detect clones as small as 0.03% or mutational hotspots of those genes[84,93]. Studies have reported a CH prevalence of 30–90% by age 90 years[94,95]. Despite the sensitivity of detection this information is not sufficient to predict which individuals with CH will be predisposed to increased incidence of hematologic malignancy such as leukemia, coronary heart disease, ischemic stroke, or other complications[96,97]. This prediction is currently not possible due to a lack of understanding of the mechanisms by which clonal HSC expansion and disease development occurs. A natural question arising from clinical studies is whether CH is a cause or consequence, with the possibility that both CH and associated diseases may be a result of aging and related processes[98,99]. Clonal expansion of mutant clones is likely due to a combination of advantages in cell-intrinsic fitness over normal HSCs and preferential survival in the dysfunctional and dysregulated aged microenvironment. In adult patients these clones are typically pre-existing and are selected for after disease treatment. Alternatively in children these clones typically appear after therapy or treatment, although both the sequencing depth and low prevalence of CH in children should be taken into consideration[87].

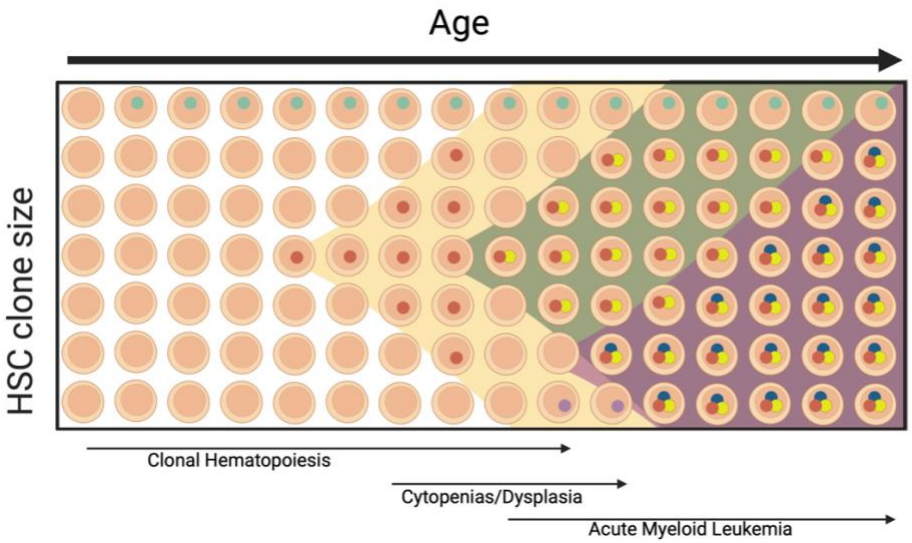

Figure 1.3: Somatic mutations, clonal hematopoiesis, and aging
HSCs acquire somatic mutations with age. Most of the acquired mutations are inconsequential, but rare mutations will lead to clonal expansion of HSCs. If additional mutations are acquired, cytopenias, and/or blood cancers may result. Created with BioRender.com licensed by The Jackson Laboratory.

1.5.1 Mouse Models of CH

By creating and utilizing genetically engineered mouse models, many research groups have reported functional and molecular consequences of the most common human CH-associated mutations in *DNMT3A*, *TET2*, and *ASXL1*[97,100-103]. Specific promoters for hematopoietic studies driving the Cre-recombinase, most commonly *Mx1*-Cre[104] and *Vav*-Cre[105], are used to achieve tissue-specific or temporal activation via external mechanisms. *Vav*-Cre expresses constitutively in hematopoietic tissues, whereas the *Mx1*-Cre expresses Cre under the control of an interferon-responsive promoter. This allows inducible activation of Cre upon injection of polyinosinic-polycytidylic acid (polyI:C), an ribonucleic acid (RNA) analog that induces an antiviral interferon response[106]. Utilizing these mouse model studies it was discovered that CH-mutant HSCs

have different molecular and functional responses to pro-inflammatory cytokine signaling[107,108] and that the enhanced competitive fitness of CH-mutant HSCs may be supported by or require simultaneous dysfunction of the aged BM niche. In Loberg et al. the Trowbridge laboratory created an *Mx1*-cre-inducible mouse model engineered to express the most common *Dnmt3a* mutation associated with CH and acute myeloid leukemia (*Dnmt3a*^{R878H})(Figure 1.4)[109]. In studies of *Dnmt3a*-mutant hematopoiesis it was discovered that elevated levels of interferon gamma (IFNg)[110,111], interleukin 6 (IL-6)[112] and tumor necrosis factor alpha (TNFα or TNFa)[113] are associated with this CH mutation. More work in human patients supported by mouse models is needed to understand if, and in which direction, cause and consequence relationships exist between inflammation and specific CH mutations.

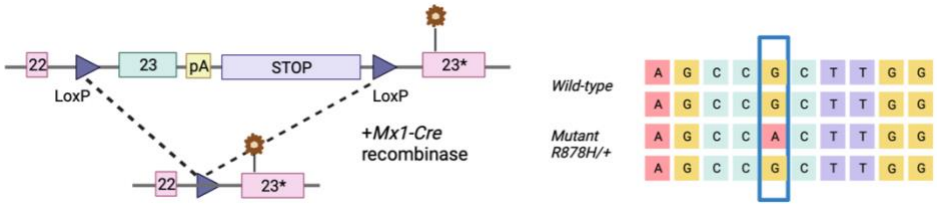

Figure 1.4: Schematic diagram of the design of the *Dnmt3a*$^{fl\text{-}R878H/+}$ allele
Asterisk indicates 2633G>A in exon 23 to encode the R878H mutation. Created with BioRender.com licensed by The Jackson Laboratory.

1.6 Cytokines and Inflammation

The process of how CH is initiated and how the mutant clones are maintained still remains to be fully understood. CH mutant HSPCs are thought to have a different proliferative state, which may result in increased self-renewal or differentiation. This is often seen in response to external stimuli such as pro-inflammatory cytokines. Cytokines are membrane-bound or secreted proteins that are responsible for the differentiation,

growth, and activation of immune cells[114]. They also play a role in disease progression and are frequently implicated in cancer and autoimmune disorders[115]. The tight regulation of the presence and timing of certain cytokines is critical to the inflammatory response to infection, development, cognitive function, tissue maintenance and aging[116,117]. In human studies, increased levels of pro-inflammatory cytokines have been associated with CH, even in cases where the CH was donor-derived following HSCT[95,118,119].

1.6.1 IL-6 Family Cytokines

One of the more prominent families in HSC aging and differentiation is the IL-6 cytokine family which is comprised of IL-6, IL-11, IL-27, IL-31, OSM, leukemia inhibitory factor (LIF), ciliary neurotrophic factor (CNTF), cardiotrophin 1 (CT-1) and cardiotrophin-like cytokine factor 1 (CLCF1)[120]. Members of this family have a significant role in various health conditions such as chronic inflammation, autoimmunity, infectious disease, and cancer, where they often act as diagnostic or prognostic indicators of disease activity and response to therapy[121]. With such widespread and often overlapping properties, the challenge remains to establish how the individual characteristics of these cytokines contribute to disease progression and the comorbidities presented by patients with complex chronic and malignant illnesses[122].

1.6.2 Oncostatin M

OSM has been shown to have a significant role in development, malignancy, and homeostasis of various tissue types[123]. It is mainly secreted by mature activated hematopoietic cells: monocytes, T lymphocytes, neutrophils, macrophages, and dendritic cells[124]. In 1986 OSM was first isolated as it was found to inhibit the proliferation of A375 melanoma tumor cells without having measurable effect on normal human fibroblasts[125]. For this role it was given the name oncostatin M: "onco" for cancer and "statin" for its ability to inhibit cancer cell proliferation. The sequence analysis from this experiment confirmed the 1814-base-pair cDNA sequence of this cytokine and a predicted a 252-amino-acid protein[125,126]. Interestingly it is relatively stable compared to other cytokines as it is stable at pH values between 2 and 11 and withstands temperatures of 56 °C for 1 h while being sensitive to 90 °C[125,127]. Some theorize that OSM is a gene duplication of LIF as they share high homology in structure and function. The LIF and OSM genes are only separated by about 16 kilobase (kb) on chromosome 22q12[128,129]. The close physical linkage of these two related genes supports the idea that they are evolutionarily related. Despite this evidence there is a low degree of sequence homology suggesting rapid evolution following this historic gene duplication event[128,130]. The 3′-UTR of OSM mRNAs contains a potential AU-rich cis-element consisting of five AUUUA pentamers embedded in a highly conserved AU-rich sequence. These regions are conserved between human and mouse OSM mRNAs and are involved in the regulation of mRNA stability effectively increasing the half-life of OSM mRNAs present[131].

1.6.3 Oncostatin M Receptor Binding

Secreted OSM can interact with two different receptor complexes, type I or type II[132-134]. The type I receptor complex is composed of the LIF receptor (LIFR) and glycoprotein 130 (gp130 or IL6ST) while the type II receptor complex is composed of oncostatin m specific receptor subunit beta (OSMRβ) and gp130 (Figure 1.5)[132,135]. In addition to full-length OSMRβ (4171 base-pair, GenBank No. NM003999), there are two other types of OSMRβ, including a short-form OSMR (1620 base-pair OSMRs GenBank No. BC010943) with the absence of an intracellular region and a soluble type of the OSMRβ (sOSMR)[136]. Within the IL-6 family, OSM is regarded as unique due to its ability to bind to two different receptor complexes and yet much is still unknown regarding the binding and interactions of OSM with its receptor complexes[137]. OSM first binds to the extracellular cytokine binding homology region of gp130 with a high affinity (10^{-8} M) and then recruits either protein to form receptor complex type I or II[138-140]. Recently it has been shown that OSM binds to the LIFR type I receptor complex with significantly lower affinity than its specific receptor[141,142]. The ability to signal through two different receptors was first described for human OSM (hOSM) as well as rat OSM[143,144]. In contrast mouse OSM (mOSM) mainly acts through the type II receptor complex but has been shown to have limited activity through the type I receptor[144]. Despite their structural similarity, mouse and human OSM are unable to signal through the other species' OSMR: hOSM signals through the murine LIFR but not mouse OSMR whereas mOSM cannot activate any of the human receptors[144,145]. Recently, a study was published exploring the molecular basis for such species-specific signaling. Adrian-Segarra et al. generated chimeric mouse-human cytokines to study the dynamics of species-specific

binding and determine the AB loop amino acids are responsible for receptor selection. By substituting individual amino acids in this loop structure, they were able to alter OSM signaling capabilities in hOSM and mOSM[144]. Identification of these critical amino acids could result in the generation of mouse OSM variants that share more functional features with human OSM to facilitate more pre-clinical studies in mice[134]. The need for better pre-clinical models and more studies is critical as overexpression of OSM and OSMR has been detected in various cancers and more recently in COVID-19[146].

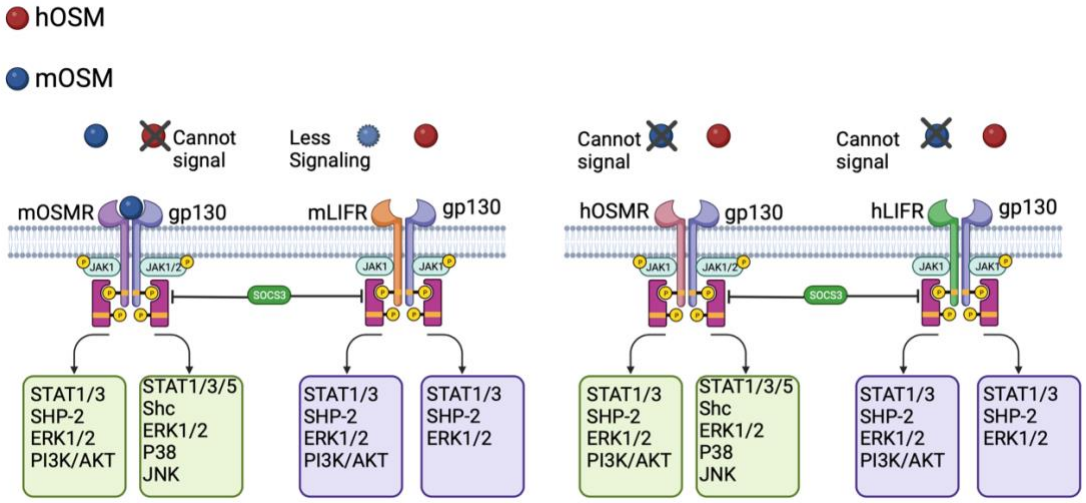

Figure 1.5: Differences in murine/human OSM signaling via OSMR and LIFR
Mouse and human OSM possess different capabilities for receptor signaling. Created with BioRender.com licensed by The Jackson Laboratory.

1.6.4 Oncostatin M Signaling

After binding to the OSMR complex several signaling pathways are activated in humans and mice including the Janus-activated kinase/signaling transducer and activator of transcription 3 (JAK/STAT3), the mitogen-activated protein kinase/extracellular regulator kinase (MAPK/ERK), the c-Jun N-terminal Kinase (JNK) and the phosphotydylinositol-3-kinase protein kinase B (PI3K/AKT) pathways[123,147]. The most

abundantly activated downstream signaling molecule of OSM is STAT3 which plays a key role in cell proliferation, invasion, and survival of cancer cells[147]. Overexpression of the OSM and OSMR has been detected in various cancers including colon cancer, breast cancer, pancreatic cancer, myeloma, brain tumors, chronic lymphocytic leukemia, and hepatoblastoma[146,148]. Additionally in genome-wide associated loci studies performed in humans utilizing BioBank Japan, the UK BioBank, and FinnGen, genetic variants in *Osm* have been identified as a likely causal gene for changes in leukocyte count, as well as CH associated diseases such as myocardial infarction and coronary artery disease[149]. Significantly increased *Osm* transcript production has also been associated with age in both in the aged human thymus[150] and aged mouse HSCs compared to young tissues[151]. The detection of the OSM expression can be used as a key biomarker to stratify and identify patients that are at risk of cancer progression or recurrence[152-155]. The transcription of OSM can be stimulated by STAT proteins and is regulated by C/EBP and GC-rich elements[156,157]. Therefore, other STAT-activator cytokines, including IL-2, IL-3, GM-CSF, EPO and OSM itself can lead to increased expression of OSM[156]. Despite 30 years of implications in inflammatory diseases there has been little to no success in the development of an anti-OSM clinal therapeutic reaching FDA approval due to poor significance and inconclusive results. There has been recent success in development of a small molecule inhibitor of OSM renewing interest in this pleiotropic cytokine.

1.7 Inflammation and CH: Friend or Foe?

Given the correlations between individual CH mutations and concurrent pro-inflammatory environment recent studies have explored the idea of a mutation-dependent

anti-inflammatory pathway resulting in a pro-survival and expansion phenotype unique to mutant HSPCs in this context. It is critical to understand the pro-survival pathways utilized by mutant HSPCs resulting in clonal expansion to utilize them for therapeutic approaches[158]. In one study *Tet2*$^{-/-}$ lineage marker-negative marrow cells and TET2-mutant human HSPCs were cultured in an *in vitro* environment that contains the proinflammatory cytokine TNFα. This environment and inflammatory state are associated with TET2 inactivation and/or "inflammaging" and were found to be associated with myeloid skewing and resistance to apoptosis[159]. This study is the first to identify a positive feedback loop involving *Tet2* mutations promoting clonal dominance with aging, producing inflammatory cytokines by myeloid skewing, and conferring TNFα resistance to mutant BM progenitors while also propagating such an inflammatory environment. The conclusion being that *Tet2*-mutant clones may have greater fitness in an inflammatory environment of aging than their wild-type counterparts. In a related study, Cai et al. explore the anti-apoptotic mechanism governing *Tet2*-mutant CH HSPCs fitness advantage and found it is the result of hyperactivation of the SHP2-STAT3 signaling axis[160]. Through this signaling pathway *Tet2*-mutant CH HSPCs selectively downregulate the apoptotic protein Bim via the anti-apoptotic long non-coding RNA *Morrbid*[161]. Lastly recent work using a zebrafish model of human *ASXL1*-mutant CH found a protective response to pro-inflammatory cytokines in HSPCs via upregulation of *socs3a*, *atf3* and *nr4a1*[162]. These genes encode anti-inflammatory proteins that act as negative regulators of major signaling pathways such as STAT3. Without the capacity to upregulate *nr4a1* and *nr4a3*, the *Asxl1*-mutant HSPCs lost their self-renewal capacity and selective growth advantage. Understanding the interplay between mutant and neighboring

wild-type HSPCs and cues from the local environment in model systems is an important step in uncovering the chronic selective forces allowing for the establishment, maintenance, and malignant transformation of CH clones.

1.8 Conclusions:

As the proportion of individuals ≥ 65 years old in the United States is expected to increase from 15% of the population in 2014 to 24% (~98 million individuals) by the year 2060, the overall incidence of clonal hematopoiesis (CH) is expected to increase significantly. Individuals with CH have a 10- to 15-fold increased risk of progression to hematologic malignancy compared to age-matched controls, as well as higher all-cause mortality especially due to a high risk of coronary heart disease and ischemic stroke. Understanding the cellular and molecular mechanisms underlying the selective advantage of HSPCs harboring somatic mutations, and how and in whom this is a risk factor for age-associated disease, will further inform our understanding of CH-associated conditions. The inflammatory environment plays a role in driving CH and the selective advantage of mutant cells, but we do not yet understand how this is initiated or how to intervene. To address this, I explored previously a identified target gene, Oncostatin M, as a candidate contributor to age-related *Dnmt3a*-mutant CH (**Chapter 2**), and the utility of OSMRβ knockout mouse models to study the role of OSM in HSCs and CH (**Chapter 3**).

Chapter 2: Oncostatin M is a Master Regulator of an Inflammatory Network in *Dnmt3a*-Mutant Hematopoietic Stem Cells

Schwartz, L. S., Young, K. A., Stearns, T. M., Boyer, N., Mujica, K. D., & Trowbridge, J. J. (2023) Submitted to Stem Cell Reports, 8/10/2023.

2.1 Introduction

The process of aging has a profound impact on tissues and cells throughout the body. In the hematopoietic stem and progenitor cell (HSPC) compartment, aging is accompanied by acquisition of somatic mutations. Given the long-lived nature of the HSPC pool, these mutations can be propagated for many cellular generations and through most mature hematopoietic cell progeny. While most of these somatic mutations are considered 'neutral', a subset can confer a selective growth advantage to HSPCs, leading to a condition termed age-associated clonal hematopoiesis (CH). The most common CH mutations are found in a subset of genes that encode canonical epigenetic or chromatin regulatory proteins such as DNA methyltransferase 3A (DNMT3A), tet methylcytosine dioxygenase 2 (TET2) and additional sex combs like-1 (ASXL1)[97,102]. While CH is not a disease *per se*, it is associated with increased risk of age-associated pathologies such as blood cancers and ischemic stroke[97,101,102,163-166]. Understanding the cellular and molecular mechanisms underlying the selective advantage of HSPCs harboring somatic mutations, and how and in whom this is a risk factor for age-associated disease, will further inform our understanding of CH-associated conditions.

By creating and utilizing genetically engineered mouse models, many research groups have reported functional and molecular consequences of the most common human CH-associated mutations in *DNMT3A*, *TET2*, and *ASXL1*[97,100-103]. In some of these studies, chronic stress and inflammation were found to act as selective pressures contributing to expansion of CH and development of CH-associated pathologies[97,118,167]. CH-mutant HSCs have different molecular and functional responses to pro-inflammatory cytokine

signaling[107,108], and recent work suggests that CH-mutant hematopoietic cells can induce and maintain a pro-inflammatory state[168]. For example, *Dnmt3a*-mutant hematopoiesis is associated with elevated levels of IFNg[110,111], IL-6[112] and TNFα[113]. *Tet2*-mutant hematopoiesis is associated with elevated levels of IL-6[160], IL-8[169], IL-1b[95,170,171] and TNFa[159]. *Asxl1*-mutant CH is associated with increased IFNg and TNFa[172]. The extent to which multiple cytokines activate the same underlying inflammatory network contributing to CH and CH-associated pathologies, or whether individual cytokines have context-dependent effects, remains unknown. Addressing this gap in knowledge is important when considering therapeutic interventions that will be most effective in individuals at risk of CH-associated pathologies.

Using a Cre-inducible mouse model that we previously engineered to express a specific *Dnmt3a* mutation associated with CH and acute myeloid leukemia (*Dnmt3a*^{R878H})[109], we found that placing *Dnmt3a*-mutant HSPCs in a middle-aged BM microenvironment in the context of elevated pro-inflammatory cytokines promoted their selective advantage[113]. We discovered that TNFa:TNFR1 signaling was a key mediator of the selective advantage of *Dnmt3a*-mutant HSCs in the context of a middle-aged BM microenvironment[113]. However, as described above, TNFa is not the only cytokine known to contribute to *Dnmt3a*-mutant CH. Here, we report on our findings that Oncostatin M (OSM) is a key pro-inflammatory cytokine associated with CH in *Dnmt3a*-mutant mice.

2.2 Materials and Methods

2.2.1 Animals

C57BL/6J (JAX:000664) and B6.SJL-*PtprcaPepcb*/BoyJ[45] (JAX:002014, referred to as CD45.1^{+}) mice were obtained from, and aged within, The Jackson Laboratory. *Dnmt3a*$^{fl\text{-}R878H/+}$ mice (JAX:032289) were crossed to B6.Cg-Tg(*Mx1*-cre)1Cgn/J mice (JAX:003556, referred to as Mx-Cre). In all experiments, control (+/+) mice carried a single copy of Mx-Cre allele. The Jackson Laboratory's Institutional Animal Care and Use Committee approved all experiments. To induce Mx-Cre, mice were intraperitoneally injected once every other day for five total injections with 15 mg/kg high molecular weight polyinosinic-polycytidylic acid (polyI:C) (InvivoGen). In all experiments, mice were used >4 weeks following polyI:C administration.

2.2.2 Peripheral Blood Analysis

Blood was collected from mice via the retro-orbital sinus and red blood cells were lysed prior to staining with the following fluorochrome-conjugated antibodies: BV650 CD45.1 (BioLegend clone A20), AlexaFluor700 CD45.2 (BioLegend clone 104), BUV496 B220 (BD Biosciences clone RA3-6B2), PerCP-Cy5.5 CD3e (BioLegend clone 145-2C11), APC-Cy7 CD11b (BioLegend clone M1/70), APC Ly6g (BioLegend clone 1A8), BV605 Ly6c (BioLegend clone HK1.4), BV421 Ter-119 (BioLegend clone TER-119), PE-Cy7 F4/80 (Invitrogen BM8). Data was collected using a LSRII (BD Biosciences) and analyzed using FlowJo V10 (BD Biosciences).

2.2.3 Isolation and Phenotyping of Hematopoietic Stem and Progenitor Cells

BM cells were isolated from pooled and crushed femurs, tibiae, iliac crests, sternums, forepaws, and spinal columns of individual mice. BM mononuclear cells (MNCs) were isolated by Ficoll-Paque (GE Healthcare Life Sciences) density centrifugation or 1X RBC Lysis Buffer (eBioscience) and stained with a combination of fluorochrome-conjugated antibodies: c-Kit (BD Biosciences, BioLegend clone 2B8), Sca-1 (BioLegend clone D7), CD150 (BioLegend clone TC15-12F12.2), CD48 (BioLegend clone HM48-1), CD34 (BD Biosciences clone RAM34), FLT3 (BioLegend clone A2F10), CD11b (BioLegend clone M1/70), mature lineage (Lin) marker mix (B220 (BD Biosciences, BioLegend clone RA3-6B2), CD4 (BioLegend clone RM4-5), CD5 (BioLegend clone 53- 7.3), CD8a (Biosciences, BioLegend clone 53-6.7), Ter-119 (BioLegend clone TER-119), and Gr-1 (BioLegend, Invitrogen clone RB6-8C5)), and the viability stain propidium iodide (PI) or 4′,6-diamidino-2-phenylindole (DAPI). For transplants CD45.1 (BioLegend clone A20), and CD45.2 (BioLegend clone 104) antibodies were used to distinguish genotypes of donor and recipient mice. The following cell surface markers were used to isolate or phenotype HSCs: Lin- Sca-1+ c-Kit+ Flt3- CD150+ CD48-, HSPCs: Lin- Sca-1+ c-Kit+, $MPP^{G/M}$: Lin- Sca-1+ c-Kit+ Flt3- CD150- CD48+, CMP: Lin- Sca-1- c-Kit+ CD34+ FcgR-, GMP: Lin- Sca-1- c-Kit+ CD34+ FcgR+. Data was collected using a BD FACSymphony A5 or cells were prospectively isolated using a FACSymphony S6 (BD Biosciences). All flow cytometry data was analyzed using FlowJo V10.

2.2.4 Cell Cycle Analysis

5,000 HSPCs were sorted directly into TC-treated 96-well plates (Falcon) containing StemSpan™ SFEM II (Stemcell Technologies) with Pen-Strep (Fisher Scientific) and SCF (100 ng/ml, BioLegend), TPO (50 ng/ml, Peprotech), with or without OSM (500 ng/ml, BioLegend) for 24hrs at 37^{o}C and 5% CO2. Cells were stained with Ghost UV450 viability dye (Cytek Biosciences) and fixed with the FIX & PERM™ Cell Permeabilization Kit (Invitrogen) following the manufacturer's protocol. Following fixation cells were stained with FITC anti-mouse/human Ki-67 (BioLegend) and DAPI. Data was collected on a BD FACSymphony A5.

2.2.5 Apoptosis Analysis

5,000 HSPCs were sorted directly into 96-well plates containing SFEMII with Pen-Strep and SCF (100 ng/ml), TPO (50 ng/ml), with or without OSM (500 ng/ml) for 24hrs at 37^{o}C and 5% CO2. Cells were stained with Annexin V and Propidium iodide using the Annexin A5 Apoptosis Detection Kit (BioLegend). Data was collected on a FACSymphony A5 (BD Biosciences).

2.2.6 Colony-Forming Unit (CFU) Assay

HSCs or HSPCs were isolated and plated in MethoCult GF M3434 (StemCell Technologies), with or without OSM (500 ng/ml) and cultured at 37^{o}C and 5% CO2. Colonies were scored between 6- and 14-days post-plating using a Nikon Eclipse TS100 inverted microscope. For serial replating, cells were harvested by washing the plates and

10,000 cells (from HSCs) or 15,000 cells (from HSPCs) were replated into fresh MethoCult GF M3434 with or without OSM (500 ng/ml).

2.2.7 *In Vitro* Culture with Cytokine-Rich and -Poor Media

We followed a published protocol to generate cytokine-rich and cytokine-poor medias[173]. Briefly, 500 cells were sorted directly into 96-well plates in 200µl of IMDM containing 5% FBS, 50 U/ml penicillin, 50mg/ml streptomycin, 2mM L-glutamine, 0.1mM non-essential amino acids, 1mM sodium pyruvate and 50µM 2-mercaptoethanol. For cytokine-rich media, this was supplemented with SCF (25 ng/ml), TPO (25 ng/ml), Flt3L (25 ng/ml), IL-11 (25 ng/ml), IL-3 (10 ng/ml), GM-CSF (10 ng/ml) and EPO (4 U/ml) (all from PeproTech). For cytokine-poor media, this was supplemented with SCF (25 ng/ml) and G-CSF (25 ng/ml, PeproTech). PBS or OSM was added at 500ng/ml to both medias. After 48hr culture at 37^{o}C and 5% CO2, cells were harvested, DAPI was used to determine live cells and data collected on a FACSymphony A5.

2.2.8 PVA Culture and *In Vivo* Transplantation

For the non-competitive PVA culture and transplant experiment, 50 CD45.2+ HSCs were sorted into a 96-well plate with Ham's F12 media containing 1X pen/strep/glutamine (Gibco), 10 mmol/l HEPES (Gibco), 1X insulin/transferrin/selenium/ethanolamine (Gibco), 100 ng/ml rmTPO (BioLegend), 10 ng/ml rmSCF (STEMCELL Technologies) and 1 mg/ml polyvinyl alcohol (Sigma), with or without 500 ng/ml rmOSM, and cultured for 7 days at 37°C and 5% CO2, as previously described[53,54]. 500 ng/ml OSM or vehicle

was added to the cultures on days 4 and 6. On day 7, the wells were harvested, mixed with 106 CD45.1+ BM MNCs, and transplanted into young, lethally irradiated (12Gy gamma irradiation, split dose) CD45.1+ recipients. PB and BM data were collected at 6 months after transplant using a BD LSR II instrument.

For competitive PVA culture and transplant, 25 $CD45.2^+$ HSCs from control or R878H/+ donors ($CD45.2^+$) and 25 $CD45.1^+CD45.2^+$ HSCs from WT F1 mice were sorted into a 96-well plate with Ham's F12 media containing 1X pen/strep/glutamine (Gibco), 10 mmol/l HEPES (Gibco), 1X insulin/transferrin/selenium/ethanolamine (Gibco), 100 ng/ml rmTPO (BioLegend), 10ng/ml rmSCF (STEMCELL Technologies) and 1mg/ml polyvinyl alcohol (Sigma), with or without 500 ng/ml rmOSM, and cultured for 7 days at 37°C and 5% CO2, as previously described[54]. 500 ng/ml rmOSM or vehicle was added to the cultures on days 4 and 6. On day 7, the wells were harvested, mixed with 10^6 $CD45.1^+$ BM MNCs, and transplanted into young, lethally irradiated (12 Gy gamma irradiation, split dose) $CD45.1^+$ recipients. PB and BM were collected at 6 months after transplant using a BD LSR II instrument.

2.2.9 Fluorescent OSM Binding

100 mg rmOSM (BioLegend) was concentrated by centrifugation (Amicon Ultra-0.5 Centrifugal Filter Unit) and fluorescently labeled using the AlexaFluor™ 488 Antibody Labeling Kit following the manufacturers protocol. 10^7 WBM cells were treated with FC block then stained for 30min with PBS or fluorescently labelled rmOSM at 37°C for 30min. After 30min, cells were stained with an antibody cocktail for identification of

HSCs and HSPCs as detailed above. Cells were washed and ran on a BD FACSymphony A5 SE. As positive control, a single cell suspension of liver cells was prepared using the Miltenyi Liver Kit (MiltenyiBiotec).

2.2.10 Phospho-Flow Cytometry

1000 LSK cells were sorted into StemSpan SFEM II media (STEMCELL Technologies). Cells were pelleted and resuspended in StemSpan SFEM II with or without 500 ng/ml rmOSM and incubated at 37°C for 20, 60 or 80min. Cells were then fixed using 16% PFA for 10min at room temperature followed by ice-cold acetone for 10min. Cells were then pelleted, washed and stained with AlexaFluor 488 Mouse Anti-Stat3 (Tyr705) (D3A7) XP Rabbit mAb (Cell Signaling Technologies) or PE-Cy7 Mouse Anti-Stat5 (pY694) (BD) for 30min at room temperature before data collection using a BD FACSymphony A5 SE.

2.2.11 RNA Sequencing

2,000 HSCs were sorted into StemSpan SFEM II media with TPO (50 ng/ml) and SCF (100 ng/ml). PBS or OSM (500 ng/ml) was added to each well and incubated at 37°C for 60min. Total RNA was isolated from flash-frozen pellets using the RNeasy Micro kit (Qiagen) including the optional DNase digest step. RNA concentration and quality were assessed using the RNA 6000 Pico Assay (Agilent Technologies). Libraries were constructed using the SMARTer Stranded Total RNA-Seq Kit v2-Pico (Takara), according to the manufacturer's protocol. Library concentration and quality were

assessed using the D5000 ScreenTape (Agilent Technologies) and Qubit dsDNA HS Assay (ThermoFisher). Libraries were sequenced (2021) 75 base pair (bp) paired-end on an Illumina NextSeq 500 using the High Output Reagent Kit v2.5 (2022)150 bp paired-end on an Illumina NovaSeq 6000 using the S4 Reagent Kit v1.5 both at a sequencing depth of >35 million reads per sample. Trimmed alignment files were processed using RSEM (v1.3.3). Alignment was completed using Bowtie 2 (v2.4.1). Expected read counts per gene produced by RSEM were rounded to integer values, filtered to include only genes that had at least two samples within a sample group having a counts per million reads >1, and passed to R (v4.1.3) and edgeR (v3.36.0) for differential expression analysis. A negative binomial generalized log-linear model was fit to the read counts for each gene. The dispersion trend was estimated by Cox-Reid approximate profile likelihood followed by empirical Bayes estimate of the negative binomial dispersion parameter for each tag, with expression levels specified by a log-linear model. Likelihood ratio tests for coefficient contrasts in the linear model were evaluated producing a p-value per contrast. The Benjamini and Hochberg's algorithm (P value adjustment) was used to control the false discovery rate (FDR). Differentially expressed genes were investigated for overlap with published datasets using Gene Set Enrichment Analysis, and upstream regulators were predicted using Ingenuity Pathway Analysis software. Features with fold change (FC) > 1.5 or < -1.5, and $P < 0.05$, were declared significantly differentially expressed.

2.2.12 Socs3 mRNA Expression Assays

For *Socs3* expression assays, HSPCs were sorted into 750 ml of StemSpan SFEM II with vehicle or 500 ng/ml OSM and incubated at 37°C for 20, 40, 60 or 80min. Following

each incubation, actinomycin D (Sigma) was added and cells were incubated for an additional 20min at 37°C. Samples were pelleted and flash frozen. For *Socs3* stability assays, HSPCs were sorted into 750 ml of StemSpan SFEM II with vehicle or 500 ng/ml OSM and incubated at 37°C for 60min. Actinomycin D was added for 20, 40, 60 or 80min at 37°C. Samples were pelleted and flash frozen. From all samples, RNA was isolated using the RNeasy Microkit (Qiagen) and cDNA was made using the qPCR Bio cDNA synthesis kit (PCR Biosystems). Quantitative PCR was performed using Power SYBR on the QuantStudio 7 Real-Time PCR System (ThermoFisher Scientific). mRNA expression levels were calculated relative to the housekeeping gene, *B2m*.

2.2.13 ELISA

Bone marrow fluid was collected from 3mo, 14mo, and 22mo C57BL/6J mice by needle flushing of femurs with 200 ml PBS. OSM concentration was determined using the Quantikine ELISA for mouse Oncostatin M (R&D Systems) using a Spectramax i3 (Molecular Devices) plate reader.

2.2.14 Statistical Analysis

All statistical tests including evaluation of the normal distribution of data and examination of variance between groups were performed using Prism 9 software (GraphPad). Figure 2.7 was created using BioRender.com licensed to The Jackson Laboratory.

2.2.15 Data Availability

Raw RNA-seq data is available at the Gene Expression Omnibus (GEO) under accession number GSE236693.

2.3 Results

2.3.1 *Dnmt3a*-Mutant HSCs Activate Oncostatin M (OSM) Signaling in an Aged Bone Marrow Microenvironment

Our previously published work profiled molecular signatures associated *Dnmt3a*-mutant (R878H/+) hematopoiesis in a middle-aged BM microenvironment by performing RNA sequencing (RNA-seq) on independent biological replicates of control and *Dnmt3a*-mutant HSCs re-isolated from young and middle-aged recipient mice[113] (Figure 2.1A). In new analysis of these data, enrichment of a hallmark inflammatory response signature was observed in *Dnmt3a*-mutant HSCs compared to control HSCs in middle-aged recipient mice but not in young recipient mice (Figure 2.1B), suggesting that a middle-aged environment promotes transcriptional responses in *Dnmt3a*-mutant HSCs to inflammatory factors. Examining the top leading-edge genes using gene set enrichment analysis (GSEA), increased expression of the IFNg-regulated genes *Bst2, Klf6* and *Icam1*, the inflammatory-responsive receptors *Tlr2* and *Ccrl2*, and the copper transporter *Slc31a2* was observed. *Osm* was the only leading-edge gene encoding a secreted molecule, Oncostatin M (OSM), which is an IL-6 family cytokine known to be involved in the immunopathogenesis of solid tumors and myeloma [174-178]. Given this observation, we hypothesized that increased expression of *Osm* results in a feed-forward loop of activation of the OSM signaling pathway.

To test this hypothesis, we interrogated the expression of a subset of genes known to be involved in and/or regulated by OSM signaling including transcripts encoding OSM signaling receptors (*Osmr, Il6st*), downstream kinases and signaling molecules (ex. *Shc1, Mapk14, Prkcb, Nfkb1*), and transcription factor targets (ex. *Egr1, Fos, Junb, Jund*). We observed trends toward increased expression and significant increase in expression ($P<0.05$) in most genes examined in *Dnmt3a*-mutant HSCs compared to control HSCs in middle-aged recipient mice but not in young recipient mice (Figure 2.1C). We used the upstream regulator analysis feature of ingenuity pathway analysis (IPA) as a complementary approach to examine activation of OSM signaling in *Dnmt3a*-mutant HSCs compared to control HSCs in middle-aged recipient mice. Activation of an OSM-driven IL-6:STAT3 module was observed in *Dnmt3a*-mutant HSCs in middle-aged recipient mice (Figure 2.1D). These results are consistent with activation of OSM signaling in *Dnmt3a*-mutant HSCs in the specific context of a middle-aged environment.

2.3.2 Acute OSM Stimulation Does Not Impact Cell Cycle, Apoptosis, Proliferation or Myeloid Differentiation of Young *Dnmt3a*-Mutant HSPCs

Given that activation of OSM signaling is associated with expanded *Dnmt3a*-mutant hematopoiesis in an aged BM microenvironment, we hypothesized that OSM as a single stimulus would be sufficient to promote the selective advantage of young *Dnmt3a*-mutant HSPCs. To test the effect of recombinant OSM on young *Dnmt3a*-mutant HSPC cycling, cell cycle status was evaluated using Ki-67 and DAPI staining. Control and *Dnmt3a*-mutant HSPCs were prospectively isolated from young adult mice (3-6 months old) and stimulated overnight with 0, 100 or 500ng/ml recombinant murine OSM. Following flow cytometry analysis, cells were gated into G0 (Ki-67- DAPI-), G1 (Ki-67+ DAPI-) and

S/G2/M (Ki-67+ DAPI+) fractions. No significant differences were observed in these proportions across any of the conditions, although there was a trend towards increased S/G2/M in *Dnmt3a*-mutant HSPCs with increasing doses of OSM (Figure 2.2A). To test the effect of recombinant OSM on young *Dnmt3a*-mutant HSPC survival, apoptosis was assessed using Annexin V and PI staining. Control and *Dnmt3a*-mutant HSPCs were prepared and stimulated overnight as detailed above. Following flow cytometry analysis, cells were gated into live (Annexin V- PI-), early apoptotic (Annexin V+ PI-), late apoptotic (Annexin V+ PI+), and necrotic (Annexin V- PI+) fractions. No significant differences in these proportions were observed across any of the conditions (Figure 2.2B). Together, these data suggest that young control and *Dnmt3a*-mutant HSPCs do not respond to acute OSM stimulation with respect to altered cell cycle and apoptosis parameters.

To test the effect of recombinant OSM on myeloid differentiation potential, control and *Dnmt3a*-mutant HSPCs were prospectively isolated from young adult mice and plated into a myeloid methylcellulose media to quantify colony-forming units (CFU). The myeloid methylcellulose media was supplemented with 0, 100 or 500ng/ml recombinant murine OSM. After 7-day culture, no differences in CFU formation were observed across any of the conditions (Figure 2.2C). This result suggests that control and *Dnmt3a*-mutant HSPCs do not respond to OSM with respect to altering their myeloid differentiation potential. To examine CFU re-plating potential, control and *Dnmt3a*-mutant HSPCs as well as HSCs with 0 or 500ng/ml recombinant murine OSM continued to be passaged. As expected, increased CFU re-plating potential from *Dnmt3a*-mutant vs. control HSPCs and

HSCs was observed (Figure 2.2D). However, there was no observed effect of OSM on either control or *Dnmt3a*-mutant CFU re-plating capacity.

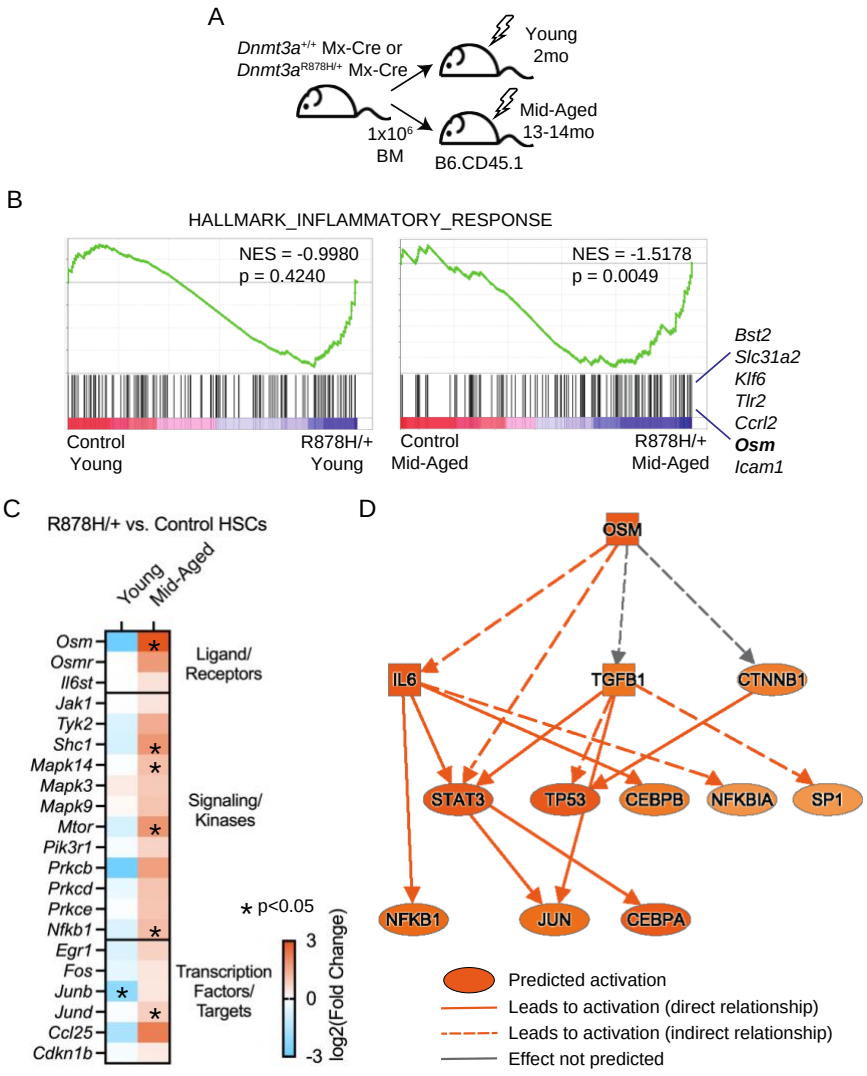

Figure 2.1: *Dnmt3a*-mutant HSCs upregulate *Osm* and OSM signaling genes in a middle-aged BM environment.
(A) Schematic of transplant design into young (2mo) and middle-aged (13-14mo) recipient mice. HSCs (Lin- c-Kit+ Sca-1+ Flt3- CD150+ CD48-) were isolated at 4 months post-transplant and used for RNA-sequencing[112]. n = 3-4 biological replicates. (B) Gene set enrichment analysis of a hallmark inflammatory response signature in control vs. *Dnmt3a*-mutant (R878H/+) HSCs in young recipient mice (left) and in middle-aged recipient mice (right). (C) Heatmap of log2(FC) expression in OSM signaling pathway genes in *Dnmt3a*-mutant (R878H/+) compared to control HSCs in young (left column) and middle-aged (right column) recipient mice. *P<0.05. (D) Ingenuity pathway analysis showing predicted activation of OSM signaling in *Dnmt3a*-mutant (R878H/+) vs. control HSCs in middle-aged recipient mice.

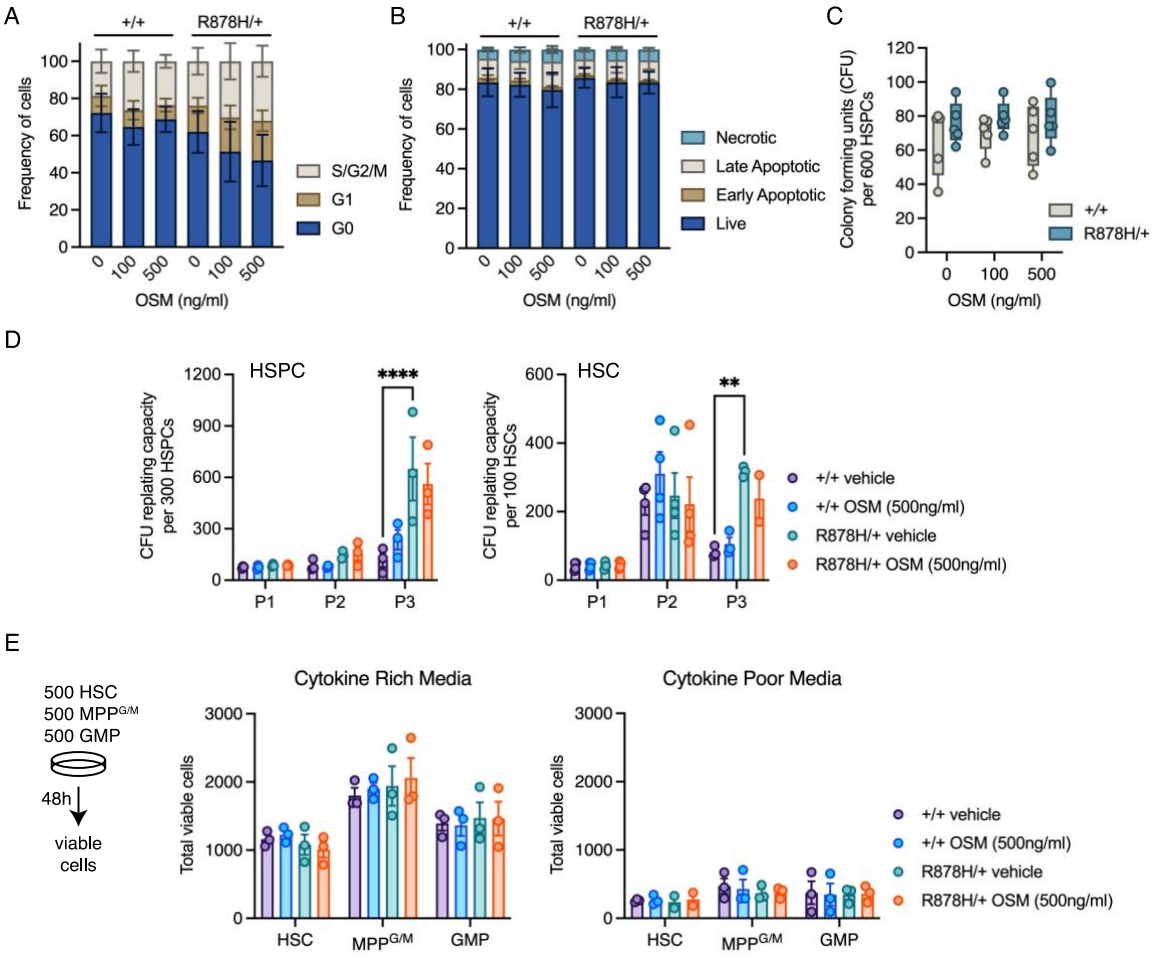

Figure 2.2: Cell cycle, apoptosis, proliferation, and myeloid differentiation in young *Dnmt3a*-mutant HSPCs are unaltered by acute OSM stimulation
(A) Frequency of control (+/+) and *Dnmt3a*-mutant (R878H/+) HSPCs in G0, G1, and S/G2/M cell cycle phases after stimulation with 0, 100, or 500ng/ml OSM for 24hrs. Bars represent mean ± SEM of $n = 3$. (B) Frequency of control (+/+) and *Dnmt3a*-mutant (R878H/+) HSPCs in live, early apoptotic, late apoptotic or necrotic gates after stimulation with 0, 100, or 500ng/ml OSM for 24hrs. Bars represent mean ± SEM of $n = 3$. (C) Colony-forming units (CFU) in control (+/+) and *Dnmt3a*-mutant (R878H/+) HSPCs with 0, 100 or 500ng/ml OSM. Dots show individual mice. $n = 5$. (D) Serial CFU in control (+/+) and *Dnmt3a*-mutant (R878H/+) HSPCs (left) and HSCs (right) with 0 or 500ng/ml OSM. Dots show individual mice, bars represent mean ± SEM of $n = 3$-4. $^{**}p < 0.01$; $^{****}p < 0.0001$ by two-way ANOVA with Tukey's multiple comparisons test. (E) Total viable cells from control (+/+) and *Dnmt3a*-mutant (R878H/+) HSCs, $MPP^{G/M}$ and GMP after 48h culture with 0 or 500ng/ml OSM. Dots show individual mice, bars represent mean ± SEM of $n = 3$.

A limitation of the above CFU studies is that the effect of OSM is being evaluated in the presence of a full complement of cytokines that drive robust myeloid/erythroid cell

differentiation (SCF, IL-3, IL-6, and EPO). To examine the effects of OSM on HSPC proliferation in conditions replicating stress, 0 or 500ng/ml recombinant murine OSM was added to previously defined 'cytokine-poor' (SCF, G-CSF) and 'cytokine-rich' (SCF, GM-CSF, IL-3, IL-11, Flt3L, TPO, EPO) medias[173] to replicate stress and non-stress conditions, respectively. Control and *Dnmt3a*-mutant HSCs, as well as two progenitor populations (granulocyte/macrophage-primed multipotent progenitors or $MPP^{G/M}$ and granulocyte-macrophage progenitors or GMPs), were prospectively isolated from young adult mice and cultured in cytokine-poor and cytokine-rich medias for 48 hours. After this culture period, total viable cell counts were obtained using flow cytometry. No significant differences in total viable cell counts were observed between genotype and treatment groups for any of the input cell populations (Figure 2.2E). Together, these data suggest that young control and young *Dnmt3a*-mutant HSPCs do not respond to acute OSM stimulation by altered cell cycling, apoptosis, myeloid differentiation, or proliferation.

2.3.3 Acute OSM Stimulation Does Not Alter Engraftment Potential or Lineage Output from Young *Dnmt3a*-Mutant HSPCs

As *in vitro* assays do not fully reflect the *in vivo* functional potential of HSPCs, we next tested the hypothesis that recombinant OSM as a single stimulus would be sufficient to promote the selective advantage of young *Dnmt3a*-mutant (R878H/+) HSPCs and HSCs *in vivo*. First, 50 prospectively isolated HSCs from young adult donor CD45.2+ control or *Dnmt3a*-mutant mice were cultured in conditions designed to promote HSC self-renewal[54] supplemented with 500ng/ml recombinant murine OSM or vehicle control

(Figure 2.3A). After 7d culture, the resulting cells in each well were transplanted into lethally irradiated CD45.1+ recipient mice to assess hematopoietic engraftment and lineage potential. At 16wks post-transplant, no significant differences were observed in donor engraftment (% CD45.2+) in the peripheral blood or bone marrow of recipient mice (Figure 2.3B). Analysis of lineage composition of the peripheral blood graft revealed an increased proportion of B cells from *Dnmt3a*-mutant vs. control vehicle-treated HSCs, as we have previously observed[113] (Figure 2.3C). However, no significant differences were observed in peripheral blood lineage composition in recipient mice based on acute OSM stimulation. We also did not observe changes in donor-derived bone marrow HSPCs subsets due to acute OSM stimulation, including HSCs, $MPP^{G/M}$, common myeloid progenitors (CMP) and GMP (Figure 2.3D).

To evaluate the effect of OSM on cellular competition between *Dnmt3a*-mutant and control hematopoiesis, we utilized competitive transplantation. 25 prospectively isolated HSCs from young adult donor CD45.2+ control or *Dnmt3a*-mutant mice were mixed with 25 prospectively isolated HSCs from competitor CD45.2+ CD45.1+ (F1 hybrid) mice. These were cultured in the same conditions as above, supplemented with 500ng/ml recombinant murine OSM or vehicle control (Figure 2.3E). After 7-day culture, the resulting cells in each well were transplanted into lethally irradiated CD45.1+ recipient mice to assess hematopoietic engraftment and lineage potential. At 16wks post-transplant, no significant differences in donor engraftment (% CD45.2+) were observed in the peripheral blood or bone marrow of recipient mice (Figure 2.3F). Analysis of lineage composition of the peripheral blood graft revealed an increased proportion of B

cells from *Dnmt3a*-mutant vs. control vehicle-treated HSCs (Figure 2.3G), consistent with the findings above. However, no significant differences were observed in peripheral blood lineage composition in recipient mice based on acute OSM stimulation. In addition, no changes were observed in donor-derived bone marrow HSPCs subsets due to acute OSM stimulation, including HSCs, $MPP^{G/M}$, CMP and GMP (Figure 2.3H). Together, these data suggest that acute OSM stimulation does not lead to changes in engraftment or lineage potential of young *Dnmt3a*-mutant HSPCs in non-competitive or competitive transplant.

2.3.4 Young *Dnmt3a*-Mutant HSCs are Responsive to Acute OSM Stimulation via STAT3 Phosphorylation and Transcriptional Alterations

Based on a lack of phenotypic alterations associated with recombinant OSM stimulation of young control and young *Dnmt3a*-mutant HSCs *in vitro* and *in vivo*, we evaluated the extent to which these cells have the capacity to directly bind and respond to recombinant murine OSM. We first considered antibody-based assessment of levels of the OSM receptor subunit OSMR on the cell surface. Due to a lack of specific and commercially available anti-mouse OSMR antibodies[179], recombinant OSM was fluorescently labeled (OSM-AF488) and used to test binding and labelling of *Dnmt3a*-mutant and control HSCs, in comparison to negative (no OSM-AF488) and positive (liver cells with OSM-AF488) controls. OSM-AF488 was found to bind both control and R878H/+ HSCs (Figure 2.4A), supporting that control and *Dnmt3a*-mutant HSCs are capable of directly binding recombinant murine OSM.

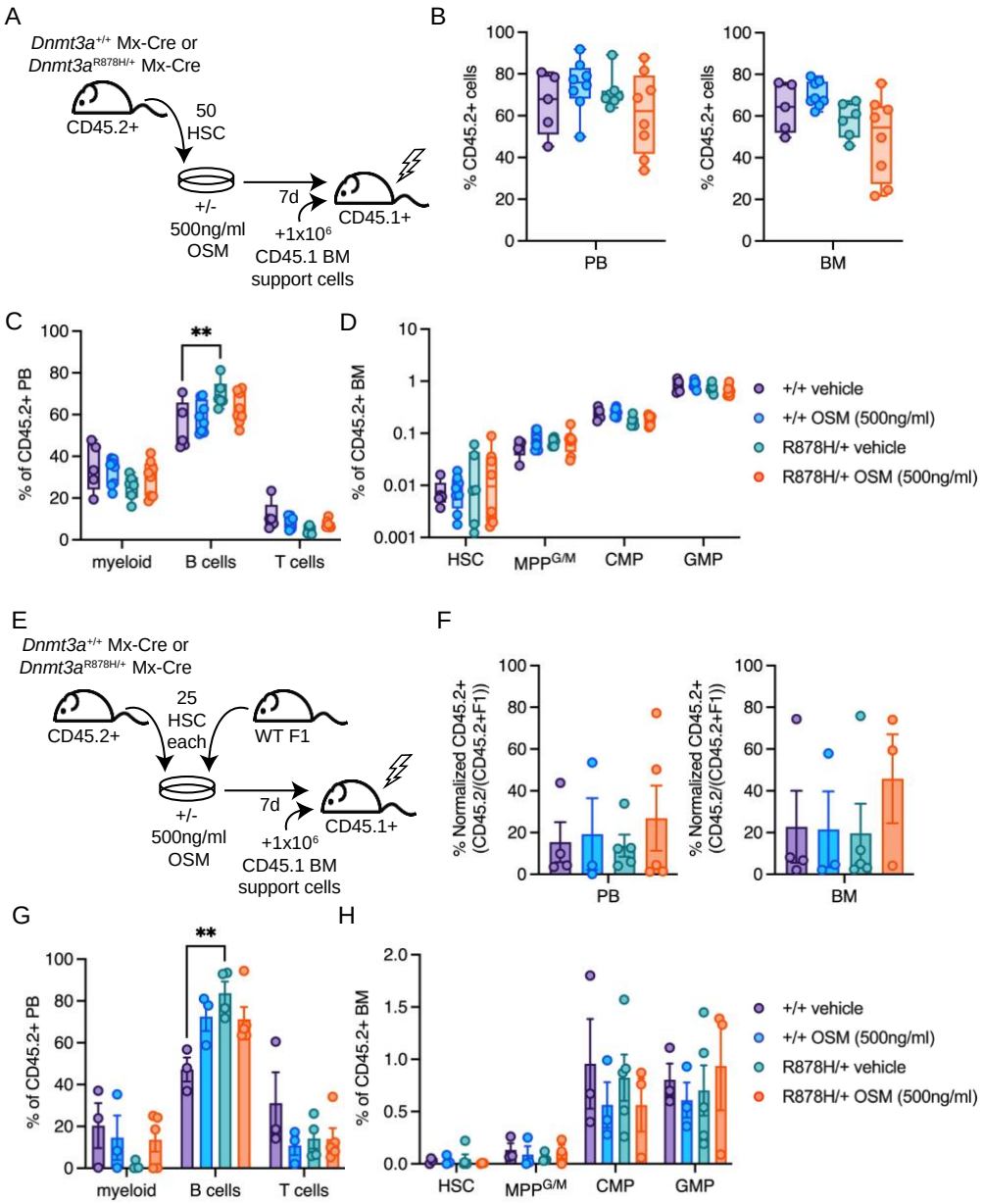

Figure 2.3: Engraftment potential and lineage output from young *Dnmt3a*-mutant HSPCs is unaltered by acute OSM stimulation.

(A) Schematic of transplant design. (B) Frequency of donor CD45.2$^+$ cells in the peripheral blood (PB) and bone marrow (BM) at 16wks post-transplant of control (+/+) and *Dnmt3a*-mutant (R878H/+) HSCs treated with 0 or 500ng/ml OSM for 7d. (C) Donor-derived PB lineage (myeloid, B and T cell) frequencies. (D) Donor-derived BM hematopoietic stem and progenitor cell frequencies. (E) Schematic of competitive transplant design. (F) Normalized frequency of donor CD45.2$^+$ cells in PB and BM at 16wks post-transplant of control (+/+) and *Dnmt3a*-mutant (R878H/+) HSCs treated with 0 or 500ng/ml OSM for 7d. (G) Donor-derived PB lineage (myeloid, B and T cell) frequencies. (H) Donor-derived BM hematopoietic stem and progenitor cell frequencies. In all figures, dots show individual mice and bars represent mean ± SEM of n = 3-8. **p < 0.01 by two-way ANOVA with Tukey's multiple comparisons test.

To test STAT3 activation by recombinant OSM, we prospectively isolated control and *Dnmt3a*-mutant HSPCs from young adult mice, stimulated *ex vivo* with 500ng/mL of recombinant murine OSM over a time course and evaluated phosphorylation of STAT3 and STAT5 by flow cytometry (Figure 2.5A). Acute OSM stimulation of *Dnmt3a*-mutant HSPCs resulted in greater pSTAT3 compared to vehicle-stimulated *Dnmt3a*-mutant HSPCs as well as compared to OSM-stimulated control HSPCs after 60min (Figure 2.5B). No differences were observed in pSTAT3 in any condition after 20min stimulation or 80min stimulation, indicating tight regulation of the OSM-STAT3 signaling response. No differences were observed in pSTAT5 in any condition at any of the tested time points (Figure 2.4B), demonstrating selectivity of acute OSM signaling response towards STAT3 activation in young *Dnmt3a*-mutant HSPCs.

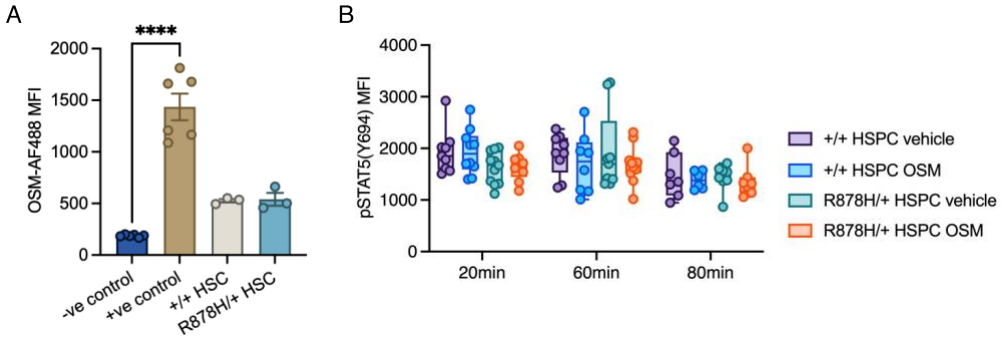

Figure 2.4: Binding of OSM to control and *Dnmt3a*-mutant HSPCs and induction of pSTAT5

(A) Mean fluorescence intensity (MFI) of fluorescently labeled OSM (OSM-AF488) in negative control (no OSM), positive control (liver), control (+/+) and *Dnmt3a*-mutant (R878H/+) HSCs. Dots show individual mice, bars represent mean ± SEM of n = 3-6. ****p < 0.0001 by one-way ANOVA with Dunnett's T3 multiple comparisons test. (B) MFI of pSTAT5 (Y694) in control (+/+) and *Dnmt3a*-mutant (R878H/+) HSPCs treated with 0 or 500ng/ml OSM for 20, 60 and 80min. Dots show individual mice and bars represent mean ± SEM of n = 6-10. **p < 0.01; ***p < 0.001 by mixed-effects analysis with Tukey's multiple comparisons test.

We tested the transcriptional consequences of OSM-STAT3 signaling in a more purified control and *Dnmt3a*-mutant HSC population. Control and *Dnmt3a*-mutant HSCs were prospectively isolated from young adult mice, stimulated *ex vivo* with 500ng/mL of recombinant murine OSM or vehicle control for 60min and immediately flash froze cell pellets for RNA extraction and RNA-seq. We identified significantly differentially expressed genes comparing OSM- vs. vehicle-treated control HSCs, and OSM- vs. vehicle-treated *Dnmt3a*-mutant HSCs, using $P < 0.05$ and fold change (FC) ± 1.5 cutoffs. This analysis revealed OSM-treated control HSCs had 385 genes increased in expression and 391 genes decreased in expression (Figure 2.5C). In contrast, OSM-treated *Dnmt3a*-mutant HSCs had 507 genes increased in expression and 299 genes decreased in expression (Figure 2.5D). Of the 385 OSM-activated genes in control HSCs and the 507 OSM-activated genes in *Dnmt3a*-mutant HSCs, only 19 were overlapping, suggesting a fundamentally distinct transcriptional response of young *Dnmt3a*-mutant HSCs to acute OSM. Delving further into specific gene alterations, we noted that acute OSM-stimulated *Dnmt3a*-mutant HSCs had robust upregulation of several key inflammatory molecules, receptors and response factors including *Il6, Il1b, Tnf, Il1r2, Csf3r, Ccr1* and *Irf1*. Apart from *Il1b,* these were not upregulated in OSM-stimulated control HSCs. These data suggests that a 60min stimulation of young *Dnmt3a*-mutant HSCs with recombinant OSM is sufficient to induce transcriptional upregulation of inflammatory cytokines associated with *Dnmt3a*-mutant clonal hematopoiesis.

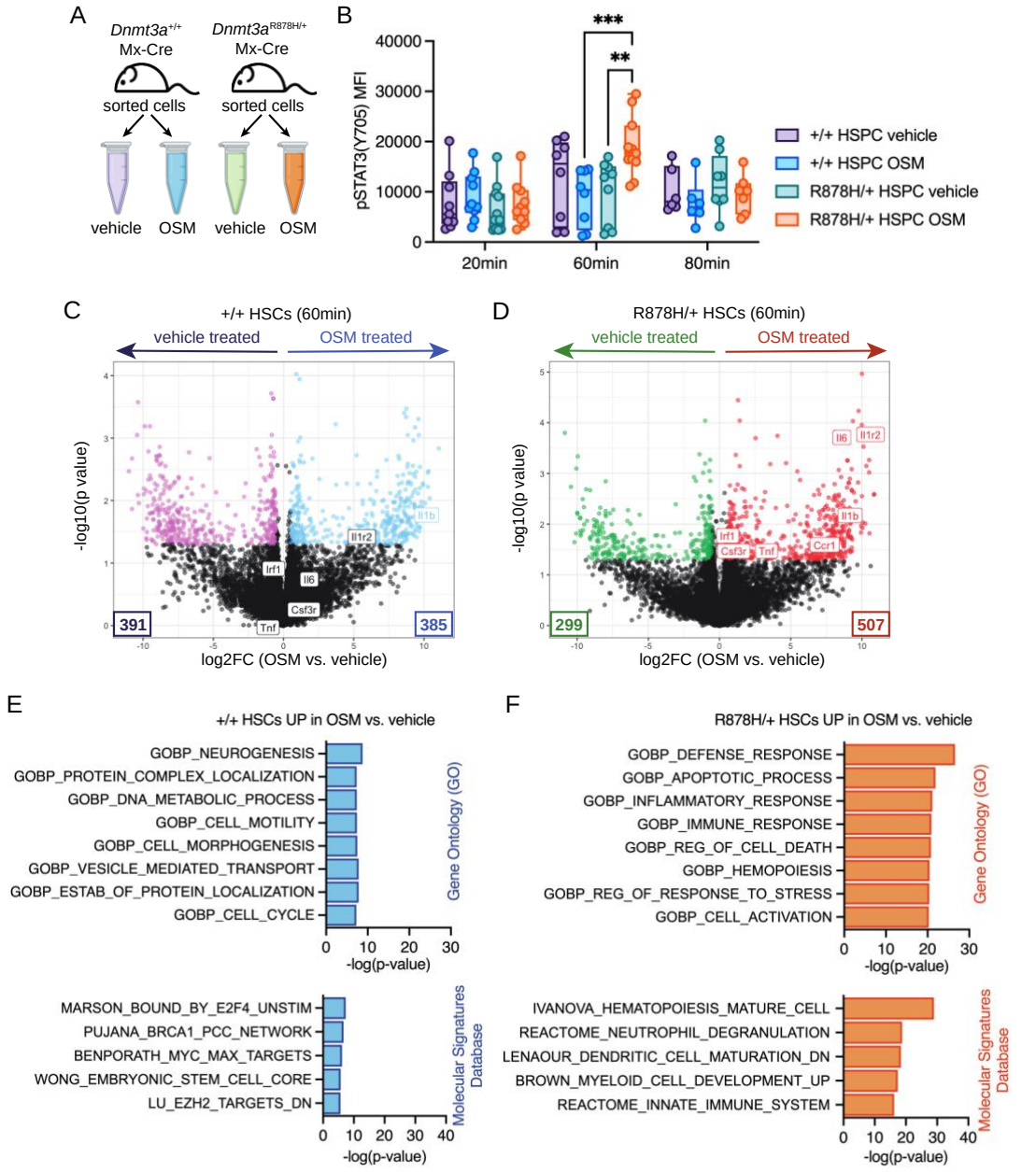

Figure 2.5: Acute OSM stimulation activates STAT3 phosphorylation and transcriptional responses in young *Dnmt3a*-mutant HSCs.
(A) Schematic of experimental design. (B) Mean fluorescence intensity (MFI) of pSTAT3 (Y705) in control (+/+) and *Dnmt3a*-mutant (R878H/+) HSPCs treated with 0 or 500ng/ml OSM for 20, 60 and 80min. Dots show individual mice and bars represent mean ± SEM of n = 6-10. **p < 0.01; ***p < 0.001 by mixed-effects analysis with Tukey's multiple comparisons test. (C, D) Volcano plot showing differential gene expression of (C) control (+/+) and (D) *Dnmt3a*-mutant (R878H/+) HSCs treated with 0 or 500ng/ml OSM for 60min. n = 6 biological replicates. Select genes involved in STAT3 signaling and inflammation are labelled. (E, F) Enrichment analysis of significantly differentially expressed genes in (E) control (+/+) and (F) *Dnmt3a*-mutant (R878H/+) HSCs treated with 500ng/ml vs. 0ng/ml OSM for 60min.

To further interrogate these transcriptional signatures, we performed enrichment analyses using Gene Ontology (GO) terms as well as using the molecular signatures database (MSigDB). Acute OSM-stimulated genes in *Dnmt3a*-mutant HSCs were enriched for focused signatures of inflammation, apoptosis, immune defense/stress responses, innate immunity, hematopoiesis, and myeloid cell development (Figure 2.5F). In contrast, OSM-stimulated genes in control HSCs were enriched for generic signatures of DNA metabolic processes, cell motility and morphogenesis, vesicle-mediated transport, and cell cycle-related processes (Myc/Max targets and E2F4 binding) (Figure 2.5E). Together, acute stimulation of *Dnmt3a*-mutant HSCs with recombinant OSM results in OSM binding, STAT3 phosphorylation, and transcriptional activation of an inflammatory gene network including the inflammatory cytokines IL-6, TNFa and IL-1b that are associated with *Dnmt3a*-mutant clonal hematopoiesis in mice and humans.

2.3.5 *Dnmt3a*-mutant HSCs Upregulate Anti-Inflammatory Genes in Response to Acute OSM Stimulation but not Chronic Stimulation in an Aged Environment Context

We sought to resolve the disconnect we observed between acute OSM-driven STAT3 signaling and transcriptional activation in *Dnmt3a*-mutant (R878H/+) HSCs and the lack of phenotypic changes in *Dnmt3a*-mutant HSCs and HSPCs. Previous studies have found elevated expression of suppressors of inflammation such as *Socs3, Nr4a1* and *Atf3* in CH-mutant HSPCs[162], and OSM has been reported to stimulate expression of *Socs3* in other cell types[161,180]. Thus, we hypothesized that acute OSM stimulation of young *Dnmt3a*-mutant HSCs results in enhanced expression of suppressors of inflammation.

Interrogating our OSM- vs. vehicle-treated *Dnmt3a*-mutant HSC RNA-seq data revealed that *Socs3, Nr4a1* and *Atf3* were increased in expression after acute OSM stimulation (Figure 2.6A).

To evaluate the dynamics of transcript induction, we focused on *Socs3*. Control and R878H/+ HSPCs were prospectively isolated from young adult mice and stimulated with 0 or 500ng/ml recombinant murine OSM for up to 80min. Cells were flash-frozen for RNA extraction, cDNA synthesis and quantitative real-time PCR for *Socs3*. OSM stimulation of control HSPCs resulted in a small, but significant, increase in *Socs3* after 60min (Figure 2.6B). In contrast, OSM stimulation of *Dnmt3a*-mutant HSPCs resulted in robust increase in *Socs3* at 20, 40 and 60min. This result demonstrates that *Dnmt3a*-mutant HSPCs rapidly respond to OSM stimulation by upregulating *Socs3*, at both greater levels and a faster rate compared to control HSPCs.

To evaluate stability of the *Socs3* mRNA transcript, we prospectively isolated control and *Dnmt3a*-mutant HSPCs from young adult mice and stimulated with 0 or 500ng/ml recombinant murine OSM for 60min, a timepoint we have consistently shown to result in STAT3 phosphorylation and transcriptional responses in *Dnmt3a*-mutant HSPCs. OSM stimulation was followed by incubating cells for 0, 20, 60 and 80 minutes with Actinomycin D, to pause transcription and allow the study of transcript stability over time[181]. Cells were flash-frozen for RNA extraction, cDNA synthesis and real-time PCR for *Socs3*. Consistent with the above results, *Socs3* was robustly increased in *Dnmt3a*-mutant HSPCs by 60min of OSM stimulation (Figure 2.6C). Furthermore, OSM-

stimulated *Dnmt3a*-mutant HSPCs maintained increased levels of *Socs3* for up to 80 minutes of Actinomycin D treatment. These results suggest that OSM-stimulated *Dnmt3a*-mutant HSPCs have a robust increase in *Socs3* transcript expression, and that this transcript is stably maintained for up to 140 minutes following exposure to OSM. We posit that *Socs3* activation may suppress STAT3 signaling, silencing transcriptional responses to OSM before functional outcomes are realized.

At the beginning of our study, we discovered a transcriptional program of inflammation response in *Dnmt3a*-mutant compared to control HSCs in middle-aged, but not young, transplant recipient mice (Figure 2.1B). Thus, we hypothesized that middle-aged mice have elevated 'chronic' levels of OSM and that *Dnmt3a*-mutant HSCs in a middle-aged microenvironment lose the capacity to upregulate suppressors of inflammation such as *Socs3, Nr4a1,* and *Atf3*. Bone marrow fluid was collected from young adult (3mo), middle-aged (14mo) and old (22mo) wild-type C57BL/6 mice and quantified OSM abundance using ELISA. A significant and progressive increase was observed in the quantity of OSM in the bone marrow fluid from young to middle-aged to old mice (Figure 2.6D). We examined our published RNA-seq data of control and *Dnmt3a*-mutant HSCs re-isolated from transplanted middle-aged wild-type recipient mice, focusing on the key inflammatory molecules identified in our acute OSM-stimulated *Dnmt3a*-mutant HSCs (Figure 2.5D) as well as *Socs3, Nr4a1* and *Atf3*. *Dnmt3a*-mutant HSCs compared to control HSCs in transplanted middle-aged recipient mice had robust upregulation of *Il1r2, Il1b*, *Ccr1, Tnf,* and *Csf3r* (Figure 2.6E). Unlike acute OSM-stimulated *Dnmt3a*-mutant HSCs, we did not observe increased expression of *Socs3, Nr4a1* or *Atf3.*

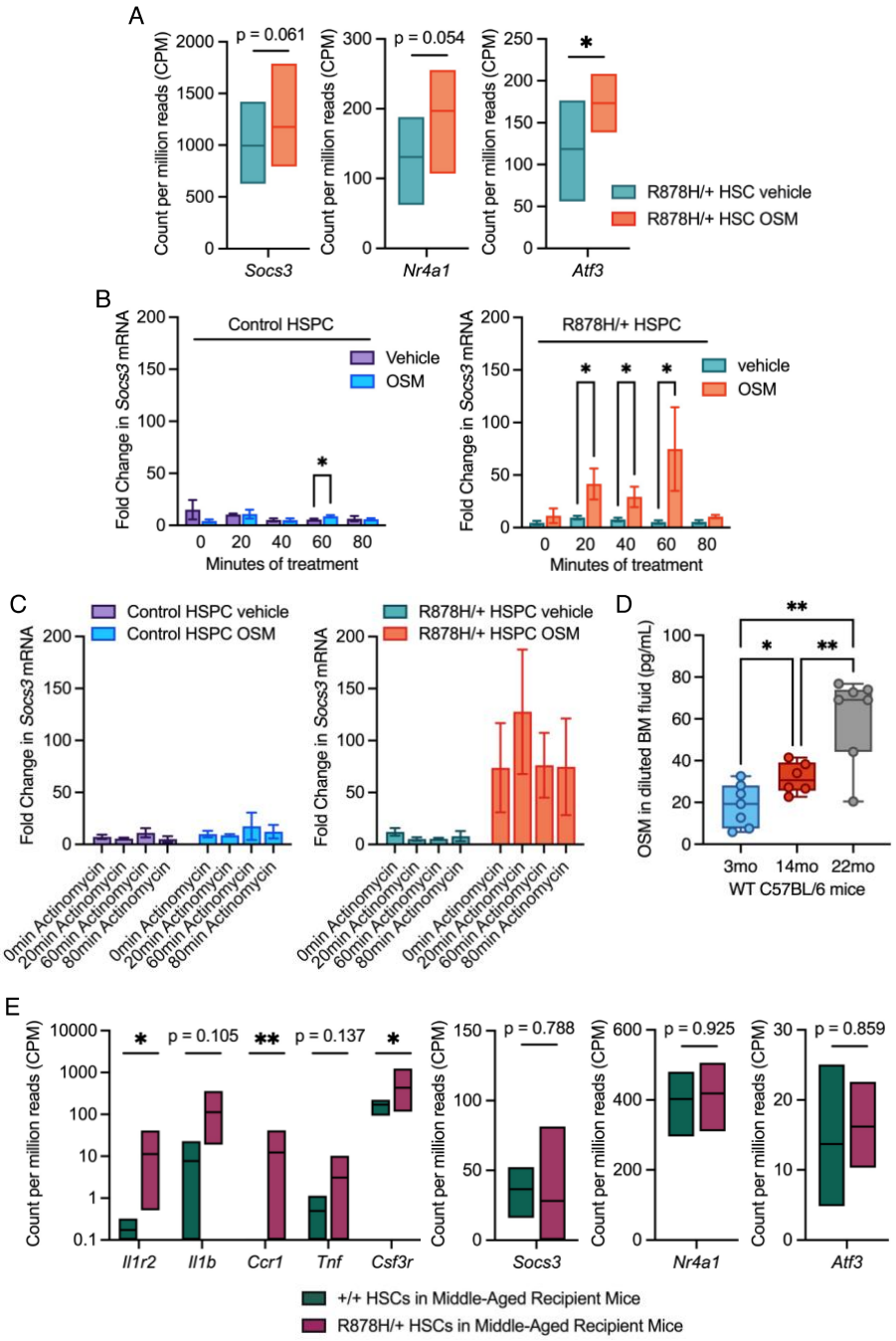

Figure 2.6: Engraftment potential and lineage output from young *Dnmt3a*-mutant HSPCs is unaltered by acute OSM stimulation.

(A) *Socs3*, *Nr4a1* and *Atf3* expression in control (+/+) and *Dnmt3a*-mutant (R878H/+) HSCs stimulated with 0 or 500ng/ml OSM for 60min. Box plots summarize n = 6 replicates per condition. *p < 0.05. (B) *Socs3* expression in control (+/+) and *Dnmt3a*-mutant (R878H/+) HSPCs stimulated with 0 or 500ng/ml OSM for described amount of time. Bars represent mean ± SEM of n = 3-4 replicates. *p < 0.05 by multiple-ratio, paired sample t test. (C) *Socs3* expression in control (+/+) and *Dnmt3a*-mutant (R878H/+) HSPCs stimulated with 0 or 500ng/ml of OSM for 60min followed by

actinomycin D for 0, 20, 60 and 80min. Bars represent mean ± SEM of n = 4 replicates. (D) OSM concentration in bone marrow fluid in young (3mo), middle-aged (14mo) and old (22mo) wild-type C57BL/6 mice. Dots show individual mice, bars represent mean ± SEM of n = 6-7. *p < 0.05; **p < 0.01 by Brown-Forsythe and Welch's ANOVA with multiple comparisons. (E) Expression of inflammatory genes *Il1r2*, *Il1b*, *Ccr1*, *Tnf*, and *Csf3r*, and the anti-inflammatory genes *Socs3*, *Nr4a1*, and *Atf3* in control (+/+) and *Dnmt3a*-mutant (R878H/+) HSCs after 4mos post-transplant in middle-aged recipient mice. Box plots summarize n = 3-4 replicates per condition. *p < 0.05; **p < 0.01 by multiple-ratio, paired sample t test.

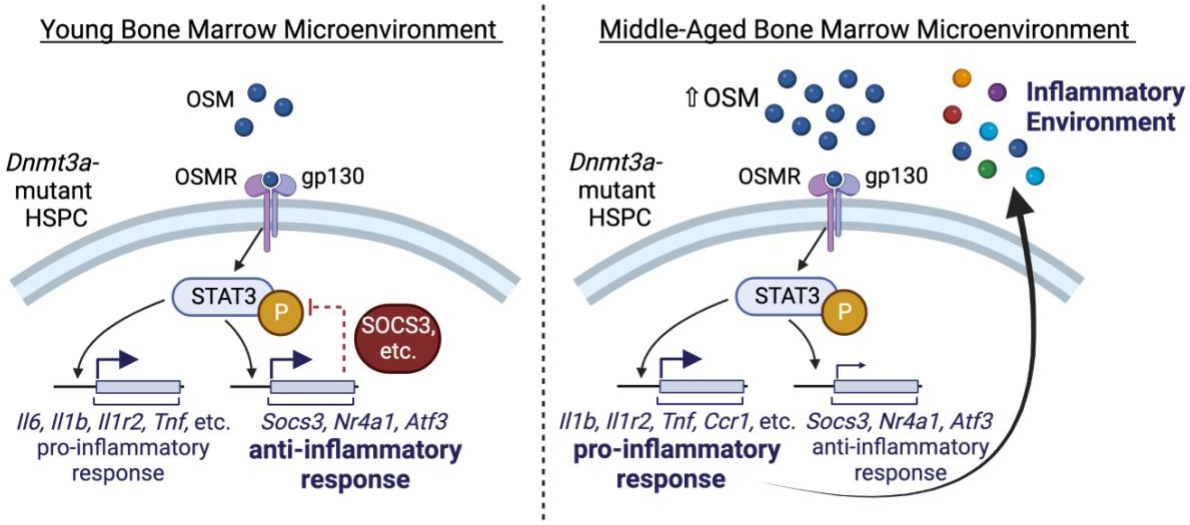

Figure 2.7: Working model of OSM signaling in *Dnmt3a*-mutant HSPCs in the context of the young and middle-aged BM environment
Created with BioRender.com licensed by The Jackson Laboratory.

2.4 Discussion

We have uncovered a role for Oncostatin M (OSM) as a master regulator of an inflammatory cytokine network active in *Dnmt3a*-mutant CH. Our initial discovery was based on transcriptional signatures indicating active OSM signaling in *Dnmt3a*-mutant HSCs specifically in the context of a middle-aged bone marrow microenvironment. In functional experiments, OSM stimulation of young *Dnmt3a*-mutant HSCs did not impact hematopoietic cell function or output *in vitro* or *in vivo*, however, it did result in STAT3 phosphorylation and a transcriptional inflammatory response including upregulation of *Il6, Il1b* and *Tnf*. Focused studies of transcript production and stability revealed a negative feedback mechanism in young *Dnmt3a*-mutant HSCs where OSM signaling results in increased transcription and transcript stability of anti-inflammatory genes including *Socs3, Nr4a1* and *Atf3* (Figure 2.7). In the context of a middle-aged bone marrow microenvironment, which has chronically increased levels of OSM, *Dnmt3a*-mutant HSCs upregulate an inflammatory response transcriptional signature which is not accompanied by upregulation of anti-inflammatory genes. Together, our work suggests that OSM is upstream of an inflammatory cytokine network in *Dnmt3a*-mutant HSCs. We speculate that chronic inflammation or exposure to ligands such as OSM with aging exhausts the regulatory mechanisms present in young *Dnmt3a*-mutant HSCs that resolve inflammatory states.

OSM is an IL-6 family cytokine known to be involved in the immunopathogenesis of colon cancer, breast cancer, pancreatic cancer, myeloma and hepatoblastoma[179]. Whereas IL-6 represents one of the most studied cytokines to date, the physiological activities of

OSM are less well known. OSM is predominantly produced by T lymphocytes, macrophages, and neutrophils[160], and in mice, signals through the heterodimeric receptor gp130/OSMR[182]. OSM is a strong inducer of JAK/STAT signaling leading to activation of STAT3 and STAT5[146,183]. OSM is an important regulator of the bone marrow microenvironment in both steady state and in regeneration after injury[184,185] with endothelial and mesenchymal cells being major cell types expressing OSMR[179], and plays a role in HSC mobilization via its effects on non-hematopoietic cells in the bone marrow microenvironment[179]. These data and models support a role for OSM as a cytokine produced by mature hematopoietic cells that impacts functionality of non-hematopoietic cells in the bone marrow microenvironment. Previous studies performed in young adult mice have shown that *Osmr* is not detected in HSPCs or myeloid cells[179] and thus it has been suggested that HSCs and their progeny do not directly respond to OSM. However, *Osmr* is one of the most upregulated transcripts in old HSCs compared to young HSCs across six independent datasets[151] suggesting that in certain contexts, such as aging, HSCs and their progeny gain the capacity to respond to OSM. Our data show that HSCs, in the context of a CH-relevant mutation in *Dnmt3a*, do have the capacity to phosphorylate STAT3 and undergo transcriptional alterations in response to OSM.

The consequences of OSM signaling are also context dependent, resulting in pro-inflammatory as well as anti-inflammatory/anti-proliferative outcomes[146]. This is consistent with our data in young *Dnmt3a*-mutant HSCs where both pro-inflammatory cytokines as well as anti-inflammatory molecules are expressed in response to OSM. This anti-inflammatory negative feedback loop may be a conserved mechanism facilitating the

selective advantage of mutant HSCs in CH. Recent work using a zebrafish model of human *ASXL1*-mutant CH found a protective response to pro-inflammatory cytokines in HSPCs via upregulation of *socs3a*, *atf3* and *nr4a1*[162]. Without the capacity to upregulate *nr4a1* and *nr4a3*, the *Asxl1*-mutant HSPCs lost their self-renewal capacity and selective growth advantage. In addition to induction of these anti-inflammatory transcripts that work in part through silencing STAT3 activation, complementary mechanisms may allow mutant HSCs to survive in a chronic inflammatory environment associated with aging. For example, in *Tet2*-mutant CH, HSPCs with hyperactivated SHP2-STAT3 signaling downregulate the apoptotic protein Bim via the anti-apoptotic long non-coding RNA *Morrbid*[161]. In the context of a middle-aged BM microenvironment, which has chronically elevated levels of OSM, *Dnmt3a*-mutant HSCs no longer upregulate key anti-inflammatory genes. We speculate that chronic inflammation prompts epigenetic rewiring or selection of *Dnmt3a*-mutant HSCs such that they lose the ability to silence these signals, which merits further experimentation and exploration.

Identification of OSM as a master regulator of inflammatory cytokine production opens the possibly of therapeutic interventions targeting OSM to reduce inflammation in aging-associated *Dnmt3a*-mutant CH. To provide evidence for blocking OSM:OSMRβ signaling in a mouse model of sepsis was found to reduce serum levels of IL-6 and TNFa and prolong mouse survival[186] and human monoclonal OSMRβ-targeting antibodies such as Vixarelimab are utilized clinically to manage such conditions as prurigo nodularis, a debilitating chronic skin disease[187]. Alternatively, identifying a transcriptional feedback loop that silences pro-inflammatory responses in *Dnmt3a*-mutant HSCs, but is

dysfunctional in the context of aging, also represents a targetable mechanism for therapeutic intervention. Re-engagement of this negative feedback loop by transient activation of *Socs3* or other anti-inflammatory factors may help to suppress inflammatory myeloid cell production that is a major contributor to CH-associated diseases including cardiovascular disease and myeloid malignancy.

2.5 Declarations

J.J.T. has received research support from H3 Biomedicine, Inc., and patent royalties from Fate Therapeutics. All other authors declare no competing interests.

2.5.1 Author Contributions

L.S.S. and J.J.T. conceptualized the project and designed experiments. L.S.S. performed experiments and analyzed data, with assistance from K.A.Y., N.B. and K.D.M. RNA-seq data was analyzed and graphed by L.S.S. and T.M.S. The manuscript was written by L.S.S. and J.J.T. All authors edited the manuscript.

2.5.2 Acknowledgements

This work was supported by National Institutes of Health grants R01DK118072, R01AG069010, U01AG077925, and an EvansMDS Discovery Research Grant to J.J.T. This work was supported in part by the NIH/NCI Cancer Center Support Grant P30CA034196. J.J.T. was supported by a Leukemia & Lymphoma Society Scholar Award and The Dattels Family Endowed Chair. L.S.S. was supported by F31DK127573 and The Tufts University Scheer-Tomasso Fund philanthropic gift. We thank all members of the Trowbridge Lab for experimental support and manuscript editing. We

thank the Scientific Services at The Jackson Laboratory including flow cytometry and genome technologies. We thank Drs. Carol Bult, Ryan Tewhey, Cliff Rosen, and Phil Hinds for their critical input into this work.

2.6 Supplementary Tables

The following table(s) have been uploaded onto ProQuest.

Table 2.1: Differential Gene Expression Analysis of OSM-Stimulated vs. Vehicle-Treated *Dnmt3a*-mutant HSCs from RNA-Seq Data

Table 2.2: Differential Gene Expression Analysis of OSM-Stimulated vs. Vehicle-Treated Control *Mx1*-Cre HSCs from RNA-Seq Data

Table 2.3: Differential Gene Expression Analysis of Vehicle-Treated *Dnmt3a*-mutant HSCs vs. Control *Mx1*-Cre HSCs from RNA-Seq Data

Table 2.4: Differential Gene Expression Analysis of OSM-Stimulated *Dnmt3a*-mutant HSCs vs. Control *Mx1*-Cre HSC

Chapter 3: Characterization of an *Osmr* Conditional Knockout Mouse Model

Schwartz L.S., Saxl L. R., Stearns, T., Trowbridge, J.J. Submitted to Nature Lab Animal 10/03/23

3.1 Introduction

OSM, belonging to the IL-6 family, plays an important role in development, malignancy, and homeostasis of various human and mouse tissue types[124,127,146,176,188]. OSM is primarily produced by mature activated hematopoietic cells such as monocytes, T lymphocytes, neutrophils, macrophages, and dendritic cells[125,127,189]. OSM was first isolated based on its ability to inhibit the proliferation of melanoma tumor cells, while having no significant effect on normal human fibroblasts[125]. Due to this unique characteristic, it was given the name oncostatin M, where "onco" referred to cancer, "statin" to its ability to inhibit cell proliferation, and “M” to melanoma. Despite the initial identification of OSM as a tumor suppressor, a pro-inflammatory role of OSM has been reported in colon cancer, breast cancer, pancreatic cancer, myeloma, brain tumors, chronic lymphocytic leukemia, hepatoblastoma and COVID-19[146,176,190]. OSM, like IL-6, has been linked to tumor growth and is often found in high concentrations in the serum and tumor sites of patients and animal models of cancer[146,176,190]. Significantly increased *Osm* transcript production has also been associated with aging in both the human thymus and mouse hematopoietic stem cells (HSCs) compared to young tissues[150,151]. Human OSM interacts with two distinct receptor complexes termed type I and type II. The type I receptor complex contains leukemia inhibitory factor receptor alpha (LIFR) and interleukin 6 signal transducer (IL6ST; gp130), while the type II receptor complex contains oncostatin M receptor (OSMRβ) and IL6ST[127,132,191,192]. While recent studies have shown that OSM has a lower affinity for the type I receptor complex than the type II receptor complex[141,142], much remains unknown about how OSM interacts with these complexes in different contexts. An additional complexity in studying OSM signaling is

that while human OSM is known to signal through both the type I and type II receptor complexes, mouse OSM is reported to signal only through the type II receptor complex[143,144,193].

To understand the role of OSM signaling in aging and disease in a physiologically relevant *in vivo* setting, mouse knockout models are essential. Two existing mouse models are commonly used to investigate loss of receptor complex II signaling through knockout of *Osmr*. The first, *Osmr*^{tm1Mtan}, was reported by Tanaka et al. in 2003[194]. This model disrupts the first coding exon of *Osmr* by knock-in of a lacZ and neomycin expression cassette into the proximal region and is non-conditional in nature[194]. These *Osmr*$^{-/-}$ mice were viable and fertile, born at expected Mendelian ratios, and had normal adult body weights[194]. Knockout of *Osmr* was confirmed by loss of mRNA in lung tissue[194]. This model exhibited hematopoiesis phenotypes showing reduced numbers of erythroid and megakaryocytic progenitors and their mature counterparts[194]. However, these were attributed to both cell-autonomous and cell non-autonomous effects of *Osmr*$^{-/-}$ on hematopoietic progenitor cells and non-hematopoietic cells in the bone marrow microenvironment[194], which are best resolved by the use of a conditional knockout model. The second existing model, B6;129-*Osmr*$^{tm1.1Nat}$/J, is a conditional knockout model in which loxP sites flank the first coding exon of the *Osmr* gene. Additionally, adjacent to the second loxP site is an Frt site remaining after excision of a PGK-neomycin selectable marker. This model was originally designed to study *Osmr* in the retina and is available in The Jackson Laboratory's mouse repository; however, characterization of the model has not been published by the donating investigators. To

investigate cell-autonomous effects of *Osmr* conditional knockout on hematopoiesis, we obtained the B6;129-*Osmr*$^{tm1.1Nat}$/J (referred to as *Osmr*$^{fl/fl}$) model and crossed these mice to an interferon-inducible *Mx1*-Cre allele[104], which is commonly used in the study of adult hematopoiesis. We characterized *Osmr*$^{fl/fl}$ *Mx1*-Cre mice using classical methods such as the development of a PCR reaction to evaluate recombination of the *Osmr*^{fl} allele, real-time PCR and RNA sequencing for *Osmr* mRNA transcript, and Western blotting to evaluate OSMRβ at the protein level. We investigated both hematopoietic tissue (bone marrow) as well as non-hematopoietic tissues (liver, lung, kidney) in which OSMRβ is also expressed. Our results demonstrate variable alterations in mRNA and protein expression in various tissues isolated from *Osmr*$^{fl/fl}$ *Mx1*-Cre compared to control *Mx1*-Cre mice.

3.2 Results

3.2.1 DNA Recombination in Bone Marrow Cells, Lung, Liver, and Kidney Cells of *Osmr*$^{fl/fl}$ *Mx1*-Cre Mice

To generate an inducible *Osmr* knockout model, the B6;129-*Osmr*$^{tm1.1Nat}$/J strain was crossed to *Mx1*-Cre[104]. *Mx1*-Cre is an interferon-inducible cre recombinase that is highly efficient in expression in progenitor and mature cells of the adult hematopoietic lineages. Thus, in the *Osmr*$^{fl/fl}$ *Mx1*-Cre model, the *Osmr*^{fl} allele should remain unrecombined with wild-type expression at the transcript and protein levels prior to administration of the double-stranded RNA poly(I:C), which then induces an interferon response and expression of cre recombinase. After crossing B6;129-*Osmr*$^{tm1.1Nat}$/J to *Mx1*-Cre to generate *Osmr*$^{fl/fl}$ *Mx1*-Cre and control *Mx1*-Cre animals, we genotyped three control and three experimental animals alongside positive (parental *Osmr*$^{fl/fl}$ and *Mx1*-Cre mice) and

negative (wild-type C57BL/6J) controls. At the *Osmr* locus, genomic DNA from *Osmr*$^{fl/fl}$ *Mx1*-Cre mice contained a loxP site (230bp) and genomic DNA from control *Mx1*-Cre mice did not contain a loxP site (170bp), recognized by primers flanking exon 2 (Figure 3.1A). Genomic DNA from all *Osmr*$^{fl/fl}$ *Mx1*-Cre and control *Mx1*-Cre mice were also positive for the transgenic cre allele (100bp) (Figure 3.1B).

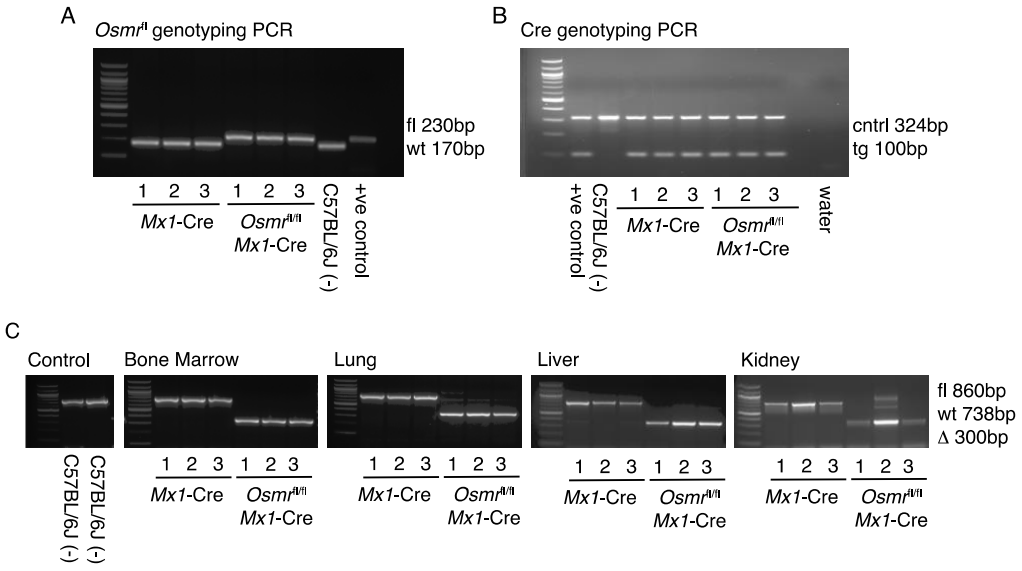

Figure 3.1: Recombination of the *Osmr*^{fl} Locus in Tissues from *Osmr*$^{fl/fl}$ *Mx1*-Cre Mice

Agarose gel electrophoresis (2% agarose) of PCR-amplified products. In all gels a 100bp ladder was used for size estimation located in lane 0. (A) Genotyping PCR for *Osmr*<tm1.1Nat>. Lanes 1-3 use genomic DNA samples from *Mx1*-Cre control mice, lanes 4-6 use genomic DNA samples from *Osmr*$^{fl/fl}$ *Mx1*-Cre mice, lane 7 uses genomic DNA from a wild-type C57BL/6J mouse and lane 8 uses a positive control *Osmr*$^{fl/fl}$ from a mouse confirmed by The Jackson Laboratory's in-house genotyping service. (B) Genotyping PCR for *Mx1*-Cre. Lane 1 shows a positive control, lane 2 shows wild-type C57BL/6J, lanes 3-5 show *Mx1*-Cre control mice and lanes 6-8 show *Osmr*$^{fl/fl}$ *Mx1*-Cre mice. (C) Recombination PCR assay results in control, bone marrow, lung, liver, and kidney tissues. From left: Lanes 1-2 show wild-type C57BL/6J control mice. In the remaining images, samples are ordered as lanes 1-3 being *Mx1*-Cre control samples and lanes 4-6 being *Osmr*$^{fl/fl}$ *Mx1*-Cre samples.

Following injection with poly(I:C) to induce *Mx1*-Cre-mediated recombination of the *Osmr*^{fl} locus, we isolated DNA from bone marrow, lung, liver, and kidney tissues. These tissues were selected based on expression of both *Osmr* and *Mx1* transcripts using publicly available databases including the human protein atlas[195-197], Mouse Genome Informatics[198] and The Bgee suite[198]. A recombination PCR assay was designed to assess *Osmr*^{fl} recombination efficiency. The primers generate a product spanning the loxP-flanked exon 2 and bind to both the wild-type and modified *Osmr* loci generating product sizes of ~860bp for the floxed (fl) allele, 738bp for the wild-type (wt) allele and ~300bp for the recombined (D) allele. This PCR assay detected a ~300bp recombined allele in all tissue samples from *Osmr*$^{fl/fl}$ *Mx1*-Cre mice (
Figure 3.1C), demonstrating that recombination of the *Osmr*^{fl} locus occurred efficiently following poly(I:C) injection in the bone marrow, lung, liver, and kidney.

3.2.2 Tissue-Dependent Reduction in *Osmr* Transcript and Protein Expression *Osmr*$^{fl/fl}$ *Mx1*-Cre Mice

We next evaluated levels of *Osmr* transcript in cells from the lung, liver, kidney, and bone marrow of *Osmr*$^{fl/fl}$ *Mx1*-Cre and control *Mx1*-Cre animals. Following harvest, cells were flash-frozen and used for RNA extraction, cDNA synthesis and semi-quantitative real-time PCR. TaqMan probes annealing to a target amplicon spanning *Osmr* exons 17 and 18, downstream of exon 2 deletion, were used. In control *Mx1*-Cre mice, *Osmr* transcript was detected at a low level in lung cells and robustly detected in liver, kidney, and bone marrow (Figure 3.2A). In *Osmr*$^{fl/fl}$ *Mx1*-Cre mice, *Osmr* transcript in lung and liver was detected at similar levels as in control *Mx1*-Cre mice. In the kidney, *Osmr*

transcript was significantly reduced in *Osmr*$^{fl/fl}$ *Mx1*-Cre mice compared to control *Mx1*-Cre. In the bone marrow, *Osmr* transcript trended toward a decrease in *Osmr*$^{fl/fl}$ *Mx1*-Cre mice compared to control *Mx1*-Cre.

Given this tissue-dependent variation in *Osmr* transcript levels, we performed western blotting with a published OSMR antibody[141,144,179,199] to quantify protein expression in the lung, liver, kidney, and bone marrow isolated from *Osmr*$^{fl/fl}$ *Mx1*-Cre and control *Mx1*-Cre mice. OSMR protein expression showed modest reduction in the lung of *Osmr*$^{fl/fl}$ *Mx1*-Cre mice compared to control *Mx1*-Cre mice (Figure 3.2B and C). OSMR expression in the liver was undetectable in *Osmr*$^{fl/fl}$ *Mx1*-Cre mice, and OSMR expression in the kidney and bone marrow were reduced to very low levels in *Osmr*$^{fl/fl}$ *Mx1*-Cre mice. Together, these data suggest that *Osmr*$^{fl/fl}$ *Mx1*-Cre mice have reduced OSMR in cell lysates prepared from lung, liver, kidney, and bone marrow and that the level of reduction in OSMR protein is tissue dependent.

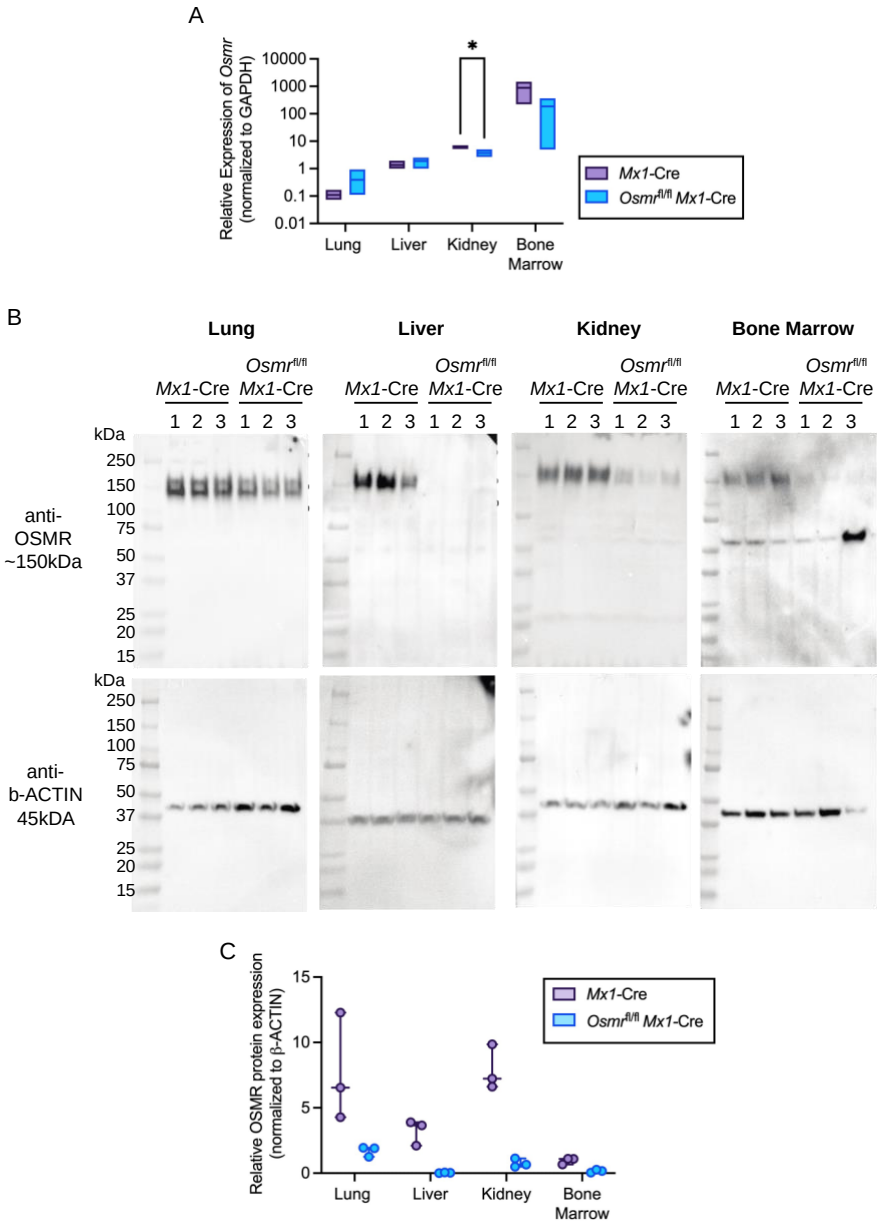

Figure 3.2: *Osmr*$^{fl/fl}$ *Mx1*-Cre Mice Have Variable and Tissue-Dependent *Osmr* Expression at the Transcript and Protein Levels

(A) Relative *Osmr* expression assessed by real-time PCR in lung, liver, kidney, and bone marrow from *Mx1*-Cre control and *Osmr*$^{fl/fl}$ *Mx1*-Cre mice (n = 3-4). Bars show low to high values with a line at the mean. *$p < 0.05$ by paired t test. (B) Western blots of cell lysates from lung, liver, kidney, and bone marrow probed with antibodies against OSMR and β-actin. (C) Relative protein expression assessed by Western blot imaging using ImageJ. OSMR band densities were normalized to β-actin (n = 3). Dots show individual bands/mice.

3.2.3 Exploring Transcriptional Alterations in *Osmr*$^{fl/fl}$ *Mx1*-Cre Hematopoietic Stem Cells (HSCs)

Given the reduction in OSMR protein detected in bone marrow lysates of *Osmr*$^{fl/fl}$ *Mx1*-Cre mice, we utilized this model to investigate *Osmr* signaling in hematopoietic stem cells (HSCs) which are a small subset of bone marrow hematopoietic cells. HSCs were prospectively isolated from the bone marrow of mice using fluorescence-activated cell sorting. HSCs from *Osmr*$^{fl/fl}$ *Mx1*-Cre and control *Mx1*-Cre mice were placed into serum-free media with or without 500ng/mL of recombinant murine OSM or vehicle control for 60min, then flash frozen for RNA sequencing (RNA-seq). Significantly differentially expressed genes were defined based on stringent cutoffs ($p < 0.01$ and log2(FC) > 3 or < -3) (Figure 3.3A**,** Table 3.1: Differential Gene Expression Analysis of $^{Osmrfl/}$fl Mx1-Cre vs. Control Mx1-Cre HSCs from RNA-Seq Data). Consistent with our real-time PCR analysis of bone marrow cells, no difference in *Osmr* transcript abundance was observed in *Osmr*$^{fl/fl}$ *Mx1*-Cre HSCs compared to control *Mx1*-Cre HSCs (Figure 3.3B). We removed predicted genes and pseudogenes from this list, resulting in a total of 91 significantly differentially expressed genes between *Osmr*$^{fl/fl}$ *Mx1*-Cre and control *Mx1*-Cre HSCs. Of these, 59 genes were increased in expression and 32 were decreased in expression in *Osmr*$^{fl/fl}$ *Mx1*-Cre HSCs. The top differentially expressed genes based on fold change included increased expression of *Gbp2b, Myh3, Cplx3, Gpr31c* and decreased expression of *Wdpcp*, *Lgalsl*, *Tesk2*, *Tigar*. Functional annotation of differentially expressed genes in *Osmr*$^{fl/fl}$ *Mx1*-Cre compared to control *Mx1*-Cre HSCs identified enrichment of signatures related to proliferation, actin binding, RNA Pol II activity and protein binding, and depletion of signatures related to smoothened pathway

signaling, intraciliary transport, and protein phosphorylation (Figure 3.3C). These data suggest that modest transcriptional differences are observed in HSCs isolated from *Osmr*$^{fl/fl}$ *Mx1*-Cre compared to *Mx1*-Cre mice, despite lack of detectable differences in *Osmr* transcript itself.

Next, we utilized our RNA-seq dataset to explore how control *Mx1*-Cre versus *Osmr*$^{fl/fl}$ *Mx1*-Cre HSCs respond to stimulation with recombinant OSM. Using the same stringent cutoffs defined above to identify significantly upregulated genes, control *Mx1*-Cre HSCs had 37 genes increased in expression following OSM stimulation compared to vehicle treatment (Figure 3.3D**,** Table 3.2: Differential Gene Expression Analysis of OSM-Stimulated vs. Vehicle-Treated *Control* Mx1-Cre HSCs from RNA-Seq Data). Examining these 37 genes in *Osmr*$^{fl/fl}$ *Mx1*-Cre HSCs stimulated with OSM (Table 3.3: Differential Gene Expression Analysis of OSM-Stimulated vs. Vehicle-Treated Osmrfl/*fl* Mx1-Cre HSCs from RNA-Seq Data.) revealed several patterns; (I) 17 genes were no longer induced by OSM in *Osmr*$^{fl/fl}$ *Mx1*-Cre HSCs, (II) 6 genes were induced by OSM in both control *Mx1*-Cre and *Osmr*$^{fl/fl}$ *Mx1*-Cre HSCs, and (III) 10 genes were induced by OSM in control *Mx1*-Cre HSCs but repressed by OSM in *Osmr*$^{fl/fl}$ *Mx1*-Cre HSCs. The 17 genes that were induced by OSM in control *Mx1*-Cre HSCs but not induced in *Osmr*$^{fl/fl}$ *Mx1*-Cre HSCs were enriched for signatures of extracellular matrix disassembly, G1/S transition, endonuclease, and hydrolase activity (Figure 3.3E). In contrast, the 10 genes that were induced by OSM in control *Mx1*-Cre HSCs but repressed by OSM in *Osmr*$^{fl/fl}$ *Mx1*-Cre HSCs were enriched for signatures of epithelial to mesenchymal transition, endothelial cell proliferation and ion channel binding (Figure 3.3F). These data suggest

that a subset of genes transcriptionally upregulated in response to OSM signaling in control *Mx1*-Cre HSCs are no longer upregulated in response to OSM in *Osmr*$^{fl/fl}$ *Mx1*-Cre HSCs, consistent with genetic knockout and functional loss of OSMR. However, as a subset of OSM signaling target genes are increased in expression in *Osmr*$^{fl/fl}$ *Mx1*-Cre HSCs, and other genes are no longer induced by OSM signaling, these results suggest that there is an incomplete loss of OSMRβ and/or that these genes are not *bona fide* targets of OSM-OSMRβ signaling.

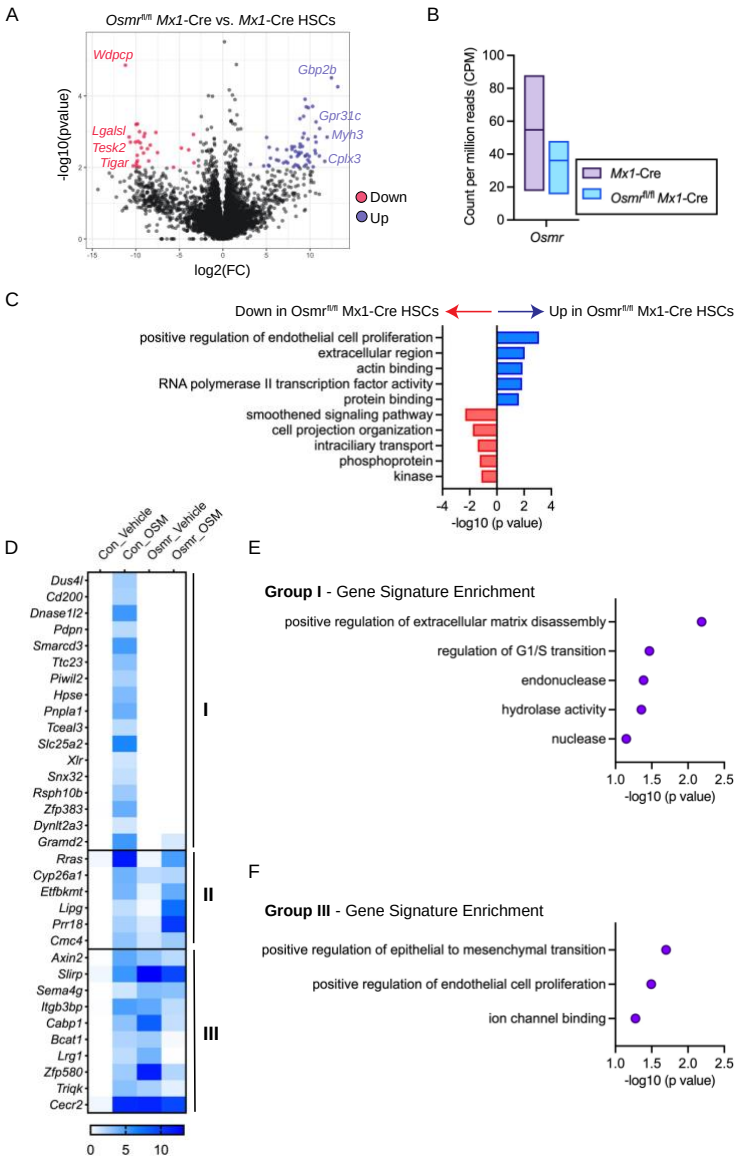

Figure 3.3: Differential Expression Analysis in *Osmr*$^{fl/fl}$ *Mx1*-Cre HSCs
(A) Volcano plot showing differential gene expression of analysis of *Osmr*$^{fl/fl}$ *Mx1*-Cre vs. control *Mx1*-Cre HSCs (n = 3-6 biological replicates). Select significantly differentially expressed genes ($p < 0.01$, log2(FC) > 3 or < -3) are shown in red (down) or blue (up) font. (B) Count per million reads of *Osmr* transcript in control *Mx1*-Cre and *Osmr*$^{fl/fl}$ *Mx1*-Cre HSCs. Bars show low to high values with a line at the mean. (C) Gene signature enrichment within differentially expressed genes between *Osmr*$^{fl/fl}$ *Mx1*-Cre and control *Mx1*-Cre HSCs. (D) Heatmap of 37 genes induced by 60min OSM stimulation in control *Mx1*-Cre HSCs. Three patterns were observed: Group (I) genes were no longer induced by OSM in *Osmr*$^{fl/fl}$ *Mx1*-Cre HSCs, group (II) genes induced by OSM in both control *Mx1*-Cre and *Osmr*$^{fl/fl}$ *Mx1*-Cre HSCs, and group (III) genes induced by OSM in control *Mx1*-Cre HSCs but repressed by OSM in *Osmr*$^{fl/fl}$ *Mx1*-Cre HSCs. (E) Gene signature enrichment within group (I) genes. (F) Gene signature enrichment within group (III) genes.

3.3 Discussion

Our data show that *Osmr*$^{fl/fl}$ *Mx1*-Cre mice have near-complete recombination of the genomic *Osmr*^{fl} locus in bone marrow, lung, liver, and kidney tissue. However, the extent of reduction in *Osmr* transcript and OSMRβ protein expression in *Osmr*$^{fl/fl}$ *Mx1*-Cre tissues compared to *Mx1*-Cre tissues was dependent upon the tissue type examined. These findings are consistent with a previous study of the B6;129-*Osmr*$^{tm1.1Nat}$/J model showing reduced OSMRβ, as opposed to a complete knockout, in K5+ epidermis[141,144,179,199]. Additionally, despite the lack of observable differences in *Osmr* transcript expression in HSCs isolated from *Osmr*$^{fl/fl}$ *Mx1*-Cre compared to *Mx1*-Cre mice, we observed alterations in the levels of other transcripts. Focusing on genes induced by OSM signaling in control *Mx1*-Cre HSCs, we found that only some of these genes are no longer induced by OSM signaling in *Osmr*$^{fl/fl}$ *Mx1*-Cre HSCs. We interpret this data to mean that residual OSMRβ expression in *Osmr*$^{fl/fl}$ *Mx1*-Cre HSCs permits some OSM signaling to occur. In addition, HSCs with reduction or loss of OSMRβ appear to incur compensatory activation of OSM-stimulated genes indicating a more complex, tissue-dependent regulation of OSM- OSMRβ signaling than was previously understood.

Future studies will be necessary to understand the mechanisms underlying tissue-dependent differences in *Osmr* transcript abundance and OSMRβ protein abundance in the B6;129-*Osmr*$^{tm1.1Nat}$/J model. It is possible that tissue-dependent differences in transcript isoforms and/or splicing underly differences in abundance of transcript and protein. For example, transcripts lacking exon 2 may be sufficient to produce OSMRβ

protein in the lung but not the liver or bone marrow. The appearance of two high molecular weight bands in the OSMRβ western blot in the lung but not in other tissues is consistent with multiple protein products being present in this tissue. In the bone marrow, a lower molecular weight band was visible in the OSMRβ western blot, which may indicate a shorter OSMRβ isoform that is still produced in *Osmr*$^{fl/fl}$ *Mx1*-Cre cells.

Utilizing mouse models to understand the role of OSM signaling in human pathophysiology is essential but is an inherent challenge due to the previously characterized differences in receptor binding between mice and humans. Other studies have reported novel and innovative tools to aid in overcoming this challenge. For example, with the knowledge that specific charged residues in the AB loop of OSM are crucial for selection of binding to receptor complex I versus complex II, "humanized" murine OSM variants have been generated to gain more accurate insights into the role of human OSM in mouse models[144]. In addition, a potent and specific inhibitor of OSM signaling has been engineered using a receptor fusion protein that contains the ligand binding domains of murine OSMRβ and murine gp130[200]. This construct can be delivered into cells using viral vectors and has been used in multiple studies investigating the hematopoietic stem cell niche in the bone marrow and the role of OSM in irritable bowel disease[179,201]. Using this construct to generate transgenic animals would be very useful for future *in vivo* studies. Moving forward, we advise that other tools be utilized in parallel to the B6;129-*Osmr*$^{tm1.1Nat}$/J model and/or that studies include a detailed characterization of *Osmr* transcript and protein levels in the tissue and cell type of focus.

3.4 Methods

3.4.1 Animals

C57BL/6J (JAX:000664) mice were obtained from The Jackson Laboratory. B6;129-*Osmr*$^{tm1.1Nat}$/J (JAX: 011081) were crossed to B6.Cg-Tg(*Mx1*-cre)1Cgn/J mice (JAX:003556). In all experiments, experimental and control mice carried a single copy of the *Mx1*-Cre transgenic allele. To induce *Mx1*-Cre, mice were intraperitoneally injected once every other day for five total injections with 15 mg/kg high molecular weight polyinosinic-polycytidylic acid (polyI:C) (InvivoGen). Mice used for experiments were at least 10-weeks following polyI:C administration. Tissues with medium-to-high expression of *Mx1* and *Osmr* were selected using publicly available databases such as the human protein atlas[195-197], Mouse Genome Informatics[198] and The Bgee suite[198]. The Jackson Laboratory's Institutional Animal Care and Use Committee approved all experiments.

3.4.2 Genotyping and Recombination PCR

Genomic DNA was extracted from lysed peripheral blood samples using the DNeasy Blood & Tissue Kit (Qiagen) for genotyping. Genotyping primers were used as suggested on the B6;129-*Osmr*$^{tm1.1Nat}$/J (JAX: 011081) mice webpage (protocol ID 29086 and 23692). Images were taken using the InGenuis LHR2 Gel imaging system (Syngene). Recombination of the *Osmr*^{fl} locus was evaluated by PCR using the following primers: Forward: 5'-GGAAATACCTTGGCAGTGGTG and Reverse: 5'-GCTACCAAACCTCGGTAATCC.

3.4.3 *Osmr* mRNA Expression

RNA was isolated using the RNeasy Minikit (Qiagen) and cDNA was made using the qPCR Bio cDNA synthesis kit (PCR Biosystems). Quantitative PCR was performed using TaqMan™ Fast Advanced Master Mix (Applied Biosystems) on the QuantStudio 7 Real-Time PCR System (ThermoFisher Scientific). mRNA expression levels for *Osmr* (Taqman probe #Mm01307326_m1) were calculated relative to the housekeeping gene, *Gapdh* (Taqman probe # Mm99999915_g1*).*

3.4.4 RNA Sequencing

Bone marrow (BM) cells were isolated from *Osmr*$^{fl/fl}$ *Mx1*-Cre and *Mx1*-Cre control mice from pooled and crushed femurs, tibiae, iliac crests, sternums, forepaws, and spinal columns of individual mice. BM mononuclear cells (MNCs) were isolated by 1X Red Blood Cell lysis Buffer (eBioscience) and stained with a combination of fluorochrome-conjugated antibodies: c-Kit (BD Biosciences, BioLegend clone 2B8), Sca-1 (BioLegend clone D7), CD150 (BioLegend clone TC15-12F12.2), CD48 (BioLegend clone HM48-1), FLT3 (BioLegend clone A2F10), (Lin) marker mix (B220 (BD Biosciences, BioLegend clone RA3-6B2), and the 4′,6-diamidino-2-phenylindole (DAPI). 2,000 hematopoietic stem cells (HSCs) were sorted based on the cell surface marker combination: Lin- Sca-1+ c-Kit+ Flt3- CD150+ CD48- on a FACSAria into StemSpan SFEM II media with SCF (100 ng/ml, BioLegend), TPO (50 ng/ml, Peprotech), with or without OSM (500 ng/ml, BioLegend) and incubated at 37°C for 60min. RNA preparation, sequencing and analysis was performed following a previously published method[202]. Significantly differentially expressed genes were identified based on criteria of $p < 0.01$ and log2(FC)>3 or <-3. Predicted genes and pseudogenes were removed from the list of significantly differentially expressed genes before downstream comparisons were performed. The

DAVID bioinformatics resource[203,204] was used for functional annotation of significantly differentially expressed gene lists.

3.4.5 Western Blotting for OSMRβ

Total protein was extracted from snap frozen tissues with a Tissue Lyser II (Qiagen) using 5mm Bead Beater balls (Qiagen) after the addition of 50mM HEPES pH 7.5 (Gibco) and 6M urea (Sigma-Aldrich) at 1.5mL per 200mg tissue. Insoluble material was spun out at 21,000 x g for 20m. Total protein concentration of each sample was determined by microBCA (ThermoFisher). SDS-PAGE gel samples were prepared. Two 4–15% Mini-PROTEAN TGX Precast, 1.0mm, 15-well, SDS-PAGE Gel (Bio-Rad) were loaded with 25ug total protein per well. The gels were run at 150V for 1h at room temperature in Tris·Glycine·SDS buffer (Bio-Rad) then transferred overnight at 4°C at 40mAmp to 0.22mm PVDF (Bio-Rad) in Tris·Glycine buffer (Bio-Rad) with 10% methanol. The blots were placed in Block (2% BSA + 4% Dry Milk) at room temperature for 1h. The blots were then placed in primary antibody Polyclonal Goat IgG anti-mouse OSMR (R&D systems AF662) diluted in fresh block at 1:2500 and incubated on an orbital shaker at 4°C overnight. Then the blots were washed with TBS with 0.03% Tween 20 (TBS-T) for 15min and three more washes for 5 minutes each. Then the blots were placed in Peroxidase AffiniPure Bovine Anti-Goat IgG (H+L)(Jackson Immuno Research) diluted 1:5,000 in block. The blots rotated for 1h at room temperature and then were washed with TBS-T for 15min and three more washes for 5 minutes each. The blot was then developed with (ThermoFisher) SuperSignal West Pico Plus reagents (ThermoFisher) and visualized with a Syngene G-Box. The blots were then stripped with Restore™ PLUS Western Blot Stripping Buffer (ThermoFisher) at room temperature for

5min. The blots were re-blocked and then incubated with b-actin (Cell Signaling Technology clone D6A8) at 1:5000 for 1h at room temperature. Then the blots were washed with TBS-T for 15min and three more washes for 5 minutes each. Then the blots were placed in Goat Anti-Rabbit IgG (H+L)-HRP (Bio-Rad) diluted 1:5,000 in block. The blots rotated for 1h at room temperature and then were washed with TBS-T for 15min and three more washes for 5 minutes each. The blot was then developed with (ThermoFisher) SuperSignal West Femto Maximum Sensitivity reagents (ThermoFisher) and visualized with a Syngene G-Box. Images were quantified by ImageJ by relative intensity, adjusted for background and normalized to β-ACTIN expression per sample.

3.5 Data Availability

Raw RNA-seq data is available at the Gene Expression Omnibus under GSE236693 and GSE244544.

3.6 Author Contributions

L.S. and J.J.T. conceptualized the project and designed experiments. L.S. performed experiments, and L.S and J.J.T. analyzed data. R.S. performed Western blot experiments and image analysis. T.S. assisted in analysis of RNA-seq data. L.S. and J.J.T. wrote the manuscript.

3.7 Acknowledgments

This work was supported by National Institutes of Health grants R01DK118072, R01AG069010, U01AG077925, and an EvansMDS Discovery Research Grant to J.J.T.

This work was supported in part by the NIH/NCI Cancer Center Support Grant P30CA034196. J.J.T. was supported by a Leukemia & Lymphoma Society Scholar Award and The Dattels Family Endowed Chair. L.S.S. was supported by F31DK127573 and The Tufts University Scheer-Tomasso Fund philanthropic gift. We thank Drs. Jeremy Nathans and Amir Rattner for providing detailed information regarding the design of the B6;129-*Osmr*$^{tm1.1Nat}$/J allele. We thank all members of the Trowbridge Lab, particularly Jayna Mistry, for experimental support and manuscript editing. We thank the Scientific Services at The Jackson Laboratory including flow cytometry, monoclonal antibody and protein production service, and genome technologies. We thank Elli Hartig, Carol Bult, Ryan Tewhey, Cliff Rosen, and Phil Hinds for discussion and input into this work.

3.8 Supplementary Tables

The following table(s) have been uploaded onto ProQuest.

Table 3.1: Differential Gene Expression Analysis of *Osmr*$^{fl/fl}$ *Mx1*-Cre vs. Control *Mx1*-Cre HSCs from RNA-Seq Data

Table 3.2: Differential Gene Expression Analysis of OSM-Stimulated vs. Vehicle-Treated Control *Mx1*-Cre HSCs from RNA-Seq Data

Table 3.3: Differential Gene Expression Analysis of OSM-Stimulated vs. Vehicle-Treated *Osmr*$^{fl/fl}$ *Mx1*-Cre HSCs from RNA-Seq Data.

.

Chapter 4: Discussion

My thesis highlights a pivotal role for OSM as a master regulator within an inflammatory cytokine network, particularly in the context of *Dnmt3a*-mutant HSCs associated with CH. In **Chapter 2** I describe the discovery of a negative feedback mechanism whereby OSM signaling led to increased transcription and enhanced transcript stability of anti-inflammatory genes to provide a selective advantage to young *Dnmt3a*-mutant HSCs within the context of CH. In this chapter I also explore the effect of chronic inflammation or aging-related OSM exposure and how this might disrupt the regulatory mechanisms that normally resolve inflammatory states in young *Dnmt3a*-mutant HSCs. In **Chapter 3** I detail the investigation of a readily available conditional *Osmr*$^{fl/fl}$ mouse model (B6;129-*Osmr*$^{tm1.1Nat/J}$) and how loss of *Osmr* exon 2 variably impacts mRNA and protein expression in individual tissues. Here I will briefly summarize the main points from each chapter, enumerate unanswered questions and important next steps, and provide predictions for the role of OSM in the field of clonal hematopoiesis.

The process of aging has a profound impact on tissues and cells throughout our bodies. Focusing on the changes that occur in the HSPC compartment, with aging comes the acquisition of somatic mutations in the stem cell pool. As HSPCs in the stem cell pool are long lived, these mutations can persist across many cellular generations and affect most mature hematopoietic cell progeny. While the majority of these mutations are generally considered 'neutral,' a subset of them can give HSPCs a competitive edge, leading to a condition known as age-associated CH (Figure 1.3). The most common CH mutations are found in a subset of genes that encode canonical epigenetic or chromatin regulatory

proteins such as DNMT3A. While CH is considered a non-malignant condition, individuals with CH will be predisposed to increased incidence of hematologic malignancy such as leukemia, coronary heart disease, ischemic stroke, or other complications. Understanding the cellular and molecular mechanisms underlying the selective advantage of HSPCs carrying these somatic mutations, and how and in whom this is a risk factor for age-associated disease, will further inform our understanding of CH-associated conditions.

Recurrent somatic mutations that were originally identified in adult acute myeloid leukemia (AML) including a missense mutation in *DNMT3A* at R882H/C have also been found in a non-malignant state of aging associated CH. Using an inducible *Dnmt3a*-mutant mouse model of CH (*Dnmt3a*$^{R878H/+}$)(Figure 1.4), we previously reported that transplant of *Dnmt3a*-mutant HSCs into 14-month-old recipient mice promotes their selective growth advantage compared to transplant into 2-month-old recipient mice[113]. This led us to hypothesize that differences in soluble factors in the middle-aged versus young BM contribute to *Dnmt3a*-mutant HSC expansion. I began with re-analysis of our HSC RNA-seq data from that study, identifying a hallmark inflammatory response signature in *Dnmt3a*-mutant versus control HSCs in middle-aged but not in young recipient mice. Examining this gene signature, I found that the top gene encoding a soluble factor and was also increased in expression in *Dnmt3a*-mutant HSCs, and this gene was *Osm* (Figure 2.1).

OSM has been shown to have a significant role in development, malignancy, and homeostasis of various human and mouse tissue types[123]. It is mainly secreted by mature activated hematopoietic cells: monocytes, T lymphocytes, neutrophils, macrophages, and dendritic cells[124]. Secreted OSM can interact with two different receptor complexes, type I or type II[132-134]. The type I receptor complex contains LIFR and gp130, while the type II receptor complex contains OSMRβ and gp130[127,132,191,192](Figure 1.5). After binding to the OSMR complex several signaling pathways are activated in humans and mice including the JAK/STAT3 pathway[123,147]. OSM/Osm is an important regulator of the BM microenvironment in both steady state and in regeneration after injury in mice and zebrafish[184,185], and plays a role in mouse and human HSC mobilization[179]. Previous studies performed in young adult mice have shown that *Osmr* is not detected in HSPCs or myeloid cells[164] and thus it has been suggested that HSCs and their progeny do not directly respond to OSM. However, *Osmr* is one of the most upregulated transcripts in old HSCs compared to young HSCs across six independent datasets[135] suggesting that in certain contexts, such as aging, HSCs and their progeny gain the capacity to respond to OSM.

Given that activation of OSM signaling is associated with expanded *Dnmt3a*-mutant hematopoiesis in the middle-aged BM microenvironment, I hypothesized that OSM as a single stimulus would be sufficient to promote the selective advantage of young *Dnmt3a*-mutant HSPCs. I found that recombinant OSM did not result in altered proliferation, apoptosis, hematopoietic engraftment, or myeloid differentiation of young *Dnmt3a*-mutant HSCs (Figure 2.2, Figure 2.3). Despite this, I found that young *Dnmt3a*-mutant

HSCs do transcriptionally upregulate an inflammatory cytokine network in response to acute OSM stimulation as evidenced by significant upregulation of the genes encoding IL-6, IL-1b and TNFα (Figure 2.5). OSM-stimulated *Dnmt3a*-mutant HSCs also demonstrate upregulation of the anti-inflammatory genes including *Socs3, Atf3* and *Nr4a1* which creates a negative feedback loop that limits sustained activation of the inflammatory network (Figure 2.6). In the context of an aged BM with chronically elevated levels of OSM, *Dnmt3a*-mutant HSCs upregulate pro-inflammatory response transcriptional signature but not the anti-inflammatory genes *Socs3, Atf3* and *Nr4a1*. The results from my studies suggest that chronic inflammation with aging exhausts the regulatory mechanisms that HSCs in young mice use to resolve inflammatory states and that OSM is a master regulator of an inflammatory network that contributes to age-associated CH (Figure 2.7).

The identification of OSM as a master regulator of inflammatory cytokine production opens the possibly of therapeutic interventions targeting OSM to reduce inflammation in aging-associated *Dnmt3a*-mutant CH. To investigate the loss of OSM- OSMRβ signaling in the context of adult hematopoiesis, aging, and aging-associated *Dnmt3a*-mutant CH I utilized the readily available conditional *Osmr*$^{fl/fl}$ mouse model B6;129-*Osmr*$^{tm1.1Nat}$/J, which is poorly characterized in the literature. This model contains loxP sites flanking exon 2 of the *Osmr* gene. I crossed *Osmr*$^{fl/fl}$ mice to interferon-inducible *Mx1*-Cre (B6.Cg-Tg(Mx1-cre)1Cgn/J), which is robustly induced in adult hematopoietic cells. I observed complete recombination of the *Osmr*^{fl} allele and loss of exon 2 in hematopoietic (BM) as well as non-hematopoietic (liver, lung, kidney) tissues (

Figure 3.1). Despite recombination of the genomic *Osmr*^{fl} locus the extent of reduction in *Osmr* transcript and OSMRβ protein expression in *Osmr*$^{fl/fl}$ *Mx1*-Cre tissues compared to *Mx1*-Cre tissues was dependent upon the tissue type examined (Figure 3.2). RNA-seq analysis of a subpopulation of BM cells (HSCs) finds that some OSM-stimulated genes, but not all, are suppressed in *Osmr*$^{fl/fl}$ *Mx1*-Cre cells (Figure 3.3). Together, these data suggest that the B6;129-*Osmr*$^{tm1.1Nat}$/J model should be utilized with caution as loss of *Osmr* exon 2 has variable and tissue-dependent impact on mRNA and protein expression.

The findings revealed in my studies suggest that other tools should be utilized in parallel to the B6;129-*Osmr*$^{tm1.1Nat}$/J model in future studies. Innovative groups have generated novel tools to aid in this challenge. For example, with the knowledge that specific charged residues in the AB loop of OSM are crucial for selection of binding to receptor complex I versus complex II, "humanized" murine OSM variants have been generated to gain more accurate insights into the role of human OSM in mouse models[144]. Following these findings the same group used this human-like OSM (hlOSM) mutant protein to study the activation of LIFR and OSMR in normoxic and hypoxic conditions in cardiomyocytes[205]. The authors found that post-infarction delivery of this hlOSM was able to improve cardiac architecture and contractility following a myocardial infarction.

In addition, a potent and specific inhibitor of OSM signaling has been engineered consisting of fused domains of the mouse gp130 and mouse OSMR connected by a flexible linker acted as a potent and specific inhibitor of mOSM[200]. It is generated by single gene and therefore is easy to deliver via viral vectors, the development of

transgenic mice and the investigation of the role of murine models of human diseases. This mOSM cytokine trap has been used in multiple studies such as to study the role of OSM on irritable bowel disease (IBD) and the hematopoietic stem cell niche in the BM as well as its indirect role on HSC mobilization[179,201]. Using this construct to generate transgenic animals would be very useful for future *in vivo* studies. Moving forward, we advise that other tools be utilized in parallel to the B6;129-*Osmr*$^{tm1.1Nat}$/J model and/or that studies include a detailed characterization of *Osmr* transcript and protein levels in the tissue and cell type of focus.

Together, my thesis work suggests that OSM is upstream of an inflammatory cytokine network in *Dnmt3a*-mutant HSCs. I speculate that chronic inflammation or exposure to cytokines such as OSM with aging exhausts the regulatory mechanisms present in young *Dnmt3a*-mutant HSCs that resolve inflammatory states. In my attempts to understand the relationship between CH and a loss of OSMR signaling, I utilized a conditional *Osmr*$^{fl/fl}$ mouse model B6;129-*Osmr*$^{tm1.1Nat}$/J, which is poorly characterized in the literature.
I found that there is a tissue dependent difference in mRNA and protein expression in these animals and that there is a need for increased pre-clinical models to study the effects of OSMR signaling. Additionally, I highlight the challenges of modeling OSMRβ deficiency in mouse models and the importance of continued studies of OSM- OSMRβ signaling. I identified a transcriptional feedback loop that silences pro-inflammatory responses in *Dnmt3a*-mutant HSCs, but is dysfunctional in the context of aging, and this could represent a targetable mechanism for therapeutic intervention. Re-engagement of this negative feedback loop by transient activation of *Socs3* or other anti-inflammatory

factors may help to suppress inflammatory myeloid cell production that is a major contributor to CH-associated malignancy.

4.1 Future Directions:

4.1.1 Small Molecule Inhibitors Targeting OSM Signaling

Future steps are needed to functionally explore the mechanisms governing OSM signaling and the context dependent relationship with *Dnmt3a*-mutant HSCs. To begin to understand this mechanism we need to first study the loss of OSM signaling in the context of young and aged *Dnmt3a*-mutant HSCs. While I attempted to do this using pre-existing mouse models, the work I describe in **Chapter 3** is evidence that another strategy is needed to confirm this. To this end I have initiated a collaboration with a group at Boise State University that has identified and patented a small molecule OSM inhibitor, OSM-SMI-10b(OSMi)(US9550828B2)[145]. This inhibitor was discovered using a bioactive recombinant human OSM for nuclear magnetic resonance (NMR) based screening and selected based on its ability to significantly reduce OSM-induced pSTAT3 in cancer cells upon co-incubation with OSM[145]. To begin studies I would perform a similar experiment in the context of control and *Dnmt3a*-mutant HSPCs. I am well poised to perform these experiments as I found in **Chapter 2** (Figure 2.5) that acute OSM stimulation activates STAT3 phosphorylation and transcriptional responses in young *Dnmt3a*-mutant HSCs when compared to control HSCs. I would repeat this experiment but add a condition with co-incubation of OSM and OSMi over a time course followed by phospho-flow measurements. I have shown that acute stimulation of *Dnmt3a*-mutant HSPCs of resulted in greater pSTAT3 compared to vehicle-stimulated *Dnmt3a*-mutant HSPCs after 60 minutes and I hypothesize that the inhibitor would bring the level of

STAT3 phosphorylation back down to those observed in vehicle treated HSCs. If my hypothesis is correct, I would continue with *in vivo* experiments.

In our previous studies I discovered a transcriptional program of inflammation response in *Dnmt3a*-mutant compared to control HSCs in middle-aged, but not young, transplant recipient mice (Figure 2.1B). Thus, I hypothesized that middle-aged mice have elevated 'chronic' levels of OSM and that *Dnmt3a*-mutant HSCs in a middle-aged microenvironment lose the capacity to upregulate suppressors of inflammation such as *Socs3, Nr4a1,* and *Atf3.* I hypothesize that treatment of young and middle-aged transplant recipient mice transplanted with *Dnmt3a*-mutant HSCs and treated with OSMi will prevent some or all the phenotypes associated with increased OSM on *Dnmt3a*-mutant HSCs. These studies could provide evidence that loss of OSM signaling results in a decreased inflammatory response signature and perhaps upregulation of suppressors of inflammation once again leading to a loss of the *Dnmt3a*-mutant HSC selective advantage in an aged environment.

4.1.2 Generation of Myeloid Cell Specific *Osm*-/- Mice

My studies have highlighted the challenges that come with utilizing mouse models to study the effects of loss of OSMRβ signaling. An alternative strategy to studying the loss of OSM-OSMRβ signaling would be to reduce the expression of OSM in the BM microenvironment instead of targeting OSMRβ. In a recent study researchers discovered that bacterial lipopolysaccharide (LPS) induces OSM and that airway biopsies taken from patients with severe asthma present with an OSM-driven transcriptional profile[206]. This

transcriptional profile correlates with activation of inflammatory and mucus-producing pathways. In this study, the authors utilized *Osm*-deficient murine macrophages and were able to show that macrophage-derived OSM translates LPS signals into asthma-associated pathologies. For my studies that involve a similar OSM-driven activation of inflammatory genes transcriptional profile I propose generating a cross between, C57BL/6 $Osm^{-/-}$ (C57BL/6N-A^{tm1Brd} $Osm^{tm1b(KOMP)Wtsi}$/ JMmucd Mutant Mouse Resource and Research centers (MMRRC) stock number 048921-UCD) and a tamoxifen-inducible LysM-Cre strain[207] driving OSM depletion in myeloid cells. The resulting mouse would be crossed to the control and *Dnmt3a*-mutant mice generating control and *Dnmt3a*-mutant *Osm*-/- mouse lines. Following tamoxifen induction these mice would be utilized as donors in BM transplantation assays into middle aged lethally irradiated recipient mice. I hypothesize that with the loss of OSM being produced by mature myeloid cells, in middle aged recipient mice transplanted with *Dnmt3a*-mutant BM, I will no longer observe activation of the OSM-driven anti-inflammatory network or *Dnmt3a*-mutant HSC selective advantage. Having these mice readily available will also provide our laboratory with the ability to test the effect of other target cytokines of interest in concert or separately from the effects of OSM in response to an inflammatory challenge. These data could provide vital information in the understanding of the role of OSM in *Dnmt3a*-mutant CH.

4.1.3 Studying the Effects of Short-Form and Soluble OSMRβ

In addition to full-length OSMRβ (4171 base-pair, GenBank No. NM003999), there are two other types of OSMRβ, including a short-form OSMR (1620 base-pair OSMRs

GenBank No. BC010943) with the absence of an intracellular region and a soluble type of the OSMRβ (sOSMR)[136]. The sOSMR is generated by alternative splicing and comprises all required domains for binding to OSM. sOSMR acts as an antagonist with soluble gp130 to block OSM-mediated signaling via OSMRβ acting as a soluble or decoy receptor. sOSMR is a result of an incomplete splicing at the exon 8 and intron 8 junction, in which the presence of a cryptic stop codon 48 nucleotides away from the 5′-splice site of intron 8 produces a truncated protein that is larger than the short-form of OSMR by 53 amino acid residues. The estimated molecular mass is about 43 kDa[136,208]. Additionally, the shorter transcripts are less stable with a half-life of 9 hours whereas the full-length transcripts decay slowly (half-life > 24 hours)[209].

I hypothesize that sOSMR is imperative for alternative signaling in my studies. In control HSCs I do not see a robust response to OSM, but contrastingly I do not observe differences in the transcript abundance of OSMR or binding capability of OSM-AF488 (Figure 2.4) both transcriptionally and fluorescently labeled OSM-AF488 as a proxy for OSM binding capability. It is possible that in response to *Dnmt3a*-mutant HSC generated OSM or recombinant mOSM, control HSCs produce sOSMR as their predominant protein instead of full-length OSMR as a similar response has been observed in systemic sclerosis[210]. This may explain why I observe robust activation of STAT3 signaling and anti-inflammatory proteins in young *Dnmt3a*-mutant HSCs while I do not observe any significant response in control HSCs. sOSMR may act as a decoy with soluble gp130 to block OSM-mediated signaling via OSMRβ in control HSCs. To test this hypothesis, I would use previously established assays to determine the role of short-form OSMR and

sOSMR including primers targeting distal and proximal regions of OSMR to detect the abundance of short and full-length OSMR transcripts[209]. Additionally, I would like to measure sOSMR in the sera of steady state and transplant mice using previously established ELISA assays to further understand this relationship[208]. It is possible in young control HSCs sOSMR plays a vital role in preventing OSM signaling and with aging the full-length OSMR transcript increases to compensate for the sOSMR blocked signaling. This hypothesis is supported by the finding that *Osmr* is one of the top changed genes with age revealing it has a profound role in control aged HSCs[151].

4.1.4 Exploring the Role of OSM Driven Upregulation of *Ube2n* in *Dnmt3a*-mutant CH

Another potential future direction of my studies is continued exploration of a gene, *Ube2n*, that was a top differentially regulated gene in *Dnmt3a*-mutant HSCs in response to OSM stimulation but not in control HSCs (Table **2.1**). The gene encoding ubiquitin-conjugating enzyme E2 N (*Ube2n*) encodes a member of the E2 ubiquitin-conjugating enzyme family, UBE2N (or also known as UBC13). Ubiquitination is an essential cellular mechanism for targeting abnormal or short-lived proteins for degradation[211,212]. I did not observe transcriptional increase of *Ube2n* in control HSCs stimulated with OSM. The appearance of this gene in my data is particularly interesting because recent studies have shown that dysregulation of UBE2N-dependent innate immune pathways are associated with AML[213]. In one study Barreyro et al, the authors found that UBE2N is required for leukemic cell function *in vitro* and *in vivo* by maintaining oncogenic immune signaling states. Additionally, inhibition of UBE2N abrogated the innate immune signaling pathways in AML cells. These studies provide evidence that UBE2N is an

actionable target in malignant hematopoietic cells in the context of AML and excitingly there are existing inhibitors making these studies possible[214]. This is particularly interesting because of the relationship between CH and transformation to AML. OSM may have an important role and unexplored role in the transformation of *Dnmt3a*-mutant HSCs by aiding to dysregulate and increase transcription of *Ube2n*. Another recent study showed that that STAT3 anti-inflammatory activity is facilitated by STAT3 mediated transcriptional repression of *Ube2n*[215]. In the context of STAT3 null HSCs removal of *Ube2n* mitigates hematopoietic failure, myeloid overproduction, and a majority of transcriptional dysregulation caused by the loss of STAT3 regulation. I hypothesize that OSM is in part responsible for the dysregulated immune states in CH and in AML cells by upregulating *Ube2n*. Further studies are required to understand the relationship between OSM with regards to anti-inflammatory STAT3 signaling and pro-inflammatory *Ube2n* in the context of clonal hematopoiesis.

4.2 Remaining questions

Taken together, my thesis work and proposed experiments have and will continue to elucidate our understanding of the role of OSM as a master regulator of inflammatory cytokine production in *Dnmt3a*-mutant CH and as an essential age- and disease-associated cytokine in hematopoiesis, cancers, and other malignancies. Despite the strides made in this thesis and in the field, I anticipate that we are only just beginning to understand the breadth of the significance and intricacies. In the last few years, the field has seen significant advances in the understanding of the relationship between aging, HSCs with somatic mutations and the interplay of cytokines and hematopoietic

malignancy. In this time researchers have found two concurrent discoveries: OSM is involved in many pro-inflammatory diseases and CH has many co-morbidities. Not surprisingly, many of these associated diseases overlap between the two, begging the question: cause…or consequence? Does OSM driven CH result in an increase in OSM production resulting in these comorbidities or is it all related to aging and therefore the OSM in the environment is causing general havoc. Regardless of the initiating mechanism or the driver of disease finding a therapeutic window is necessary to give patients relief.

A place to start that has been getting a lot of attention is to target downstream signaling pathways such as STAT3. As constitutively active STAT3 is involved in AML and splicing factor mutant clones in human MDS have been found to be reliant on STAT3 function and there is an opportunity to utilize STAT3 inhibitors[216-219]. In Potts et al., the authors found that splicing factor mutant cells ($SRSF2^{+/p95H}$) are sensitive to STAT3 inhibition. Pharmacologic STAT3 inhibition using STATTIC which binds to the SH2 domain and blocks phosphorylation and dimerization of STAT3 also reduced STAT3 phosphorylation in HSPCs more in mutant HSCs than wild type HSCs. And in this context OSM-stimulation was found to cause increased levels of STAT3 phosphorylation in human $SRSF2^{+/p95H}$ mutant cells when compared to wild-type K562 cells[219]. Targeting the STAT3 protein is a potentially promising strategy for many hematologic malignancies and cancers. Although no STAT3 inhibitors have been marketed yet there are many promising small molecule inhibitors and degraders in clinical trials. Targeting STAT3 is historically difficult and often considered “undruggable” as it is a ubiquitously

expressed transcription factor. In the past two decades many diverse compounds have been discovered to therapeutically target mediators of the STAT3 signaling or STAT3 signaling directly. This endeavor is promising as studies have already shown targeting STAT3 beneficial in the restoration of anti-tumor immunity. Targeting STAT3 signaling provides attractive avenues that are currently being explored for the immunotherapy of cancers both as monotherapy and in combination therapies.

Therapeutic intervention of OSM and/or OSMR is an exciting new therapeutic window due to its multi-disease implication garnering the interest of many biotech companies. While there are many approved therapies to target IL-6 and other IL-6 family members there is no current FDA approved treatment for OSM[220]. Excitingly the first molecular structure of OSM was published in 2000 by Deller et al. and this information is critical in the development of anti-OSM therapeutics[221]. As previously stated OSM consists of four alpha-helical bundles and two distinct binding sites for formation of receptor complexes. The site II motif is responsible for OSM binding to the gp130 portion of the receptor complex. Site III located between helices A and B is the site by which OSM binds to OSMR and LIFR. Four amino acids in the AB loop are responsible for denoting OSMR binding while other amino acids are necessary for the interaction of both OSMR and LIFR[138,144,182] .To date the only two anti-OSM antibodies to enter clinical trials target site II of OSM. Both clinical trials were supported by GlaxoSmithKline for the treatment of active rheumatoid arthritis and systemic scleroderma[222,223]. Unfortunately, neither clinical trial resulted in an FDA approved anti-OSM therapeutic due to the high off-rate and binding affinity of the antibodies. The antibody treatment results were also inconclusive

and did not reach significance. In the context of patients with systemic scleroderma, the higher dose treatment group patients reported at least one adverse effect such as decreased hemoglobin, platelet and neutrophil counts as well as anemia of varying degrees[223,224]. These findings and symptoms are particularly intriguing as they are the same observations seen in Tanaka et al. while characterizing an OSMR knockout mouse model, *Osmr*^{tm1Mtan} [194]. The most promising attempt to target OSM is utilizing a small molecule from Boise State University (patent US9550828B2) proposed in my future studies. This patented inhibitor is to date the only small molecule designed to target OSM.

Challenges exist from the start for targeting OSMRβ as it is included in another receptor complex with IL-31RA. This overlap between the OSMR complex and the IL-31 complex makes it difficult to target one or the other specifically. Another challenge is that surprisingly after 30 years of research the protein structure of OSMRβ is still unknown. Molecular modeling predictions of the structure have aided in the development of anti-OSMRβ therapeutics, but the mystery of the structure makes this task increasingly difficult. While patents for monoclonal antibodies targeting OSM exist for patients with skin diseases, cancer and heart disease there has been little success in this effort. Overexpression of OSM and/or OSMRβ is a commonality in many advanced tumors and linked to decreased patient survival in many cancer types such as breast cancer, cervical cancer, pancreatic cancer, lung cancer and brain cancer. While disappointingly the efforts for an anti-OSM and/or anti-OSMRβ drug have not yet succeeded in making it through

clinical trials there is hope as many laboratories and biotechnology companies are focused on this effort.

Chapter 5: Appendix

Table 5.1: Gene Details

Gene symbol	Gene Name	Identifier
ASXL1	ASXL transcriptional regulator 1	HGNC:18318
Asxl1	ASXL transcriptional regulator 1	MGI:2684063
asxl1	ASXL transcriptional regulator 1	ZDB-GENE-091116-9
Atf3	activating transcription factor 3	MGI:109384
atf3	activating transcription factor 3	ZDB-GENE-040426-728
Actb	actin, beta	MGI:87904
B2m	beta-2-microglobulin	MGI:88127
Bst2	bone marrow stromal cell antigen 2	MGI:1916800
Ccr1	C-C motif chemokine receptor 1	MGI:104618
Ccrl2	C-C motif chemokine receptor-like 2	MGI:1920904
CLCF1	cardiotrophin like cytokine factor 1	HGNC:17412
CNTF	ciliary neurotrophic factor	HGNC:2169
Csf3r	colony stimulating factor 3 receptor	MGI:1339755
CTF1	cardiotrophin 1	HGNC:2499
DNMT3A	DNA methyltransferase 3 alpha	HGNC:2978
Dnmt3a	DNA methyltransferase 3A	MGI:1261827
Egr1	early growth response 1	MGI:95295
EPO	erythropoietin	HGNC:3415
Epo	erythropoietin	MGI:95407
Flt3l	FMS-like tyrosine kinase 3 ligand	MGI:95560
Fos	FBJ osteosarcoma oncogene	MGI:95574
Gapdh	glyceraldehyde-3-phosphate dehydrogenase	MGI:95640
GM-CSF	colony stimulating factor 2	HGNC:2434
Gm-csf/Csf2	colony stimulating factor 2 (granulocyte-macrophage)	MGI:1339752
Icam1	intercellular adhesion molecule 1	MGI:96392
Ifng	interferon gamma	MGI:107656
IL-31RA	interleukin 31 receptor A	HGNC:18969
IL11	interleukin 11	HGNC:5966
Il11	interleukin 11	MGI:107613
Il1b	interleukin 1 beta	MGI:96543
Il1r2	interleukin 1 receptor, type II	MGI:96546
IL2	interleukin 2	HGNC:6001
IL27	interleukin 27	HGNC:19157
Il3	interleukin 3	MGI:96552

IL3	interleukin 3	HGNC:6011
IL31	interleukin 31	HGNC:19372
IL6	interleukin 6	HGNC:6018
Il6	interleukin 6	MGI:96559
IL6ST	interleukin 6 cytokine family signal transducer	HGNC:6021
Il6st	interleukin 6 cytokine family signal transducer	MGI:96560
Il8/Cxcl15	C-X-C motif chemokine ligand 15	MGI:1339941
Irf1	interferon regulatory factor 1	MGI:96590
Jak1	Janus kinase 1	MGI:96628
Junb	jun B proto-oncogene	MGI:96647
Jund	jun D proto-oncogene	MGI:96648
Ki-67	antigen identified by monoclonal antibody Ki 67	MGI:106035
Klf6	Kruppel-like transcription factor 6	MGI:1346318
LIF	leukemia inhibitory factor	HGNC:6596
Lif	leukemia inhibitory factor	MGI:96787
LIFR	LIF receptor subunit alpha	HGNC:6597
Lifr	LIF receptor subunit alpha	MGI:96788
MAPK	mitogen-activated protein kinase 1	HGNC:6871
Mapk1	mitogen-activated protein kinase 1	MGI:1346858
Mapk14	mitogen-activated protein kinase 14	MGI:1346865
Morrbid	myeloid RNA regulator of BCL2L11 induced cell death	MGI:3652191
Mx1	MX dynamin-like GTPase 1	MGI:97243
Nfkb1	nuclear factor of kappa light polypeptide gene enhancer in B cells 1	MGI:97312
Nr4a1	nuclear receptor subfamily 4, group A, member 1	MGI:1352454
nr4a1	nuclear receptor subfamily 4, group A, member 1	ZDB-GENE-040704-11
nr4a3	nuclear receptor subfamily 4, group A, member 3	ZDB-GENE-070824-4
OSM	oncostatin M	HGNC:8506
Osm	oncostatin M	MGI:104749
OSMR	oncostatin M receptor	HGNC:8507
Osmr	oncostatin M receptor	MGI:1330819
Prkcb	protein kinase C, beta	MGI:97596
Ptprc	protein tyrosine phosphatase receptor type C	MGI:97810

Scf/Kitl	kit ligand	MGI:96974
Shc1	src homology 2 domain-containing transforming protein C1	MGI:98296
Slc31a2	solute carrier family 31, member 2	MGI:1333844
SOCS3	suppressor of cytokine signaling 3	HGNC:19391
Socs3	suppressor of cytokine signaling 3	MGI:1201791
socs3a	suppressor of cytokine signaling 3a	ZDB-GENE-030131-7349
SRSF2	serine and arginine rich splicing factor 2	HGNC:10783
Srsf2	serine and arginine rich splicing factor 2	MGI:98284
STAG2	STAG2 cohesin complex component	HGNC:11355
STAT3	signal transducer and activator of transcription 3	HGNC:11364
Stat3	signal transducer and activator of transcription 3	MGI:103038
Stat5a	signal transducer and activator of transcription 5A	MGI:103036
TET2	tet methylcytosine dioxygenase 2	HGNC:25941
Tet2	tet methylcytosine dioxygenase 2	MGI:2443298
Tlr2	toll-like receptor 2	MGI:1346060
Tnf	tumor necrosis factor	MGI:104798
Tnfrsf1a	tumor necrosis factor receptor superfamily, member 1a	MGI:1314884
Tpo	thyroid peroxidase	MGI:98813
Ube2n	ubiquitin-conjugating enzyme E2N	MGI:1934835
UBE2N	ubiquitin-conjugating enzyme E2N	HGNC:12492
Vav1	vav 1 oncogene	MGI:98923

Chapter 6: Bibliography

1. Hart, G. (2001). Descriptions of blood and blood disorders before the advent of laboratory studies. Brit J Haematol *115*, 719-728. DOI 10.1046/j.1365-2141.2001.03130.x.

2. Meletis, J., and Konstantopoulos, K. (2010). The beliefs, myths, and reality surrounding the word hema (blood) from homer to the present. Anemia *2010*, 857657. 10.1155/2010/857657.

3. Ribatti, D. (2009). William Harvey and the discovery of the circulation of the blood. J Angiogenes Res *1*, 3. 10.1186/2040-2384-1-3.

4. Jagannathan-Bogdan, M., and Zon, L.I. (2013). Hematopoiesis. Development *140*, 2463-2467. 10.1242/dev.083147.

5. Rieger, M.A., and Schroeder, T. (2012). Hematopoiesis. Cold Spring Harb Perspect Biol *4*. 10.1101/cshperspect.a008250.

6. Weissman, I.L., and Shizuru, J.A. (2008). The origins of the identification and isolation of hematopoietic stem cells, and their capability to induce donor-specific transplantation tolerance and treat autoimmune diseases. Blood *112*, 3543-3553. 10.1182/blood-2008-08-078220.

7. Orkin, S.H., and Zon, L.I. (2008). Hematopoiesis: an evolving paradigm for stem cell biology. Cell *132*, 631-644. 10.1016/j.cell.2008.01.025.

8. Chen, T.P., and Dent, S.Y.R. (2014). Chromatin modifiers and remodellers: regulators of cellular differentiation. Nature Reviews Genetics *15*, 93-106. 10.1038/nrg3607.

9. Cossarizza, A., Chang, H.D., Radbruch, A., Abrignani, S., Addo, R., Akdis, M., Andra, I., Andreata, F., Annunziato, F., Arranz, E., et al. (2021). Guidelines for the use of flow cytometry and cell sorting in immunological studies (third edition). Eur J Immunol *51*, 2708-3145. 10.1002/eji.202170126.

10. Seita, J., and Weissman, I.L. (2010). Hematopoietic stem cell: self-renewal versus differentiation. Wiley Interdiscip Rev Syst Biol Med *2*, 640-653. 10.1002/wsbm.86.

11. Cheng, H., Zheng, Z.F., and Cheng, T. (2020). New paradigms on hematopoietic stem cell differentiation. Protein Cell *11*, 34-44. 10.1007/s13238-019-0633-0.

12. Mann, Z., Sengar, M., Verma, Y.K., Rajalingam, R., and Raghav, P.K. (2022). Hematopoietic Stem Cell Factors: Their Functional Role in Self-Renewal and Clinical Aspects. Frontiers in Cell and Developmental Biology *10*. ARTN 664261

10.3389/fcell.2022.664261.

13. Schippel, N., and Sharma, S. (2023). Dynamics of human hematopoietic stem and progenitor cell differentiation to the erythroid lineage. Exp Hematol *123*, 1-17. 10.1016/j.exphem.2023.05.001.

14. Graf, T. (2002). Differentiation plasticity of hematopoietic cells. Blood *99*, 3089-3101. DOI 10.1182/blood.V99.9.3089.

15. Challen, G.A., Pietras, E.M., Wallscheid, N.C., and Signer, R.A.J. (2021). Simplified murine multipotent progenitor isolation scheme: Establishing a consensus approach for multipotent progenitor identification. Experimental Hematology *104*, 55-63. 10.1016/j.exphem.2021.09.007.

16. Yokota, T. (2019). "Hierarchy" and "Holacracy"; A Paradigm of the Hematopoietic System. Cells *8*. 10.3390/cells8101138.

17. Tikhonova, A.N., Dolgalev, I., Hu, H., Sivaraj, K.K., Hoxha, E., Cuesta-Dominguez, A., Pinho, S., Akhmetzyanova, I., Gao, J., Witkowski, M., et al. (2019). The bone marrow microenvironment at single-cell resolution. Nature *569*, 222-228. 10.1038/s41586-019-1104-8.

18. Kowalczyk, M.S., Tirosh, I., Heckl, D., Rao, T.N., Dixit, A., Haas, B.J., Schneider, R.K., Wagers, A.J., Ebert, B.L., and Regev, A. (2015). Single-cell RNA-seq reveals changes in cell cycle and differentiation programs upon aging of hematopoietic stem cells. Genome Res *25*, 1860-1872. 10.1101/gr.192237.115.

19. Pellin, D., Loperfido, M., Baricordi, C., Wolock, S.L., Montepeloso, A., Weinberg, O.K., Biffi, A., Klein, A.M., and Biasco, L. (2019). A comprehensive single cell transcriptional landscape of human hematopoietic progenitors. Nat Commun *10*, 2395. 10.1038/s41467-019-10291-0.

20. Baccin, C., Al-Sabah, J., Velten, L., Helbling, P.M., Grunschlager, F., Hernandez-Malmierca, P., Nombela-Arrieta, C., Steinmetz, L.M., Trumpp, A., and Haas, S. (2020). Combined single-cell and spatial transcriptomics reveal the molecular, cellular and spatial bone marrow niche organization. Nat Cell Biol *22*, 38-48. 10.1038/s41556-019-0439-6.

21. Triana, S., Vonficht, D., Jopp-Saile, L., Raffel, S., Lutz, R., Leonce, D., Antes, M., Hernandez-Malmierca, P., Ordonez-Rueda, D., Ramasz, B., et al. (2021). Single-cell proteo-genomic reference maps of the hematopoietic system enable the purification and massive profiling of precisely defined cell states. Nat Immunol *22*, 1577-1589. 10.1038/s41590-021-01059-0.

22. Sommarin, M.N.E., Olofzon, R., Palo, S., Dhapola, P., Soneji, S., Karlsson, G., and Boiers, C. (2023). Single-cell multiomics of human fetal hematopoiesis define a developmental-specific population and a fetal signature. Blood Adv *7*, 5325-5340. 10.1182/bloodadvances.2023009808.

23. Matatall, K.A., Jeong, M., Chen, S., Sun, D., Chen, F., Mo, Q., Kimmel, M., and King, K.Y. (2016). Chronic Infection Depletes Hematopoietic Stem Cells through Stress-Induced Terminal Differentiation. Cell Rep *17*, 2584-2595. 10.1016/j.celrep.2016.11.031.

24. Chavez, J.S., Rabe, J.L., Nino, K.E., Wells, H.H., Gessner, R.L., Mills, T.S., Hernandez, G., and Pietras, E.M. (2023). PU.1 is required to restrain myelopoiesis during chronic inflammatory stress. Front Cell Dev Biol *11*, 1204160. 10.3389/fcell.2023.1204160.

25. Chavez, J.S., Rabe, J.L., Hernandez, G., Mills, T.S., Nino, K.E., Davizon-Castillo, P., and Pietras, E.M. (2022). PU.1 Expression Defines Distinct Functional Activities in the Phenotypic HSC Compartment of a Murine Inflammatory Stress Model. Cells *11*. 10.3390/cells11040680.

26. Pietras, E.M., Mirantes-Barbeito, C., Fong, S., Loeffler, D., Kovtonyuk, L.V., Zhang, S., Lakshminarasimhan, R., Chin, C.P., Techner, J.M., Will, B., et al. (2016). Chronic interleukin-1 exposure drives haematopoietic stem cells towards precocious myeloid differentiation at the expense of self-renewal. Nat Cell Biol *18*, 607-618. 10.1038/ncb3346.

27. Viny, A.D., Bowman, R.L., Liu, Y., Lavallee, V.P., Eisman, S.E., Xiao, W., Durham, B.H., Navitski, A., Park, J., Braunstein, S., et al. (2019). Cohesin Members Stag1 and Stag2 Display Distinct Roles in Chromatin Accessibility and Topological Control of HSC Self-Renewal and Differentiation. Cell Stem Cell *25*, 682-696 e688. 10.1016/j.stem.2019.08.003.

28. Velten, L., Haas, S.F., Raffel, S., Blaszkiewicz, S., Islam, S., Hennig, B.P., Hirche, C., Lutz, C., Buss, E.C., Nowak, D., et al. (2017). Human haematopoietic stem cell lineage commitment is a continuous process. Nat Cell Biol *19*, 271-281. 10.1038/ncb3493.

29. Simpson, E., and Dazzi, F. (2019). Bone Marrow Transplantation 1957-2019. Front Immunol *10*, 1246. 10.3389/fimmu.2019.01246.

30. Simpson, E. (2015). Medawar's legacy to cellular immunology and clinical transplantation: a commentary on Billingham, Brent and Medawar (1956) 'Quantitative studies on tissue transplantation immunity. III. Actively acquired tolerance'. Philos T R Soc B *370*. ARTN 20140382

10.1098/rstb.2014.0382.

31. Billingham, R.E., Brent, L., and Medawar, P.B. (1953). Actively acquired tolerance of foreign cells. Nature *172*, 603-606. 10.1038/172603a0.

32. Rutkowski, P., Ostrowski, J., Debska-Slizien, A., and Rutkowski, B. (2018). Nobel Prize Winners Who Contributed To Transplantation. G Ital Nefrol *35*, 55-60.

33. Curto-Garcia, N., Harrison, C., and McLornan, D.P. (2020). Bone marrow niche dysregulation in myeloproliferative neoplasms. Haematologica *105*, 1189-1200. 10.3324/haematol.2019.243121.

34. Riether, C., Schurch, C.M., and Ochsenbein, A.F. (2015). Regulation of hematopoietic and leukemic stem cells by the immune system. Cell Death Differ *22*, 187-198. 10.1038/cdd.2014.89.

35. Reya, T. (2003). Regulation of hematopoietic stem cell self-renewal. Recent Prog Horm Res *58*, 283-295. 10.1210/rp.58.1.283.

36. Dick, J.E. (2008). Stem cell concepts renew cancer research. Blood *112*, 4793-4807. 10.1182/blood-2008-08-077941.

37. Doulatov, S., Notta, F., Laurenti, E., and Dick, J.E. (2012). Hematopoiesis: a human perspective. Cell Stem Cell *10*, 120-136. 10.1016/j.stem.2012.01.006.

38. Reya, T., Morrison, S.J., Clarke, M.F., and Weissman, I.L. (2001). Stem cells, cancer, and cancer stem cells. Nature *414*, 105-111. 10.1038/35102167.

39. Orkin, S.H. (2000). Diversification of haematopoietic stem cells to specific lineages. Nat Rev Genet *1*, 57-64. 10.1038/35049577.

40. Morrison, S.J., Uchida, N., and Weissman, I.L. (1995). The biology of hematopoietic stem cells. Annu Rev Cell Dev Biol *11*, 35-71. 10.1146/annurev.cb.11.110195.000343.

41. Pinho, S., and Frenette, P.S. (2019). Haematopoietic stem cell activity and interactions with the niche. Nat Rev Mol Cell Biol *20*, 303-320. 10.1038/s41580-019-0103-9.

42. Frisch, B.J., and Calvi, L.M. (2014). Hematopoietic stem cell cultures and assays. Methods Mol Biol *1130*, 315-324. 10.1007/978-1-62703-989-5_24.

43. Wilkinson, A.C., Igarashi, K.J., and Nakauchi, H. (2020). Haematopoietic stem cell self-renewal in vivo and ex vivo. Nat Rev Genet *21*, 541-554. 10.1038/s41576-020-0241-0.

44. Park, E., Evans, M.A., Doviak, H., Horitani, K., Ogawa, H., Yura, Y., Wang, Y., Sano, S., and Walsh, K. (2021). Bone Marrow Transplantation Procedures in Mice to Study Clonal Hematopoiesis. J Vis Exp. 10.3791/61875.

45. Shen, F.W., Saga, Y., Litman, G., Freeman, G., Tung, J.S., Cantor, H., and Boyse, E.A. (1985). Cloning of Ly-5 cDNA. Proc Natl Acad Sci U S A *82*, 7360-7363. 10.1073/pnas.82.21.7360.

46. Shen, F.W., Tung, J.S., and Boyse, E.A. (1986). Further definition of the Ly-5 system. Immunogenetics *24*, 146-149. 10.1007/BF00364741.

47. Morse, H.C., 3rd, Shen, F.W., and Hammerling, U. (1987). Genetic nomenclature for loci controlling mouse lymphocyte antigens. Immunogenetics *25*, 71-78. 10.1007/BF00364270.

48. Morse, H.C., 3rd (1992). Genetic nomenclature for loci controlling surface antigens of mouse hemopoietic cells. J Immunol *149*, 3129-3134.

49. Charbonneau, H., Tonks, N.K., Walsh, K.A., and Fischer, E.H. (1988). The leukocyte common antigen (CD45): a putative receptor-linked protein tyrosine phosphatase. Proc Natl Acad Sci U S A *85*, 7182-7186. 10.1073/pnas.85.19.7182.

50. Iscove, N.N., and Nawa, K. (1997). Hematopoietic stem cells expand during serial transplantation in vivo without apparent exhaustion. Curr Biol *7*, 805-808. 10.1016/s0960-9822(06)00341-1.

51. Yamamoto, R., Morita, Y., Ooehara, J., Hamanaka, S., Onodera, M., Rudolph, K.L., Ema, H., and Nakauchi, H. (2013). Clonal analysis unveils self-renewing lineage-restricted progenitors generated directly from hematopoietic stem cells. Cell *154*, 1112-1126. 10.1016/j.cell.2013.08.007.

52. Ema, H., Takano, H., Sudo, K., and Nakauchi, H. (2000). In vitro self-renewal division of hematopoietic stem cells. J Exp Med *192*, 1281-1288. 10.1084/jem.192.9.1281.

53. Wilkinson, A.C., Ishida, R., Nakauchi, H., and Yamazaki, S. (2020). Long-term ex vivo expansion of mouse hematopoietic stem cells. Nat Protoc *15*, 628-648. 10.1038/s41596-019-0263-2.

54. Wilkinson, A.C., Ishida, R., Kikuchi, M., Sudo, K., Morita, M., Crisostomo, R.V., Yamamoto, R., Loh, K.M., Nakamura, Y., Watanabe, M., et al. (2019). Long-term ex vivo haematopoietic-stem-cell expansion allows nonconditioned transplantation. Nature *571*, 117-121. 10.1038/s41586-019-1244-x.

55. Zhang, L., Mack, R., Breslin, P., and Zhang, J.W. (2020). Molecular and cellular mechanisms of aging in hematopoietic stem cells and their niches. J Hematol Oncol *13*. ARTN 157

10.1186/s13045-020-00994-z.

56. Adelman, E.R., and Figueroa, M.E. (2021). Human hematopoiesis: aging and leukemogenic risk. Curr Opin Hematol *28*, 57-63. 10.1097/MOH.0000000000000622.

57. Young, K., Borikar, S., Bell, R., Kuffler, L., Philip, V., and Trowbridge, J.J. (2016). Progressive alterations in multipotent hematopoietic progenitors underlie lymphoid cell loss in aging. J Exp Med *213*, 2259-2267. 10.1084/jem.20160168.

58. Groarke, E.M., and Young, N.S. (2019). Aging and Hematopoiesis. Clin Geriatr Med *35*, 285-+. 10.1016/j.cger.2019.03.001.

59. Lee, J., Yoon, S.R., Choi, I., and Jung, H. (2019). Causes and Mechanisms of Hematopoietic Stem Cell Aging. Int J Mol Sci *20*. 10.3390/ijms20061272.

60. Verovskaya, E.V., Dellorusso, P.V., and Passegue, E. (2019). Losing Sense of Self and Surroundings: Hematopoietic Stem Cell Aging and Leukemic Transformation. Trends Mol Med *25*, 494-515. 10.1016/j.molmed.2019.04.006.

61. Pappas, L.E., and Nagy, T.R. (2019). The translation of age-related body composition findings from rodents to humans. Eur J Clin Nutr *73*, 172-178. 10.1038/s41430-018-0324-6.

62. Dutta, S., and Sengupta, P. (2016). Men and mice: Relating their ages. Life Sci *152*, 244-248. 10.1016/j.lfs.2015.10.025.

63. Hudgins, A.D., Tazearslan, C., Tare, A., Zhu, Y., Huffman, D., and Suh, Y. (2018). Age- and Tissue-Specific Expression of Senescence Biomarkers in Mice. Front Genet *9*, 59. 10.3389/fgene.2018.00059.

64. Zahn, J.M., Poosala, S., Owen, A.B., Ingram, D.K., Lustig, A., Carter, A., Weeraratna, A.T., Taub, D.D., Gorospe, M., Mazan-Mamczarz, K., et al. (2007). AGEMAP: a gene expression database for aging in mice. PLoS Genet *3*, e201. 10.1371/journal.pgen.0030201.

65. Young, K., Eudy, E., Bell, R., Loberg, M.A., Stearns, T., Sharma, D., Velten, L., Haas, S., Filippi, M.D., and Trowbridge, J.J. (2021). Decline in IGF1 in the bone marrow microenvironment initiates hematopoietic stem cell aging. Cell Stem Cell *28*, 1473-1482 e1477. 10.1016/j.stem.2021.03.017.

66. Geiger, H., and Florian, M.C. (2018). Mechanisms of Aging of Hematopoietic Stem Cells. Experimental Hematology *64*, S29-S29.

67. Beerman, I. (2017). Accumulation of DNA damage in the aged hematopoietic stem cell compartment. Semin Hematol *54*, 12-18. 10.1053/j.seminhematol.2016.11.001.

68. Flach, J., Bakker, S.T., Mohrin, M., Conroy, P.C., Pietras, E.M., Reynaud, D., Alvarez, S., Diolaiti, M.E., Ugarte, F., Forsberg, E.C., et al. (2014). Replication stress is a potent driver of functional decline in ageing haematopoietic stem cells. Nature *512*, 198-+. 10.1038/nature13619.

69. Poulos, M.G., Ramalingam, P., Gutkin, M.C., Llanos, P., Gilleran, K., Rabbany, S.Y., and Butler, J.M. (2017). Endothelial transplantation rejuvenates aged hematopoietic stem cell function. Journal of Clinical Investigation *127*, 4163-4178. 10.1172/Jci93940.

70. Kusumbe, A.P., Ramasamy, S.K., Itkin, T., Mae, M.A., Langen, U.H., Betsholtz, C., Lapidot, T., and Adams, R.H. (2016). Age-dependent modulation of vascular niches for haematopoietic stem cells (vol 532, pg 380, 2016). Nature *539*. 10.1038/nature19782.

71. Ungvari, Z., Tarantini, S., Donato, A.J., Galvan, V., and Csiszar, A. (2018). Mechanisms of Vascular Aging. Circulation Research *123*, 849-867. 10.1161/Circresaha.118.311378.

72. Ho, Y.H., del Toro, R., Rivera-Torres, J., Rak, J., Korn, C., Garcia-Garcia, A., Macias, D., Gonzalez-Gomez, C., del Monte, A., Wittner, M., et al. (2019). Remodeling of Bone Marrow Hematopoietic Stem Cell Niches Promotes Myeloid Cell Expansion during Premature or Physiological Aging. Cell Stem Cell *25*, 407-+. 10.1016/j.stem.2019.06.007.

73. Fox, J.G. (2007). The mouse in biomedical research, 2nd Edition (Elsevier, AP).

74. Partridge, L., Deelen, J., and Slagboom, P.E. (2018). Facing up to the global challenges of ageing. Nature *561*, 45-56. 10.1038/s41586-018-0457-8.

75. Sander, M., Oxlund, B., Jespersen, A., Krasnik, A., Mortensen, E.L., Westendorp, R.G., and Rasmussen, L.J. (2015). The challenges of human population ageing. Age Ageing *44*, 185-187. 10.1093/ageing/afu189.

76. Vollset, S.E., Goren, E., Yuan, C.W., Cao, J., Smith, A.E., Hsiao, T., Bisignano, C., Azhar, G.S., Castro, E., Chalek, J., et al. (2020). Fertility, mortality, migration, and population scenarios for 195 countries and territories from 2017 to 2100: a forecasting analysis for the Global Burden of Disease Study. Lancet *396*, 1285-1306. 10.1016/S0140-6736(20)30677-2.

77. Harper, S. (2014). Economic and social implications of aging societies. Science *346*, 587-591. 10.1126/science.1254405.

78. Crimmins, E.M., and Beltran-Sanchez, H. (2011). Mortality and Morbidity Trends: Is There Compression of Morbidity? J Gerontol B-Psychol *66*, 75-86. 10.1093/geronb/gbq088.

79. Niccoli, T., and Partridge, L. (2012). Ageing as a Risk Factor for Disease. Curr Biol *22*, R741-R752. 10.1016/j.cub.2012.07.024.

80. Crimmins, E.M. (2015). Lifespan and Healthspan: Past, Present, and Promise. Gerontologist *55*, 901-911. 10.1093/geront/gnv130.

81. Weir, H.K., Thompson, T.D., Stewart, S.L., and White, M.C. (2021). Cancer Incidence Projections in the United States Between 2015 and 2050. Prev Chronic Dis *18*. ARTN 210006

10.5888/pcd18.210006.

82. Gopal, S., Wood, W.A., Lee, S.J., Shea, T.C., Naresh, K.N., Kazembe, P.N., Casper, C., Hesseling, P.B., and Mitsuyasu, R.T. (2012). Meeting the challenge of hematologic malignancies in sub-Saharan Africa. Blood *119*, 5078-5087. 10.1182/blood-2012-02-387092.

83. Zhang, N., Wu, J., Wang, Q., Liang, Y., Li, X., Chen, G., Ma, L., Liu, X., and Zhou, F. (2023). Global burden of hematologic malignancies and evolution patterns over the past 30 years. Blood Cancer J *13*, 82. 10.1038/s41408-023-00853-3.

84. Young, A.L., Challen, G.A., Birmann, B.M., and Druley, T.E. (2016). Clonal haematopoiesis harbouring AML-associated mutations is ubiquitous in healthy adults. Nat Commun *7*, 12484. 10.1038/ncomms12484.

85. Buscarlet, M., Provost, S., Zada, Y.F., Barhdadi, A., Bourgoin, V., Lepine, G., Mollica, L., Szuber, N., Dube, M.P., and Busque, L. (2017). DNMT3A and TET2 dominate clonal hematopoiesis and demonstrate benign phenotypes and different genetic predispositions. Blood *130*, 753-762. 10.1182/blood-2017-04-777029.

86. Zink, F., Stacey, S.N., Norddahl, G.L., Frigge, M.L., Magnusson, O.T., Jonsdottir, I., Thorgeirsson, T.E., Sigurdsson, A., Gudjonsson, S.A., Gudmundsson, J., et al. (2017). Clonal hematopoiesis, with and without candidate driver mutations, is common in the elderly. Blood *130*, 742-752. 10.1182/blood-2017-02-769869.

87. Jaiswal, S., and Ebert, B.L. (2019). Clonal hematopoiesis in human aging and disease. Science *366*. 10.1126/science.aan4673.

88. Ayachi, S., Buscarlet, M., and Busque, L. (2020). 60 Years of clonal hematopoiesis research: From X-chromosome inactivation studies to the identification of driver mutations. Exp Hematol *83*, 2-11. 10.1016/j.exphem.2020.01.008.

89. Wang, Y., Sano, S., Ogawa, H., Horitani, K., Evans, M.A., Yura, Y., Miura-Yura, E., Doviak, H., and Walsh, K. (2022). Murine models of clonal haematopoiesis to assess mechanisms of cardiovascular disease. Cardiovasc Res *118*, 1413-1432. 10.1093/cvr/cvab215.

90. Gaulin, C., Kelemen, K., and Arana Yi, C. (2022). Molecular Pathways in Clonal Hematopoiesis: From the Acquisition of Somatic Mutations to Transformation into Hematologic Neoplasm. Life (Basel) *12*. 10.3390/life12081135.

91. Venney, D., Mohd-Sarip, A., and Mills, K.I. (2021). The Impact of Epigenetic Modifications in Myeloid Malignancies. Int J Mol Sci *22*. 10.3390/ijms22095013.

92. Belizaire, R., Wong, W.J., Robinette, M.L., and Ebert, B.L. (2023). Clonal haematopoiesis and dysregulation of the immune system. Nat Rev Immunol. 10.1038/s41577-023-00843-3.

93. Sperotto, A., Bochicchio, M.T., Simonetti, G., Buccisano, F., Peccatori, J., Piemontese, S., Calistri, E., Ciotti, G., Pierdomenico, E., De Marchi, R., et al.

(2023). Measurable Residual Disease and Clonal Evolution in Acute Myeloid Leukemia from Diagnosis to Post-Transplant Follow-Up: The Role of Next-Generation Sequencing. Biomedicines *11*. 10.3390/biomedicines11020359.

94. Fabre, M.A., de Almeida, J.G., Fiorillo, E., Mitchell, E., Damaskou, A., Rak, J., Orru, V., Marongiu, M., Chapman, M.S., Vijayabaskar, M.S., et al. (2022). The longitudinal dynamics and natural history of clonal haematopoiesis. Nature *606*, 335-342. 10.1038/s41586-022-04785-z.

95. Bick, A.G., Weinstock, J.S., Nandakumar, S.K., Fulco, C.P., Bao, E.L., Zekavat, S.M., Szeto, M.D., Liao, X., Leventhal, M.J., Nasser, J., et al. (2020). Inherited causes of clonal haematopoiesis in 97,691 whole genomes. Nature *586*, 763-768. 10.1038/s41586-020-2819-2.

96. Evans, M.A., Sano, S., and Walsh, K. (2020). Cardiovascular Disease, Aging, and Clonal Hematopoiesis. Annu Rev Pathol *15*, 419-438. 10.1146/annurev-pathmechdis-012419-032544.

97. Jaiswal, S., Fontanillas, P., Flannick, J., Manning, A., Grauman, P.V., Mar, B.G., Lindsley, R.C., Mermel, C.H., Burtt, N., Chavez, A., et al. (2014). Age-related clonal hematopoiesis associated with adverse outcomes. N Engl J Med *371*, 2488-2498. 10.1056/NEJMoa1408617.

98. Franceschi, C., Garagnani, P., Morsiani, C., Conte, M., Santoro, A., Grignolio, A., Monti, D., Capri, M., and Salvioli, S. (2018). The Continuum of Aging and Age-Related Diseases: Common Mechanisms but Different Rates. Front Med (Lausanne) *5*, 61. 10.3389/fmed.2018.00061.

99. Ferrucci, L., and Fabbri, E. (2018). Inflammageing: chronic inflammation in ageing, cardiovascular disease, and frailty. Nat Rev Cardiol *15*, 505-522. 10.1038/s41569-018-0064-2.

100. Busque, L., Patel, J.P., Figueroa, M.E., Vasanthakumar, A., Provost, S., Hamilou, Z., Mollica, L., Li, J., Viale, A., Heguy, A., et al. (2012). Recurrent somatic TET2 mutations in normal elderly individuals with clonal hematopoiesis. Nat Genet *44*, 1179-1181. 10.1038/ng.2413.

101. Xie, M., Lu, C., Wang, J., McLellan, M.D., Johnson, K.J., Wendl, M.C., McMichael, J.F., Schmidt, H.K., Yellapantula, V., Miller, C.A., et al. (2014). Age-related mutations associated with clonal hematopoietic expansion and malignancies. Nat Med *20*, 1472-1478. 10.1038/nm.3733.

102. Genovese, G., Kahler, A.K., Handsaker, R.E., Lindberg, J., Rose, S.A., Bakhoum, S.F., Chambert, K., Mick, E., Neale, B.M., Fromer, M., et al. (2014). Clonal hematopoiesis and blood-cancer risk inferred from blood DNA sequence. N Engl J Med *371*, 2477-2487. 10.1056/NEJMoa1409405.

103. Nagase, R., Inoue, D., Pastore, A., Fujino, T., Hou, H.A., Yamasaki, N., Goyama, S., Saika, M., Kanai, A., Sera, Y., et al. (2018). Expression of mutant Asxl1 perturbs hematopoiesis and promotes susceptibility to leukemic transformation. J Exp Med *215*, 1729-1747. 10.1084/jem.20171151.

104. Kuhn, R., Schwenk, F., Aguet, M., and Rajewsky, K. (1995). Inducible gene targeting in mice. Science *269*, 1427-1429. 10.1126/science.7660125.

105. Stadtfeld, M., and Graf, T. (2005). Assessing the role of hematopoietic plasticity for endothelial and hepatocyte development by non-invasive lineage tracing. Development *132*, 203-213. 10.1242/dev.01558.

106. Basheer, F., and Vassiliou, G. (2021). Mouse Models of Myeloid Malignancies. Cold Spring Harb Perspect Med *11*. 10.1101/cshperspect.a035535.

107. SanMiguel, J.M., Young, K., and Trowbridge, J.J. (2020). Hand in hand: intrinsic and extrinsic drivers of aging and clonal hematopoiesis. Exp Hematol *91*, 1-9. 10.1016/j.exphem.2020.09.197.

108. Trowbridge, J.J., and Starczynowski, D.T. (2021). Innate immune pathways and inflammation in hematopoietic aging, clonal hematopoiesis, and MDS. J Exp Med *218*. 10.1084/jem.20201544.

109. Loberg, M.A., Bell, R.K., Goodwin, L.O., Eudy, E., Miles, L.A., SanMiguel, J.M., Young, K., Bergstrom, D.E., Levine, R.L., Schneider, R.K., and Trowbridge, J.J. (2019). Sequentially inducible mouse models reveal that Npm1 mutation causes malignant transformation of Dnmt3a-mutant clonal hematopoiesis. Leukemia *33*, 1635-1649. 10.1038/s41375-018-0368-6.

110. Zhang, C.R.C., Nix, D., Gregory, M., Ciorba, M.A., Ostrander, E.L., Newberry, R.D., Spencer, D.H., and Challen, G.A. (2019). Inflammatory cytokines promote clonal hematopoiesis with specific mutations in ulcerative colitis patients. Exp Hematol *80*, 36-41 e33. 10.1016/j.exphem.2019.11.008.

111. Hormaechea-Agulla, D., Matatall, K.A., Le, D.T., Kain, B., Long, X., Kus, P., Jaksik, R., Challen, G.A., Kimmel, M., and King, K.Y. (2021). Chronic infection drives Dnmt3a-loss-of-function clonal hematopoiesis via IFNgamma signaling. Cell Stem Cell *28*, 1428-1442 e1426. 10.1016/j.stem.2021.03.002.

112. Zioni, N., Bercovich, A.A., Chapal-Ilani, N., Bacharach, T., Rappoport, N., Solomon, A., Avraham, R., Kopitman, E., Porat, Z., Sacma, M., et al. (2023). Inflammatory signals from fatty bone marrow support DNMT3A driven clonal hematopoiesis. Nat Commun *14*, 2070. 10.1038/s41467-023-36906-1.

113. SanMiguel, J.M., Eudy, E., Loberg, M.A., Young, K.A., Mistry, J.J., Mujica, K.D., Schwartz, L.S., Stearns, T.M., Challen, G.A., and Trowbridge, J.J. (2022). Distinct Tumor Necrosis Factor Alpha Receptors Dictate Stem Cell Fitness versus

Lineage Output in Dnmt3a-Mutant Clonal Hematopoiesis. Cancer Discov *12*, 2763-2773. 10.1158/2159-8290.CD-22-0086.

114. Zhang, J.M., and An, J. (2007). Cytokines, inflammation, and pain. Int Anesthesiol Clin *45*, 27-37. 10.1097/AIA.0b013e318034194e.

115. Moudgil, K.D., and Choubey, D. (2011). Cytokines in autoimmunity: role in induction, regulation, and treatment. J Interferon Cytokine Res *31*, 695-703. 10.1089/jir.2011.0065.

116. Dinarello, C.A. (2007). Historical insights into cytokines. Eur J Immunol *37 Suppl 1*, S34-45. 10.1002/eji.200737772.

117. Metcalf, D. (2008). Hematopoietic cytokines. Blood *111*, 485-491. 10.1182/blood-2007-03-079681.

118. Jaiswal, S., and Libby, P. (2020). Clonal haematopoiesis: connecting ageing and inflammation in cardiovascular disease. Nat Rev Cardiol *17*, 137-144. 10.1038/s41569-019-0247-5.

119. Gibson, C.J., Kim, H.T., Zhao, L., Murdock, H.M., Hambley, B., Ogata, A., Madero-Marroquin, R., Wang, S., Green, L., Fleharty, M., et al. (2022). Donor Clonal Hematopoiesis and Recipient Outcomes After Transplantation. J Clin Oncol *40*, 189-201. 10.1200/JCO.21.02286.

120. Murakami, M., Kamimura, D., and Hirano, T. (2019). Pleiotropy and Specificity: Insights from the Interleukin 6 Family of Cytokines. Immunity *50*, 812-831. 10.1016/j.immuni.2019.03.027.

121. Jones, S.A., and Jenkins, B.J. (2018). Recent insights into targeting the IL-6 cytokine family in inflammatory diseases and cancer. Nat Rev Immunol *18*, 773-789. 10.1038/s41577-018-0066-7.

122. Turner, M.D., Nedjai, B., Hurst, T., and Pennington, D.J. (2014). Cytokines and chemokines: At the crossroads of cell signalling and inflammatory disease. Biochim Biophys Acta *1843*, 2563-2582. 10.1016/j.bbamcr.2014.05.014.

123. Lantieri, F., and Bachetti, T. (2022). OSM/OSMR and Interleukin 6 Family Cytokines in Physiological and Pathological Condition. Int J Mol Sci *23*. 10.3390/ijms231911096.

124. Houben, E., Hellings, N., and Broux, B. (2019). Oncostatin M, an Underestimated Player in the Central Nervous System. Front Immunol *10*, 1165. 10.3389/fimmu.2019.01165.

125. Zarling, J.M., Shoyab, M., Marquardt, H., Hanson, M.B., Lioubin, M.N., and Todaro, G.J. (1986). Oncostatin M: a growth regulator produced by differentiated

histiocytic lymphoma cells. Proc Natl Acad Sci U S A *83*, 9739-9743. 10.1073/pnas.83.24.9739.

126. Bazan, J.F. (1991). Neuropoietic cytokines in the hematopoietic fold. Neuron *7*, 197-208. 10.1016/0896-6273(91)90258-2.

127. Tanaka, M., and Miyajima, A. (2003). Oncostatin M, a multifunctional cytokine. Rev Physiol Biochem Pharmacol *149*, 39-52. 10.1007/s10254-003-0013-1.

128. Jeffery, E., Price, V., and Gearing, D.P. (1993). Close proximity of the genes for leukemia inhibitory factor and oncostatin M. Cytokine *5*, 107-111. 10.1016/1043-4666(93)90048-a.

129. Giovannini, M., Djabali, M., McElligott, D., Selleri, L., and Evans, G.A. (1993). Tandem linkage of genes coding for leukemia inhibitory factor (LIF) and oncostatin M (OSM) on human chromosome 22. Cytogenet Cell Genet *64*, 240-244. 10.1159/000133586.

130. Giovannini, M., Selleri, L., Hermanson, G.G., and Evans, G.A. (1993). Localization of the human oncostatin M gene (OSM) to chromosome 22q12, distal to the Ewing's sarcoma breakpoint. Cytogenet Cell Genet *62*, 32-34. 10.1159/000133439.

131. Saha, S., Chakraborty, A., and Bandyopadhyay, S.S. (2016). Stabilization of Oncostatin-M mRNA by Binding of Nucleolin to a GC-Rich Element in Its 3'UTR. J Cell Biochem *117*, 988-999. 10.1002/jcb.25384.

132. Mosley, B., De Imus, C., Friend, D., Boiani, N., Thoma, B., Park, L.S., and Cosman, D. (1996). Dual oncostatin M (OSM) receptors. Cloning and characterization of an alternative signaling subunit conferring OSM-specific receptor activation. J Biol Chem *271*, 32635-32643. 10.1074/jbc.271.51.32635.

133. Kubin, T., Gajawada, P., Bramlage, P., Hein, S., Berge, B., Cetinkaya, A., Burger, H., Schonburg, M., Schaper, W., Choi, Y.H., and Richter, M. (2022). The Role of Oncostatin M and Its Receptor Complexes in Cardiomyocyte Protection, Regeneration, and Failure. Int J Mol Sci *23*. 10.3390/ijms23031811.

134. Richards, C.D. (2013). The enigmatic cytokine oncostatin m and roles in disease. ISRN Inflamm *2013*, 512103. 10.1155/2013/512103.

135. Rose, T.M., and Bruce, A.G. (1991). Oncostatin M is a member of a cytokine family that includes leukemia-inhibitory factor, granulocyte colony-stimulating factor, and interleukin 6. Proc Natl Acad Sci U S A *88*, 8641-8645. 10.1073/pnas.88.19.8641.

136. Chen, D., Chu, C.Y., Chen, C.Y., Yang, H.C., Chiang, Y.Y., Lin, T.Y., Chiang, I.P., Chuang, D.Y., Yu, C.C., and Chow, K.C. (2008). Expression of short-form

oncostatin M receptor as a decoy receptor in lung adenocarcinomas. J Pathol *215*, 290-299. 10.1002/path.2361.

137. Rose-John, S. (2018). Interleukin-6 Family Cytokines. Cold Spring Harb Perspect Biol *10*. 10.1101/cshperspect.a028415.

138. Chollangi, S., Mather, T., Rodgers, K.K., and Ash, J.D. (2012). A unique loop structure in oncostatin M determines binding affinity toward oncostatin M receptor and leukemia inhibitory factor receptor. J Biol Chem *287*, 32848-32859. 10.1074/jbc.M112.387324.

139. Olivier, C., Auguste, P., Chabbert, M., Lelievre, E., Chevalier, S., and Gascan, H. (2000). Identification of a gp130 cytokine receptor critical site involved in oncostatin M response. J Biol Chem *275*, 5648-5656. 10.1074/jbc.275.8.5648.

140. Martinez-Fabregas, J., Wilmes, S., Wang, L., Hafer, M., Pohler, E., Lokau, J., Garbers, C., Cozzani, A., Fyfe, P.K., Piehler, J., et al. (2019). Kinetics of cytokine receptor trafficking determine signaling and functional selectivity. Elife *8*. 10.7554/eLife.49314.

141. Walker, E.C., McGregor, N.E., Poulton, I.J., Solano, M., Pompolo, S., Fernandes, T.J., Constable, M.J., Nicholson, G.C., Zhang, J.G., Nicola, N.A., et al. (2010). Oncostatin M promotes bone formation independently of resorption when signaling through leukemia inhibitory factor receptor in mice. J Clin Invest *120*, 582-592. 10.1172/JCI40568.

142. Sims, N.A. (2021). Influences of the IL-6 cytokine family on bone structure and function. Cytokine *146*, 155655. 10.1016/j.cyto.2021.155655.

143. Drechsler, J., Grotzinger, J., and Hermanns, H.M. (2012). Characterization of the rat oncostatin M receptor complex which resembles the human, but differs from the murine cytokine receptor. PLoS One *7*, e43155. 10.1371/journal.pone.0043155.

144. Adrian-Segarra, J.M., Sreenivasan, K., Gajawada, P., Lorchner, H., Braun, T., and Poling, J. (2018). The AB loop of oncostatin M (OSM) determines species-specific signaling in humans and mice. J Biol Chem *293*, 20181-20199. 10.1074/jbc.RA118.004375.

145. Mass, O.A., Tuccinardi, J., Woodbury, L., Wolf, C.L., Grantham, B., Holdaway, K., Pu, X., King, M.D., Warner, D.L., Jorcyk, C.L., and Warner, L.R. (2021). Bioactive recombinant human oncostatin M for NMR-based screening in drug discovery. Sci Rep *11*, 16174. 10.1038/s41598-021-95424-6.

146. Masjedi, A., Hajizadeh, F., Beigi Dargani, F., Beyzai, B., Aksoun, M., Hojjat-Farsangi, M., Zekiy, A., and Jadidi-Niaragh, F. (2021). Oncostatin M: A mysterious cytokine in cancers. Int Immunopharmacol *90*, 107158. 10.1016/j.intimp.2020.107158.

147. Bharadwaj, U., Kasembeli, M.M., Robinson, P., and Tweardy, D.J. (2020). Targeting Janus Kinases and Signal Transducer and Activator of Transcription 3 to Treat Inflammation, Fibrosis, and Cancer: Rationale, Progress, and Caution. Pharmacol Rev *72*, 486-526. 10.1124/pr.119.018440.

148. Caligiuri, A., Gitto, S., Lori, G., Marra, F., Parola, M., Cannito, S., and Gentilini, A. (2022). Oncostatin M: From Intracellular Signaling to Therapeutic Targets in Liver Cancer. Cancers (Basel) *14*. 10.3390/cancers14174211.

149. Sakaue, S., Kanai, M., Tanigawa, Y., Karjalainen, J., Kurki, M., Koshiba, S., Narita, A., Konuma, T., Yamamoto, K., Akiyama, M., et al. (2021). A cross-population atlas of genetic associations for 220 human phenotypes. Nat Genet *53*, 1415-1424. 10.1038/s41588-021-00931-x.

150. Sempowski, G.D., Hale, L.P., Sundy, J.S., Massey, J.M., Koup, R.A., Douek, D.C., Patel, D.D., and Haynes, B.F. (2000). Leukemia inhibitory factor, oncostatin M, IL-6, and stem cell factor mRNA expression in human thymus increases with age and is associated with thymic atrophy. J Immunol *164*, 2180-2187. 10.4049/jimmunol.164.4.2180.

151. Flohr Svendsen, A., Yang, D., Kim, K., Lazare, S., Skinder, N., Zwart, E., Mura-Meszaros, A., Ausema, A., von Eyss, B., de Haan, G., and Bystrykh, L. (2021). A comprehensive transcriptome signature of murine hematopoietic stem cell aging. Blood *138*, 439-451. 10.1182/blood.2020009729.

152. Guo, A., Ross, C., Chande, N., Gregor, J., Ponich, T., Khanna, R., Sey, M., Beaton, M., Yan, B., Kim, R.B., and Wilson, A. (2022). High oncostatin M predicts lack of clinical remission for patients with inflammatory bowel disease on tumor necrosis factor alpha antagonists. Sci Rep *12*, 1185. 10.1038/s41598-022-05208-9.

153. Cao, Y., Dai, Y., Zhang, L., Wang, D., Yu, Q., Hu, W., Wang, X., Yu, P., Ping, Y., Sun, T., et al. (2022). Serum oncostatin M is a potential biomarker of disease activity and infliximab response in inflammatory bowel disease measured by chemiluminescence immunoassay. Clin Biochem *100*, 35-41. 10.1016/j.clinbiochem.2021.11.011.

154. Verstockt, S., Verstockt, B., Machiels, K., Vancamelbeke, M., Ferrante, M., Cleynen, I., De Hertogh, G., and Vermeire, S. (2021). Oncostatin M Is a Biomarker of Diagnosis, Worse Disease Prognosis, and Therapeutic Nonresponse in Inflammatory Bowel Disease. Inflamm Bowel Dis *27*, 1564-1575. 10.1093/ibd/izab032.

155. Liu, Q., Lan, T., Song, Y., Cai, J., Yu, X., and Chen, W. (2020). Oncostatin M expression and TP53 mutation status regulate tumor-infiltration of immune cells and survival outcomes in cholangiocarcinoma. Aging (Albany NY) *12*, 21518-21543. 10.18632/aging.103936.

156. Morris, R., Kershaw, N.J., and Babon, J.J. (2018). The molecular details of cytokine signaling via the JAK/STAT pathway. Protein Sci *27*, 1984-2009. 10.1002/pro.3519.

157. Ma, Y., Streiff, R.J., Liu, J., Spence, M.J., and Vestal, R.E. (1999). Cloning and characterization of human oncostatin M promoter. Nucleic Acids Res *27*, 4649-4657. 10.1093/nar/27.23.4649.

158. Avagyan, S., and Zon, L.I. (2023). Clonal hematopoiesis and inflammation - the perpetual cycle. Trends Cell Biol *33*, 695-707. 10.1016/j.tcb.2022.12.001.

159. Abegunde, S.O., Buckstein, R., Wells, R.A., and Rauh, M.J. (2018). An inflammatory environment containing TNFalpha favors Tet2-mutant clonal hematopoiesis. Exp Hematol *59*, 60-65. 10.1016/j.exphem.2017.11.002.

160. Cai, Z., Kotzin, J.J., Ramdas, B., Chen, S., Nelanuthala, S., Palam, L.R., Pandey, R., Mali, R.S., Liu, Y., Kelley, M.R., et al. (2018). Inhibition of Inflammatory Signaling in Tet2 Mutant Preleukemic Cells Mitigates Stress-Induced Abnormalities and Clonal Hematopoiesis. Cell Stem Cell *23*, 833-849 e835. 10.1016/j.stem.2018.10.013.

161. Stross, C., Radtke, S., Clahsen, T., Gerlach, C., Volkmer-Engert, R., Schaper, F., Heinrich, P.C., and Hermanns, H.M. (2006). Oncostatin M receptor-mediated signal transduction is negatively regulated by SOCS3 through a receptor tyrosine-independent mechanism. J Biol Chem *281*, 8458-8468. 10.1074/jbc.M511212200.

162. Avagyan, S., Henninger, J.E., Mannherz, W.P., Mistry, M., Yoon, J., Yang, S., Weber, M.C., Moore, J.L., and Zon, L.I. (2021). Resistance to inflammation underlies enhanced fitness in clonal hematopoiesis. Science *374*, 768-772. 10.1126/science.aba9304.

163. Colom Diaz, P.A., Mistry, J.J., and Trowbridge, J.J. (2023). Hematopoietic Stem Cell Aging and Leukemia Transformation. Blood. 10.1182/blood.2022017933.

164. Bhattacharya, R., Zekavat, S.M., Haessler, J., Fornage, M., Raffield, L., Uddin, M.M., Bick, A.G., Niroula, A., Yu, B., Gibson, C., et al. (2022). Clonal Hematopoiesis Is Associated With Higher Risk of Stroke. Stroke *53*, 788-797. 10.1161/STROKEAHA.121.037388.

165. Mooney, L., Goodyear, C.S., Chandra, T., Kirschner, K., Copland, M., Petrie, M.C., and Lang, N.N. (2021). Clonal haematopoiesis of indeterminate potential: intersections between inflammation, vascular disease and heart failure. Clin Sci (Lond) *135*, 991-1007. 10.1042/CS20200306.

166. Papaemmanuil, E., Gerstung, M., Malcovati, L., Tauro, S., Gundem, G., Van Loo, P., Yoon, C.J., Ellis, P., Wedge, D.C., Pellagatti, A., et al. (2013). Clinical and biological implications of driver mutations in myelodysplastic syndromes. Blood *122*, 3616-3627; quiz 3699. 10.1182/blood-2013-08-518886.

167. Nachun, D., Lu, A.T., Bick, A.G., Natarajan, P., Weinstock, J., Szeto, M.D., Kathiresan, S., Abecasis, G., Taylor, K.D., Guo, X., et al. (2021). Clonal hematopoiesis associated with epigenetic aging and clinical outcomes. Aging Cell *20*, e13366. 10.1111/acel.13366.

168. Florez, M.A., Tran, B.T., Wathan, T.K., DeGregori, J., Pietras, E.M., and King, K.Y. (2022). Clonal hematopoiesis: Mutation-specific adaptation to environmental change. Cell Stem Cell *29*, 882-904. 10.1016/j.stem.2022.05.006.

169. Cook, E.K., Izukawa, T., Young, S., Rosen, G., Jamali, M., Zhang, L., Johnson, D., Bain, E., Hilland, J., Ferrone, C.K., et al. (2019). Comorbid and inflammatory characteristics of genetic subtypes of clonal hematopoiesis. Blood Adv *3*, 2482-2486. 10.1182/bloodadvances.2018024729.

170. Caiado, F., Kovtonyuk, L.V., Gonullu, N.G., Fullin, J., Boettcher, S., and Manz, M.G. (2023). Aging drives Tet2+/- clonal hematopoiesis via IL-1 signaling. Blood *141*, 886-903. 10.1182/blood.2022016835.

171. Fuster, J.J., Zuriaga, M.A., Zorita, V., MacLauchlan, S., Polackal, M.N., Viana-Huete, V., Ferrer-Perez, A., Matesanz, N., Herrero-Cervera, A., Sano, S., et al. (2020). TET2-Loss-of-Function-Driven Clonal Hematopoiesis Exacerbates Experimental Insulin Resistance in Aging and Obesity. Cell Rep *33*, 108326. 10.1016/j.celrep.2020.108326.

172. Fujino, T., Goyama, S., Sugiura, Y., Inoue, D., Asada, S., Yamasaki, S., Matsumoto, A., Yamaguchi, K., Isobe, Y., Tsuchiya, A., et al. (2021). Mutant ASXL1 induces age-related expansion of phenotypic hematopoietic stem cells through activation of Akt/mTOR pathway. Nat Commun *12*, 1826. 10.1038/s41467-021-22053-y.

173. Yamashita, M., and Passegue, E. (2019). TNF-alpha Coordinates Hematopoietic Stem Cell Survival and Myeloid Regeneration. Cell Stem Cell *25*, 357-372 e357. 10.1016/j.stem.2019.05.019.

174. Tawara, K., Scott, H., Emathinger, J., Wolf, C., LaJoie, D., Hedeen, D., Bond, L., Montgomery, P., and Jorcyk, C. (2019). HIGH expression of OSM and IL-6 are associated with decreased breast cancer survival: synergistic induction of IL-6 secretion by OSM and IL-1beta. Oncotarget *10*, 2068-2085. 10.18632/oncotarget.26699.

175. Chauhan, D., Kharbanda, S.M., Ogata, A., Urashima, M., Frank, D., Malik, N., Kufe, D.W., and Anderson, K.C. (1995). Oncostatin M induces association of Grb2 with Janus kinase JAK2 in multiple myeloma cells. J Exp Med *182*, 1801-1806. 10.1084/jem.182.6.1801.

176. Chen, M., Ren, R., Lin, W., Xiang, L., Zhao, Z., and Shao, B. (2021). Exploring the oncostatin M (OSM) feed-forward signaling of glioblastoma via STAT3 in pan-cancer analysis. Cancer Cell Int *21*, 565. 10.1186/s12935-021-02260-9.

177. Lee, B.Y., Hogg, E.K.J., Below, C.R., Kononov, A., Blanco-Gomez, A., Heider, F., Xu, J., Hutton, C., Zhang, X., Scheidt, T., et al. (2021). Heterocellular OSM-OSMR signalling reprograms fibroblasts to promote pancreatic cancer growth and metastasis. Nat Commun *12*, 7336. 10.1038/s41467-021-27607-8.

178. Gu, Z.J., Costes, V., Lu, Z.Y., Zhang, X.G., Pitard, V., Moreau, J.F., Bataille, R., Wijdenes, J., Rossi, J.F., and Klein, B. (1996). Interleukin-10 is a growth factor for human myeloma cells by induction of an oncostatin M autocrine loop. Blood *88*, 3972-3986.

179. Bisht, K., McGirr, C., Lee, S.Y., Tseng, H.W., Fleming, W., Alexander, K.A., Matsumoto, T., Barbier, V., Sims, N.A., Muller-Newen, G., et al. (2022). Oncostatin M regulates hematopoietic stem cell (HSC) niches in the bone marrow to restrict HSC mobilization. Leukemia *36*, 333-347. 10.1038/s41375-021-01413-z.

180. Ehlting, C., Bohmer, O., Hahnel, M.J., Thomas, M., Zanger, U.M., Gaestel, M., Knoefel, W.T., Schulte Am Esch, J., Haussinger, D., and Bode, J.G. (2015). Oncostatin M regulates SOCS3 mRNA stability via the MEK-ERK1/2-pathway independent of p38(MAPK)/MK2. Cell Signal *27*, 555-567. 10.1016/j.cellsig.2014.12.016.

181. Ratnadiwakara, M., and Anko, M.L. (2018). mRNA Stability Assay Using transcription inhibition by Actinomycin D in Mouse Pluripotent Stem Cells. Bio Protoc *8*, e3072. 10.21769/BioProtoc.3072.

182. Adrian-Segarra, J.M., Schindler, N., Gajawada, P., Lorchner, H., Braun, T., and Poling, J. (2018). The AB loop and D-helix in binding site III of human Oncostatin M (OSM) are required for OSM receptor activation. J Biol Chem *293*, 7017-7029. 10.1074/jbc.RA118.001920.

183. Hintzen, C., Evers, C., Lippok, B.E., Volkmer, R., Heinrich, P.C., Radtke, S., and Hermanns, H.M. (2008). Box 2 region of the oncostatin M receptor determines specificity for recruitment of Janus kinases and STAT5 activation. J Biol Chem *283*, 19465-19477. 10.1074/jbc.M710157200.

184. Mukouyama, Y., Hara, T., Xu, M., Tamura, K., Donovan, P.J., Kim, H., Kogo, H., Tsuji, K., Nakahata, T., and Miyajima, A. (1998). In vitro expansion of murine multipotential hematopoietic progenitors from the embryonic aorta-gonad-mesonephros region. Immunity *8*, 105-114. 10.1016/s1074-7613(00)80463-x.

185. Mahony, C.B., Pasche, C., and Bertrand, J.Y. (2018). Oncostatin M and Kit-Ligand Control Hematopoietic Stem Cell Fate during Zebrafish Embryogenesis. Stem Cell Reports *10*, 1920-1934. 10.1016/j.stemcr.2018.04.016.

186. Salim, S.Y., AlMalki, N., Macala, K.F., Wiedemeyer, A., Mueller, T.F., Churchill, T.A., Bourque, S.L., and Khadaroo, R.G. (2023). Oncostatin M Receptor Type II

Knockout Mitigates Inflammation and Improves Survival from Sepsis in Mice. Biomedicines *11*. 10.3390/biomedicines11020483.

187. Sofen, H., Bissonnette, R., Yosipovitch, G., Silverberg, J.I., Tyring, S., Loo, W.J., Zook, M., Lee, M., Zou, L., Jiang, G.L., and Paolini, J.F. (2023). Efficacy and safety of vixarelimab, a human monoclonal oncostatin M receptor beta antibody, in moderate-to-severe prurigo nodularis: a randomised, double-blind, placebo-controlled, phase 2a study. EClinicalMedicine *57*, 101826. 10.1016/j.eclinm.2023.101826.

188. Stephens, J.M., and Elks, C.M. (2017). Oncostatin M: Potential Implications for Malignancy and Metabolism. Curr Pharm Des *23*, 3645-3657. 10.2174/1381612823666170704122559.

189. Malik, N., Kallestad, J.C., Gunderson, N.L., Austin, S.D., Neubauer, M.G., Ochs, V., Marquardt, H., Zarling, J.M., Shoyab, M., Wei, C.M., and et al. (1989). Molecular cloning, sequence analysis, and functional expression of a novel growth regulator, oncostatin M. Mol Cell Biol *9*, 2847-2853. 10.1128/mcb.9.7.2847-2853.1989.

190. Araujo, A.M., Abaurrea, A., Azcoaga, P., Lopez-Velazco, J.I., Manzano, S., Rodriguez, J., Rezola, R., Egia-Mendikute, L., Valdes-Mora, F., Flores, J.M., et al. (2022). Stromal oncostatin M cytokine promotes breast cancer progression by reprogramming the tumor microenvironment. J Clin Invest *132*. 10.1172/JCI148667.

191. Auguste, P., Guillet, C., Fourcin, M., Olivier, C., Veziers, J., Pouplard-Barthelaix, A., and Gascan, H. (1997). Signaling of type II oncostatin M receptor. J Biol Chem *272*, 15760-15764. 10.1074/jbc.272.25.15760.

192. Gearing, D.P., Comeau, M.R., Friend, D.J., Gimpel, S.D., Thut, C.J., McGourty, J., Brasher, K.K., King, J.A., Gillis, S., Mosley, B., and et al. (1992). The IL-6 signal transducer, gp130: an oncostatin M receptor and affinity converter for the LIF receptor. Science *255*, 1434-1437. 10.1126/science.1542794.

193. Ichihara, M., Hara, T., Kim, H., Murate, T., and Miyajima, A. (1997). Oncostatin M and leukemia inhibitory factor do not use the same functional receptor in mice. Blood *90*, 165-173.

194. Tanaka, M., Hirabayashi, Y., Sekiguchi, T., Inoue, T., Katsuki, M., and Miyajima, A. (2003). Targeted disruption of oncostatin M receptor results in altered hematopoiesis. Blood *102*, 3154-3162. 10.1182/blood-2003-02-0367.

195. Uhlen, M., Karlsson, M.J., Hober, A., Svensson, A.S., Scheffel, J., Kotol, D., Zhong, W., Tebani, A., Strandberg, L., Edfors, F., et al. (2019). The human secretome. Sci Signal *12*. 10.1126/scisignal.aaz0274.

196. Uhlen, M., Karlsson, M.J., Zhong, W., Tebani, A., Pou, C., Mikes, J., Lakshmikanth, T., Forsstrom, B., Edfors, F., Odeberg, J., et al. (2019). A genome-wide transcriptomic analysis of protein-coding genes in human blood cells. Science *366*. 10.1126/science.aax9198.

197. Uhlen, M., Fagerberg, L., Hallstrom, B.M., Lindskog, C., Oksvold, P., Mardinoglu, A., Sivertsson, A., Kampf, C., Sjostedt, E., Asplund, A., et al. (2015). Proteomics. Tissue-based map of the human proteome. Science *347*, 1260419. 10.1126/science.1260419.

198. Bastian, F.B., Roux, J., Niknejad, A., Comte, A., Fonseca Costa, S.S., de Farias, T.M., Moretti, S., Parmentier, G., de Laval, V.R., Rosikiewicz, M., et al. (2021). The Bgee suite: integrated curated expression atlas and comparative transcriptomics in animals. Nucleic Acids Res *49*, D831-D847. 10.1093/nar/gkaa793.

199. Wang, E.C.E., Dai, Z., Ferrante, A.W., Drake, C.G., and Christiano, A.M. (2019). A Subset of TREM2(+) Dermal Macrophages Secretes Oncostatin M to Maintain Hair Follicle Stem Cell Quiescence and Inhibit Hair Growth. Cell Stem Cell *24*, 654-669 e656. 10.1016/j.stem.2019.01.011.

200. Brolund, L., Kuster, A., Korr, S., Vogt, M., and Muller-Newen, G. (2011). A receptor fusion protein for the inhibition of murine oncostatin M. BMC Biotechnol *11*, 3. 10.1186/1472-6750-11-3.

201. West, N.R., Hegazy, A.N., Owens, B.M.J., Bullers, S.J., Linggi, B., Buonocore, S., Coccia, M., Gortz, D., This, S., Stockenhuber, K., et al. (2017). Oncostatin M drives intestinal inflammation and predicts response to tumor necrosis factor-neutralizing therapy in patients with inflammatory bowel disease. Nat Med *23*, 579-589. 10.1038/nm.4307.

202. Schwartz, L.S., Young, K.A., Stearns, T.M., Boyer, N., Mujica, K.D., and Trowbridge, J.J. (2023). Oncostatin M is a Master Regulator of an Inflammatory Network in Dnmt3a -Mutant Hematopoietic Stem Cells. bioRxiv. 10.1101/2023.07.12.548764.

203. Huang da, W., Sherman, B.T., and Lempicki, R.A. (2009). Systematic and integrative analysis of large gene lists using DAVID bioinformatics resources. Nat Protoc *4*, 44-57. 10.1038/nprot.2008.211.

204. Sherman, B.T., Hao, M., Qiu, J., Jiao, X., Baseler, M.W., Lane, H.C., Imamichi, T., and Chang, W. (2022). DAVID: a web server for functional enrichment analysis and functional annotation of gene lists (2021 update). Nucleic Acids Res *50*, W216-W221. 10.1093/nar/gkac194.

205. Lorchner, H., Adrian-Segarra, J.M., Waechter, C., Wagner, R., Goes, M.E., Brachmann, N., Sreenivasan, K., Wietelmann, A., Gunther, S., Doll, N., et al. (2021). Concomitant Activation of OSM and LIF Receptor by a Dual-Specific

hlOSM Variant Confers Cardioprotection after Myocardial Infarction in Mice. Int J Mol Sci *23*. 10.3390/ijms23010353.

206. Headland, S.E., Dengler, H.S., Xu, D., Teng, G., Everett, C., Ratsimandresey, R.A., Yan, D., Kang, J., Ganeshan, K., Nazarova, E.V., et al. (2022). Oncostatin M expression induced by bacterial triggers drives airway inflammatory and mucus secretion in severe asthma. Sci Transl Med *14*, eabf8188. 10.1126/scitranslmed.abf8188.

207. Canli, O., Nicolas, A.M., Gupta, J., Finkelmeier, F., Goncharova, O., Pesic, M., Neumann, T., Horst, D., Lower, M., Sahin, U., and Greten, F.R. (2017). Myeloid Cell-Derived Reactive Oxygen Species Induce Epithelial Mutagenesis. Cancer Cell *32*, 869-883 e865. 10.1016/j.ccell.2017.11.004.

208. Diveu, C., Venereau, E., Froger, J., Ravon, E., Grimaud, L., Rousseau, F., Chevalier, S., and Gascan, H. (2006). Molecular and functional characterization of a soluble form of oncostatin M/interleukin-31 shared receptor. J Biol Chem *281*, 36673-36682. 10.1074/jbc.M607005200.

209. Winstanley-Zarach, P., Rot, G., Kuba, S., Smagul, A., Peffers, M.J., and Tew, S.R. (2023). Analysis of RNA Polyadenylation in Healthy and Osteoarthritic Human Articular Cartilage. Int J Mol Sci *24*. 10.3390/ijms24076611.

210. de Almeida, A.R., Dantas, A.T., Pereira, M.C., de Melo Rego, M.J.B., Guimaraes Goncalves, R.S., Pitta, I.D.R., Branco Pinto Duarte, A.L., Parra Abdalla, D.S., and da Rocha Pitta, M.G. (2020). Increased levels of the soluble oncostatin M receptor (sOSMR) and glycoprotein 130 (sgp130) in systemic sclerosis patients and associations with clinical parameters. Immunobiology *225*, 151964. 10.1016/j.imbio.2020.151964.

211. Zhao, L., Zhao, J., Zhong, K., Tong, A., and Jia, D. (2022). Targeted protein degradation: mechanisms, strategies and application. Signal Transduct Target Ther *7*, 113. 10.1038/s41392-022-00966-4.

212. Ciechanover, A., and Schwartz, A.L. (1998). The ubiquitin-proteasome pathway: the complexity and myriad functions of proteins death. Proc Natl Acad Sci U S A *95*, 2727-2730. 10.1073/pnas.95.6.2727.

213. Barreyro, L., Sampson, A.M., Ishikawa, C., Hueneman, K.M., Choi, K., Pujato, M.A., Chutipongtanate, S., Wyder, M., Haffey, W.D., O'Brien, E., et al. (2022). Blocking UBE2N abrogates oncogenic immune signaling in acute myeloid leukemia. Sci Transl Med *14*, eabb7695. 10.1126/scitranslmed.abb7695.

214. Cheng, J., Fan, Y.H., Xu, X., Zhang, H., Dou, J., Tang, Y., Zhong, X., Rojas, Y., Yu, Y., Zhao, Y., et al. (2014). A small-molecule inhibitor of UBE2N induces neuroblastoma cell death via activation of p53 and JNK pathways. Cell Death Dis *5*, e1079. 10.1038/cddis.2014.54.

215. Zhang, H., Li, H.S., Hillmer, E.J., Zhao, Y., Chrisikos, T.T., Hu, H., Wu, X., Thompson, E.J., Clise-Dwyer, K., Millerchip, K.A., et al. (2018). Genetic rescue of lineage-balanced blood cell production reveals a crucial role for STAT3 antiinflammatory activity in hematopoiesis. Proc Natl Acad Sci U S A *115*, E2311-E2319. 10.1073/pnas.1713889115.

216. Redell, M.S., Ruiz, M.J., Alonzo, T.A., Gerbing, R.B., and Tweardy, D.J. (2011). Stat3 signaling in acute myeloid leukemia: ligand-dependent and -independent activation and induction of apoptosis by a novel small-molecule Stat3 inhibitor. Blood *117*, 5701-5709. 10.1182/blood-2010-04-280123.

217. Moser, B., Edtmayer, S., Witalisz-Siepracka, A., and Stoiber, D. (2021). The Ups and Downs of STAT Inhibition in Acute Myeloid Leukemia. Biomedicines *9*. 10.3390/biomedicines9081051.

218. Schuringa, J.J., Wierenga, A.T., Kruijer, W., and Vellenga, E. (2000). Constitutive Stat3, Tyr705, and Ser727 phosphorylation in acute myeloid leukemia cells caused by the autocrine secretion of interleukin-6. Blood *95*, 3765-3770.

219. Potts, K.S., Cameron, R.C., Metidji, A., Ghazale, N., Wallace, L., Leal-Cervantes, A.I., Palumbo, R., Barajas, J.M., Gupta, V., Aluri, S., et al. (2022). Splicing factor deficits render hematopoietic stem and progenitor cells sensitive to STAT3 inhibition. Cell Rep *41*, 111825. 10.1016/j.celrep.2022.111825.

220. Rose-John, S., Jenkins, B.J., Garbers, C., Moll, J.M., and Scheller, J. (2023). Targeting IL-6 trans-signalling: past, present and future prospects. Nat Rev Immunol *23*, 666-681. 10.1038/s41577-023-00856-y.

221. Deller, M.C., Hudson, K.R., Ikemizu, S., Bravo, J., Jones, E.Y., and Heath, J.K. (2000). Crystal structure and functional dissection of the cytostatic cytokine oncostatin M. Structure *8*, 863-874. 10.1016/s0969-2126(00)00176-3.

222. Choy, E.H., Bendit, M., McAleer, D., Liu, F., Feeney, M., Brett, S., Zamuner, S., Campanile, A., and Toso, J. (2013). Safety, tolerability, pharmacokinetics and pharmacodynamics of an anti- oncostatin M monoclonal antibody in rheumatoid arthritis: results from phase II randomized, placebo-controlled trials. Arthritis Res Ther *15*, R132. 10.1186/ar4312.

223. Denton, C.P., Del Galdo, F., Khanna, D., Vonk, M.C., Chung, L., Johnson, S.R., Varga, J., Furst, D.E., Temple, J., Zecchin, C., et al. (2022). Biological and clinical insights from a randomized phase 2 study of an anti-oncostatin M monoclonal antibody in systemic sclerosis. Rheumatology (Oxford) *62*, 234-242. 10.1093/rheumatology/keac300.

224. Marden, G., Wan, Q., Wilks, J., Nevin, K., Feeney, M., Wisniacki, N., Trojanowski, M., Bujor, A., Stawski, L., and Trojanowska, M. (2020). The role of the oncostatin M/OSM receptor beta axis in activating dermal microvascular

endothelial cells in systemic sclerosis. Arthritis Res Ther *22*, 179. 10.1186/s13075-020-02266-0.